

1 Data-driven modeling of carbon dioxide and methane fluxes across the 2 Arctic-boreal region: recent achievements and future opportunities

3 Anna-Maria Virkkala*^{1,2}, Mathias Göckede*³, Kyle A. Arndt*¹, McKenzie Kuhn^{1,4}, Sophia Walther³, Jacob
4 Nelson³, Olli Peltola⁵, Gerard Rocher-Ros⁶, Annett Bartsch⁷, David Bastviken⁸, Grant Falvo⁹, Alexandra Hamm²,
5 Josh Hashemi¹⁰, Sarah M. Ludwig¹¹, Susan M. Natali¹, David Olefeldt¹², Martijn Pallandt^{2, 13}, Frans-Jan W.
6 Parmentier¹⁴, Brendan M. Rogers¹, Ted Schuur¹⁵, Claire Treat¹⁰, Judith Vogt³, Carolina Voigt^{10,16}, Jennifer D.
7 Watts¹, Isabel Wargowsky¹, Birgit Wild^{17,13}, Yili Yang¹, Amanda Armstrong^{18, 19}, Valeria Briones¹, Elchin Jafarov¹,
8 Kathleen M.Orndahl²⁰, Benjamin Poulter²¹, Qing Ying¹⁸, Gustaf Hugelius^{2, 13}

9 *Shared first authorship

10 Affiliations:

11 1 Woodwell Climate Research Center, Falmouth, USA

12 2 Department of Physical Geography, Stockholm University, Stockholm, Sweden

13 3 Max Planck Institute for Biogeochemistry, Jena, Germany

14 4 Geography Department, University of British Columbia, Vancouver, Canada

15 5 Natural Resources Institute Finland, Helsinki, Finland

16 6 IceLab, Department of Ecology Environment and Geoscience, Umeå University, Umeå, Sweden

17 7 b.geos GmbH, Korneuburg, Austria

18 8 Department of Thematic Studies - Environmental Change, Linköping University, Linköping, Sweden

19 9 Department of Biological Sciences, Northern Arizona University, Arizona, USA

20 10 Alfred-Wegener Institute Helmholtz Centre for Polar and Marine Research, Potsdam, Germany

21 11 Department of Earth and Environmental Science, Columbia University, New York, NY, United States of
22 America

23 12 Department of Renewable Resources, University of Alberta, Edmonton, Canada

24 13 Bolin Centre for Climate Research, Stockholm University, Stockholm, Sweden

25 14 Centre for Biogeochemistry in the Anthropocene, Department of Geosciences, University of Oslo, Oslo, Norway

26 15 Center for Ecosystem Science and Society, and Department of Biological Sciences, Northern Arizona University,
27 Flagstaff, AZ, USA

28 16 University of Hamburg, Hamburg, Germany

29 17 Department of Environmental Science, Stockholm University, Stockholm, Sweden

30 18 Earth System Science Interdisciplinary Center, University of Maryland, College Park, MD, USA

31 19 Biospheric Sciences Laboratory, NASA Goddard Space Flight Center, Greenbelt, MD, USA

32 20 School of Informatics, Computing and Cyber Systems, Northern Arizona University, Flagstaff, AZ, USA

33 21 Spark Climate Solutions, San Francisco, California

34 Contact: avirkkala@woodwellclimate.org

35 The manuscript was submitted to Global Change Biology.

36 Abstract

37 The Arctic-boreal region contains a significant portion of the global carbon reservoir, which is
38 becoming increasingly vulnerable to atmospheric release due to climate change. Thus, it is vital
39 to monitor and model Arctic-boreal carbon flux dynamics to understand the shifting carbon
40 balance. Data-driven statistical and machine learning models are now commonly used to upscale
41 carbon dioxide (CO₂) and methane (CH₄) fluxes in northern ecosystems from local to
42 circumpolar scales. This review highlights recent progress, ongoing challenges, and new insights
43 into data-driven Arctic-boreal carbon flux modeling. We identify five key areas for future model
44 development: (1) developing comparable upscaling frameworks for terrestrial and freshwater
45 ecosystems, especially for understudied systems like lakes and rivers; (2) reducing uncertainties
46 and gaps in geospatial observations to better represent landscape heterogeneity; (3) fusing
47 process-based with upscaling models to reduce computational demands, allowing to increase
48 resolution and boost predictive power; (4) maximizing synergies between data-driven, process-
49 based, and atmospheric inversion models using hybrid modeling; and (5) collaborating with field
50 and remote sensing scientists to ingest observations in the upscaling process in near-real-time.
51 These steps will reduce carbon budget uncertainty, advance our understanding of the carbon
52 cycle, and support global climate policy.

53 1 Introduction

54 The balance of carbon fluxes, including carbon dioxide (CO₂) and methane (CH₄) from the
55 Arctic-boreal region is changing as climate warming degrades permafrost and alters vegetation
56 dynamics (Biskaborn et al., 2019; Meredith et al., 2019; Virkkala et al., 2025a; Watts et al.,
57 2025). Because permafrost and Yedoma soils in the Arctic-boreal region store over 1,700 Pg of
58 carbon, about one-third of global soil carbon (Hugelius et al., 2020, 2014; Mishra et al., 2021),
59 these changes are creating global climate feedbacks (Natali et al., 2021; Schuur et al., 2022).
60 There is high spatiotemporal complexity in carbon fluxes and drivers at scales ranging from local
61 to regional/circumpolar and disentangling this complexity is necessary to understand current and
62 expected fluxes (Euskirchen et al., 2022). The limited spatiotemporal coverage of carbon flux
63 observations in the Arctic-boreal region requires scaling approaches to project local-scale
64 information across larger-scale domains (See et al., 2024; Virkkala et al., 2025a). The most
65 common techniques available for this purpose include atmospheric inverse modeling, bottom-up
66 process modeling, and data-driven upscaling (Bruhwiler et al., 2021; Hugelius et al., 2024; Treat
67 et al., 2024).

68 Atmospheric inversion models are a method for characterizing surface-atmosphere exchange
69 across regional to global scales from the “top-down” perspective by combining measurements of
70 atmospheric mixing ratios with atmospheric transport modeling and advanced statistics
71 (Bruhwiler et al., 2021; Ciais et al., 2022). These approaches facilitate an atmospheric constraint
72 of large-scale carbon fluxes between the surface and atmosphere, with relatively coarse
73 observational footprints of hundreds of kilometers extending over regional to global extents (e.g.,
74 Houweling et al., 2017; Rödenbeck et al., 2018). Atmospheric inversions offer an independent
75 method for estimating carbon budgets compared to bottom-up scaling approaches, such as
76 process-based models or data-drive upscaling (e.g., Ramage et al., 2024). Inversions are
77 commonly informed by prior flux information as a starting point, including estimates of flux
78 magnitudes from e.g. fossil fuel inventories, land cover maps and output from process-based
79 models. In regions that lack observational constraints, such as the Arctic-boreal (e.g., Wittig et
80 al., 2024) inversions gravitate strongly to these existing priors, thus limiting their ability to add
81 information on properly attributing fluxes.

82 Process-based models simulate ecosystem dynamics using mathematical equations of
83 biophysical, biochemical, and ecological processes and their feedbacks (Heffernan et al., 2024;
84 Huntzinger et al., 2020; Mevenkamp et al., 2023). Importantly, as processed-based models
85 directly incorporate mechanisms, they may be used to predict future states outside of present-day
86 climatic boundaries (e.g., Kleinen et al., 2021), or to experiment with how changes in specific
87 inputs affect results (i.e., sensitivity analyses, e.g., De Vrese et al., 2023). But their predictive
88 capacity strongly depends on accurate representation of complex underlying processes (e.g., Gier
89 et al., 2024). The current generation of Arctic-boreal process-based models still has limitations
90 due to missing processes, such as permafrost feedbacks, limited representation of thermal and
91 moisture dynamics, as well as a poor representation of soil carbon stocks (Hugelius et al., 2024;
92 Schädel et al., 2024). Consequently, they may underestimate CO₂ and CH₄ flux variability from
93 permafrost ecosystems (Treat et al., 2024; Virkkala et al., 2025a).

94 Data-driven upscaling uses various statistical techniques applied to large but typically
95 geographically biased data volumes, to analyze relationships between in-situ carbon flux
96 measurements and explanatory variables, such as environmental conditions and ecosystem
97 characteristics (Jung et al., 2020; Kuhn et al., 2025; Virkkala et al., 2025a; Ying et al., 2025;
98 Yuan et al., 2024). These models are thus correlative in nature and can make full use of available
99 data in finding relationships between target and predictor variables in ways other modeling
100 techniques cannot. However, the strengths and directions of the relationships between target and
101 predictor variables in regional upscaling efforts are often consistent with concepts used in other
102 modeling studies (e.g., positive relationships between temperature or CH₄ fluxes and ecosystem
103 respiration are positive; (Virkkala et al., 2021; Yuan et al., 2024). Current data-driven models are
104 generally multivariate, meaning that several predictors - and often also their interactions - are
105 included. Data-driven approaches can include static predictors (e.g. fundamental physical state
106 variables such as land cover type or permafrost), and dynamic variables (e.g. temperature, soil
107 moisture, and vegetation indices), which follow the timestep of the model. Additionally, different
108 types of new predictors are continuously being explored, e.g. novel static geospatial layers (e.g.,
109 burned status) or parameters accounting for temporal lags (e.g., accounting for delayed transport
110 and release of gas, Yuan et al., 2022). Although the absence of processed-based mechanisms and
111 feedback may introduce uncertainties, the ability of data-driven models to ingest large datasets

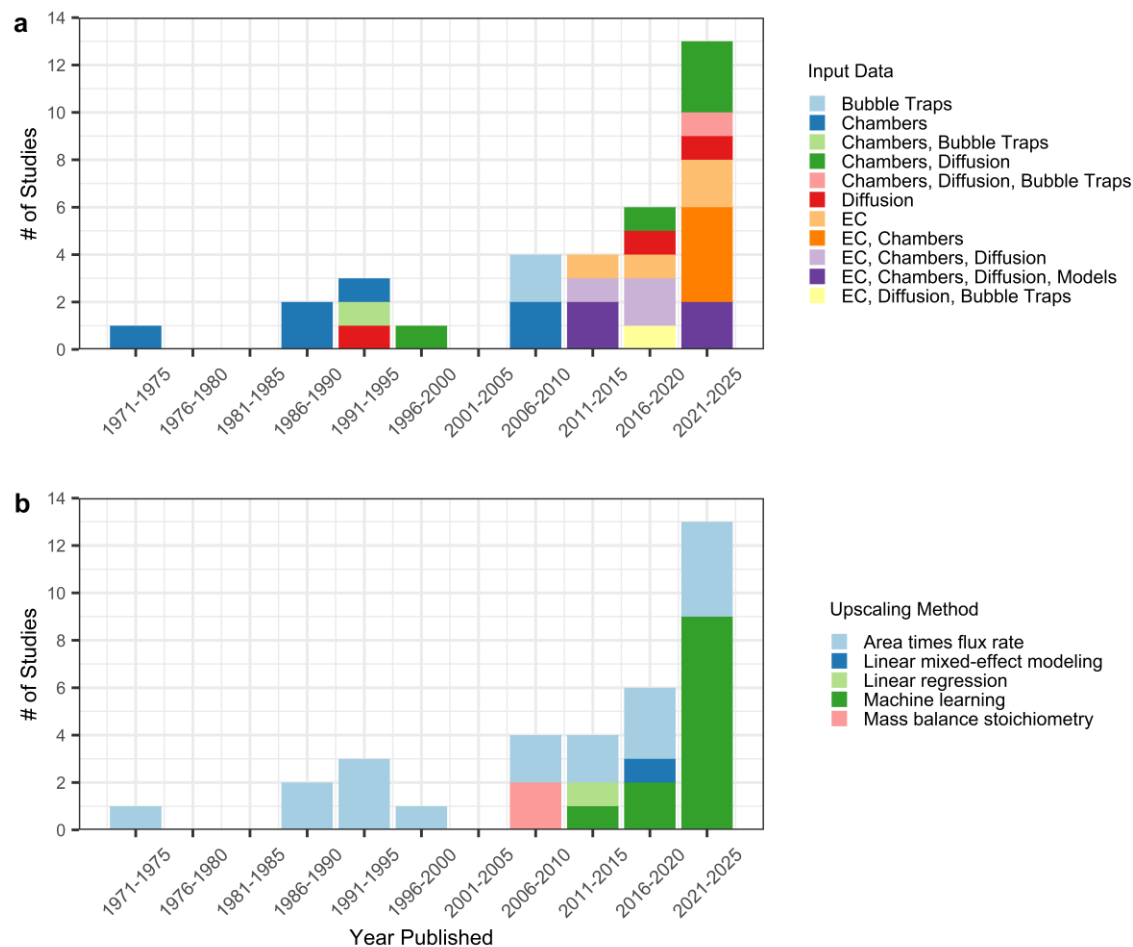
112 and the much lower computing demand make them ideal for more rapidly upscaling data and
113 modeling over larger spatial domains.

114 In this review, we examine the history, development, and current status of data-driven upscaling
115 methods, emphasizing their role in understanding carbon flux dynamics in the Arctic-boreal
116 region, the extent of which is defined here by Dinerstein et al. (2017). Our focus is on biogenic
117 surface-atmosphere carbon fluxes; CO₂ fluxes, encompassing plant carbon uptake and emissions
118 from microbial and plant respiration and CH₄ fluxes, including emissions driven by
119 methanogenesis and uptake driven by methotrophy. Different methodological approaches have
120 been used in carbon flux upscaling studies that have been conducted for terrestrial ecosystems
121 versus inland water ecosystems (including freshwater lakes, reservoirs, ponds, rivers, and
122 streams; Ramage et al., 2024), and methods have also varied depending on the carbon species
123 targeted (Johnson et al., 2022; Ramage et al., 2024; Rocher-Ros et al., 2023; Virkkala et al.,
124 2021). These differentiations have been required since relationships with covariates and data
125 coverage often differed between ecosystem types and/or carbon species. In the following, we
126 will compare scaling methods, summarize data considerations of both in-situ and gridded data
127 important for constructing and running models, and provide best practices for operating data-
128 driven upscaling frameworks. Finally, we will discuss future directions for enhancing the quality
129 of data-driven upscaling products.

130 2 History of Arctic-boreal Data Driven Upscaling

131 The first data-driven approaches to scaling carbon fluxes across Arctic-boreal ecosystems date
132 back to the 1970s (Ehhalt, 1974). These early efforts were limited to in-situ observations from a
133 handful of field sites, and geospatial information on landscape structure and climate, and
134 computational resources, were limited (Oechel et al., 1993). Accordingly, assessed carbon fluxes
135 for complex high-latitude landscapes were simplified by calculating the product of landcover
136 area and flux intensity (“paint-by-numbers”) for a few dominant landcover types to extrapolate
137 across a large region (Figure 1). First attempts to quantify northern wetland CH₄ budgets were
138 based on wetland maps and chamber-flux values from literature (Table 1; Matthews and Fung,
139 1987), on observations from a limited number of sites in Alaska (Sebacher et al., 1986), and a

140 tundra CH₄ budget for the Russian domain (Ehhalt, 1974). Similarly, early estimators of inland
 141 water carbon budgets were restricted to data from the North Slope of Alaska (Kling et al.,
 142 1992) and isolated regions of northern Siberia (Zimov et al., 1997).



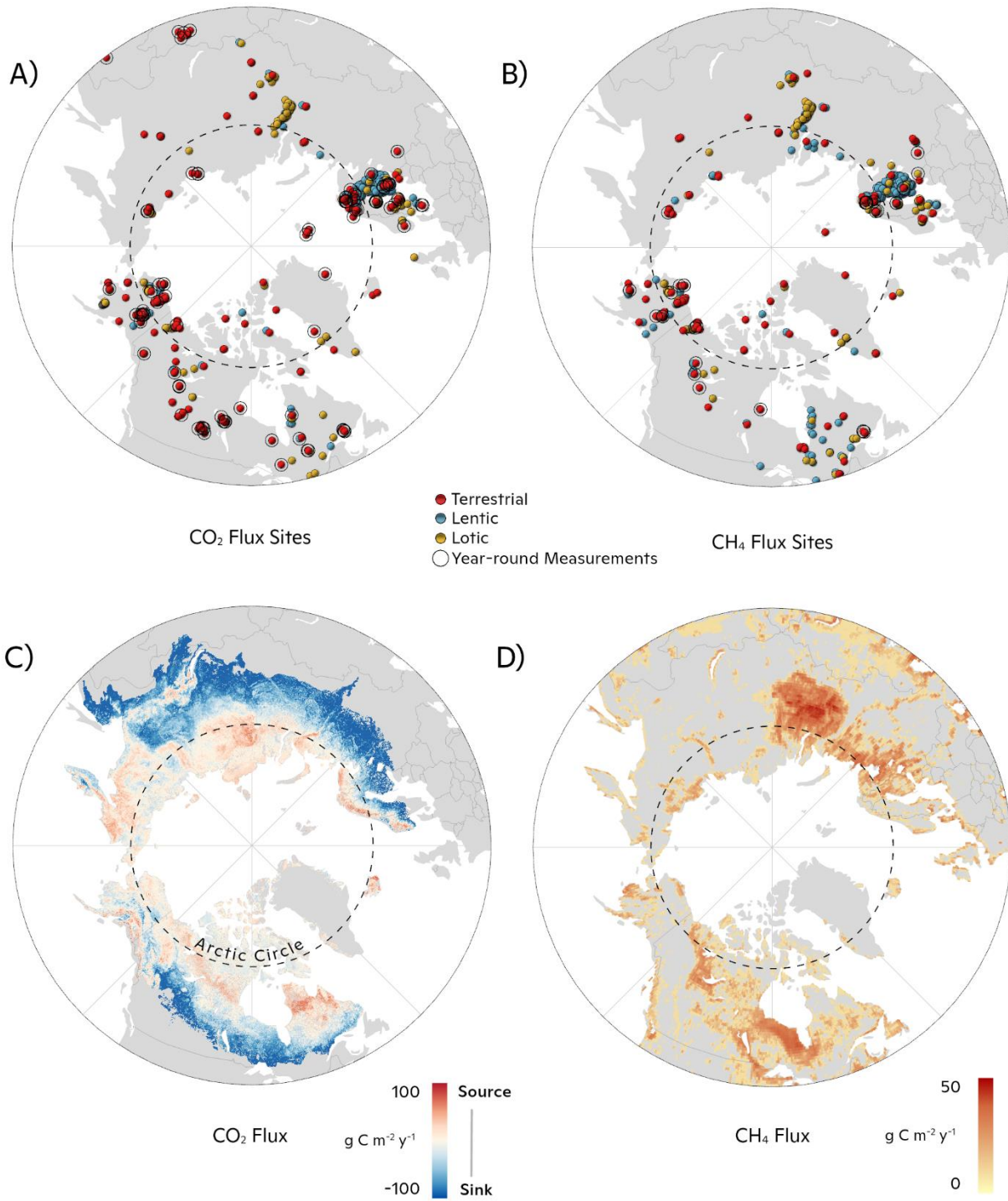
143
 144 **Figure 1.** Count of carbon flux upscaling studies based on in-situ flux data using various
 145 measurement methods **(a)** and upscaling methods **(b)** for data-driven regional budget estimates
 146 from 1971 to 2025. Based on a compilation of studies as of February 2025 where the upscaling
 147 method and input data were identified through expert assessment (SI Table 1). Chambers refer to
 148 both terrestrial and inland water ecosystems and diffusion is the diffusion flux method from
 149 inland water systems. EC is eddy covariance. Models as data input use model outputs in
 150 upscaling.

151 Starting in the 1990s, new generations of instrumentation for field observations led to a rapid
 152 expansion of Arctic-boreal carbon flux monitoring (Belshe et al., 2013; Oechel et al., 2014;

153 Pallandt et al., 2022; Suni et al., 2003; Vogt et al., 2025), initially focusing on CO₂
154 measurements. The first year-round CH₄ measurements at a boreal site were established a few
155 years later (Rinne et al., 2007). Progress in the availability of in-situ observations was
156 accompanied by improvements in spatial resolution and thematic content of geospatial data
157 layers of the explanatory variables (Ueyama et al., 2013; Wik et al., 2016). This provided the
158 foundation for the development of more sophisticated upscaling methods that included higher
159 levels of detail regarding the functional relationships between fluxes and explanatory variables,
160 or the differentiation of ecosystem types within structured landscapes. A key effort has been the
161 global upscaling framework FLUXCOM investigating e.g. how different predictor datasets and
162 machine learning models impacted upscaled global terrestrial CO₂ and energy fluxes (Jung et al.,
163 2020; Nelson & Walther et al., 2024; Tramontana et al., 2016). With the ongoing improvement
164 of methods, information, and computational resources, a generation of advanced upscaling
165 products has emerged, which makes it possible to resolve the Arctic-boreal domain at relatively
166 high spatio-temporal resolution and link fluxes and controls in a high degree of detail (Figure 2,
167 Peltola et al., 2019; Virkkala et al., 2021; Ying et al., 2025).

168 Recent wetland CH₄ budget assessments suggest wide emissions ranges based partly on the
169 regions covered and wetland maps used (Table 1, Peltola et al., 2019; Ramage et al., 2024; Ying
170 et al., 2025; Yuan et al., 2024). Other recent studies have started to focus on CH₄ uptake showing
171 emissions may be offset partially by drier ecosystems, previously process-based and inversion
172 models dominated CH₄ uptake studies (Jiang et al., 2025; Oh et al., 2020; Parmentier et al., 2024;
173 Voigt et al., 2023). In contrast, terrestrial CO₂ budgets indicate a relatively strong carbon sink in
174 the boreal region, while the tundra biome exhibits a smaller sink to near-neutral budget (Ramage
175 et al., 2024; Virkkala et al., 2025a). Recent papers suggest a wide range in estimated lake CO₂
176 emissions (Ramage et al., 2024; Song et al., 2024) and generally higher and more variable
177 estimates were reported for rivers (Lauerwald et al., 2023; Liu et al., 2022; Ramage et al., 2024;
178 Song et al., 2024), where lake CH₄ emission estimates tend to agree more than CO₂ (Johnson et
179 al., 2022; Kuhn et al., 2025; Matthews et al., 2020; Ramage et al., 2024; Sieczko et al., 2020;
180 Wik et al., 2016); however, this agreement may be incomplete because most models potentially
181 have issues capturing the spring ice-breakup period. River emission of CH₄ for the Arctic-boreal
182 region was also substantial and was estimated to 17% of the global riverine CH₄ emissions
183 (Rocher-Ros et al., 2023; Stanley et al., 2016). Human impacted ecosystems such as reservoirs

184 deserve attention as well given their prevalence in northern boreal areas and are of increasing
185 attention (Bastviken and Johnson, 2025).



186

187 **Figure 2.** The spatial distribution of the Arctic-boreal network of carbon flux observations,
188 based on a recent data synthesis (a & b; Virkkala et al., 2025b), alongside two examples of
189 upscaled Arctic-boreal carbon flux maps. (c) The average terrestrial net ecosystem exchange
190 (NEE) over 2002-2020 from Virkkala et al., (2025a), and (d) wetland methane (CH₄) emissions
191 over 2016-2022 based on Ying et al., (2025), mapped across the wetlands north of 45 °N. These
192 upscaled products were developed using random forest models together with gridded
193 meteorological, remote sensing, and soil datasets as predictors.

194 **Table 1.** Methane (CH₄) and carbon dioxide (CO₂) budgets for various data-driven upscaling studies targeting various ecosystems and
 195 regions. All units are Tg CH₄-C yr⁻¹ or Tg CO₂-C yr⁻¹.

Manuscript	Budget (Min)	Budget (Mean)	Budget (Max)	Target ecosystem(s)		Region
					Methane	
Bastviken et al. (2025)		0.3		Reservoirs		Arctic Boreal Region
Bastviken et al. (2025)		11.0		Lakes		Arctic Boreal Region
Ying et al. (2025)	11.8	17.1	38.7	Wetlands		North of 45 Degrees N
Jiang et al. (2025)		6.9		Terrestrial		Arctic Boreal Region
Ramage et al. (2024)	22.0		53.0	Terrestrial		Arctic Boreal Region
Ramage et al. (2024)	4.5	9.4	13.1	Inland Waters		Arctic Boreal Region
Song et al. (2024)	7.6	10.7	13.9	Inland Waters		Northern land cryosphere region, incl. Tibetan plateau
Song et al. (2024)	1.7	3.5	5.3	Rivers		Northern land cryosphere region, incl. Tibetan plateau
Song et al. (2024)	5.9	7.2	8.7	Lakes		Northern land cryosphere region, incl. Tibetan plateau
Yuan et al. (2024)	14.6	15.2	15.9	Wetlands		Arctic Boreal Region
Chen et al. (2024)	17.0	19.5	22.0	Wetlands		North of 30 Degrees N
Rocher-Ros et al. (2023)		3.5		Rivers		North of 50 Degrees N
McNichol et al. (2023)	8.6	12.0	15.0	Wetlands	60-90 deg. N + West	Siberian lowlands & Hudson Bay Lowlands
Johnson et al. (2022)		7.1		Lakes		North of 45 Degrees N
Matthews et al. (2020)	10.4	11.8	13.3	Lakes		North of 50 Degrees N
Peltola et al. (2019)	16.1		37.1	Wetlands		North of 45 Degrees N
Treat et al. (2018)	22.5	27.8	33.0	Wetlands		North of 40 Degrees N
Holgerson & Raymond (2016)	6.0		15.0	Lakes & ponds		Global
Wik et al. (2016)	5.5	12.4	19.3	Lakes & ponds		North of 50 Degrees N
Tan & Zhuang (2015)	6.9	8.5	10.1	Lakes		North of 60 Degrees N
McGuire et al. (2012)	0.0	11.0	22.0	Tundra		Circumpolar

Walter et al. (2007)	10.3	18.2	26.0	Lakes	North of 45 Degrees N
Bartlett and Harris (1993)		28.5		Wetlands & Tundra	North of 45 Degrees N
Mathews and Fung (1987)		49.1		Wetlands	North of 50 Degrees N
Mathews and Fung (1987)		21.9		Wetlands	North of 60 Degrees N
Sebacher et al. (1986)	33.8	56.6	79.5	Wetlands	Arctic Boreal Region
Ehhalt et al. (1974)	1.0		9.8	Tundra	Circumpolar

Manuscript	Budget (Min)	Budget (Mean)	Budget (Max)	Target ecosystem(s)	Region
Carbon Dioxide					
Mu et al. (2025)	174.0	188.0	202.0	Rivers	Arctic Boreal Permafrost Region
Virkkala et al. (2025a)	-688.0	-548.0	-408.0	Terrestrial	Arctic Boreal Region
Ramage et al. (2024)	-606.0		661.0	Terrestrial	Permafrost Region
Ramage et al. (2024)	132.4	230.6	359.8	Inland Waters	Arctic Boreal Region
Song et al. (2024)	274.0	313.4	356.6	Inland Waters	Northern land cryosphere region, incl. Tibetan plateau
Song et al. (2024)	71.2	87.5	105.5	Lakes	Northern land cryosphere region, incl. Tibetan plateau
Song et al. (2024)	202.6	225.8	250.9	Rivers	Northern land cryosphere region, incl. Tibetan plateau
Liu et al. (2022)		250.0		Rivers	"Arctic" (~boreal-Arctic region)
Virkkala et al. (2021)	-449.0		-366.0	Terrestrial	Arctic Boreal Region
Holgerson & Raymond (2016)	439.0		683.0	Lakes & Ponds	Global
Belshe et al. (2013)	84.0	462.0	840.0	Tundra	Circumpolar
McGuire et al. (2012)	-297.0	-103.0	89.0	Tundra	Circumpolar
Oechel et al. (1993)		190.0		Tundra, Lakes, & Rivers	Circumpolar

197 3 In-situ Flux and Predictor Data

198 Observational input data for both target and predictor variables are critical for upscaling, and
199 obtaining spatially and temporally representative data remains a persistent challenge (Munson,
200 2012; Tweedie et al., 1994). Ideally, observational data are collected and processed using
201 standardized protocols to ensure comparability, reproducibility and to avoid measurement error
202 and bias (Loescher et al., 2022; Pastorello et al., 2020). Upscaling efforts are based on training
203 data that are limited in space and time and in the ecosystem states they represent. A data-driven
204 model must generalize input data patterns to larger areas and to conditions not always
205 represented in the measured data. This is especially challenging in the Arctic-boreal region
206 where carbon flux networks represent less than 40% of the environmental space and are biased
207 towards warmer and undisturbed conditions (Pallandt et al., 2024, 2022; Virkkala et al., 2019).
208 Accordingly, data quantity and quality are factors limiting upscaling efforts in the Arctic-boreal
209 region, particularly during the non-growing season (Arndt et al., 2023), and important factors
210 like extent and severity of disturbances such as wildfires are often unaccounted for (Ramage et
211 al., 2024; Virkkala et al., 2025a).

212 3.1 Carbon Flux Measurements

213 3.1.1 Terrestrial observations

214 Terrestrial fluxes are primarily collected with the use of eddy covariance (EC) or flux chamber
215 techniques. Other flux methods exist such as snow diffusion fluxes (Mavrovic et al., 2025) but
216 they are less common in upscaling studies and thus are not emphasized in more detail here. EC is
217 a micrometeorological flux measurement technique used to quantify ecosystem-atmosphere
218 energy and trace gas exchange at landscape scales (i.e., 100s of m^2 to $\sim km^2$ spatial scale), based
219 on the continuous measurement of turbulent atmospheric transport using tower- or tripod-
220 mounted instruments (Aubinet et al., 2012; Baldocchi, 2003). The spatial scale and continuous
221 temporal coverage of EC measurements is convenient when connecting flux observations with
222 geospatial data products as the scale of these observations can be similar (i.e., 250 – 1000 m).
223 Chamber flux measurements (Kwon et al., 2019; Subke et al., 2021) enclose a small portion of
224 the ecosystem (usually $<1m^2$) and derive the surface-atmosphere flux from the gas concentration

225 change in the headspace over time, with data usually collected manually during episodic
226 campaigns. This allows collection of flux samples from homogeneous sub-units of a mixed
227 landscape, but due to the small footprint the representativeness of individual measurements is
228 challenging to assess.

229 Arctic-boreal data coverage currently includes around 120 active EC towers (Pallandt et al.,
230 2024), and more than 1,000 flux chamber plots, though less than 30 of those flux chamber sites
231 provide continuous data collected by automated chambers (Vogt et al., 2025). Many previous
232 upscaling studies used just one type of flux data, such as global efforts based on EC fluxes from
233 FLUXNET (Jung et al., 2020; McNicol et al., 2023; Tramontana et al., 2016). Using data from
234 both chambers and EC has the advantage of a more detailed local-scale understanding of flux
235 variability based on their different spatial coverage (Natali & Watts et al., 2019; Virkkala et al.,
236 2021; Watts et al., 2021; Yuan et al., 2024). This also fosters process-understanding given the
237 small-scale heterogeneity of carbon fluxes (Davidson et al., 2016; Juutinen et al., 2022; Virkkala
238 et al., 2024). However, at the same time combining fluxes captured by different techniques adds
239 challenges and uncertainty as these methods may not be directly comparable, although a good
240 match between EC and flux chambers can be achieved (e.g., Parmentier et al., 2011). The user
241 should decide carefully based on the scale of their study and representation of in-situ data in
242 what to include to inform their models.

243 3.1.2 Inland water observations

244 Water-atmosphere carbon fluxes can be derived using many techniques, such as direct gas flux
245 measurements using chambers (e.g., Rasilo et al., 2015) or bubble traps (e.g., Walter Anthony et
246 al., 2021, 2010), EC towers with footprints covering inland water systems (e.g., Erkkilä et al.,
247 2018; Podgrajsek et al., 2014), or diffusion outgassing estimated based on measured dissolved
248 gas concentrations using Fick's law (Jaynes and Rogowski, 1983) and models for the gas transfer
249 velocity (Hall and Ulseth, 2020; Klaus and Vachon, 2020; Raymond et al., 2012). Current
250 Arctic-boreal data coverage includes 24 EC sites with major footprint fractions placed on open
251 water bodies, while episodic flux chamber data and dissolved gas measurements are available for
252 more than 1300 locations (Vogt et al., 2025). Global and regional data syntheses of carbon fluxes
253 using different techniques have been published for lakes (Golub et al., 2022; Kuhn et al., 2021),

254 rivers and stream (Liu et al., 2022; Stanley et al., 2023), and inland waters in combination (i.e.
255 lakes, rivers and streams; Song et al., 2024). Furthermore, dissolved gas concentrations were
256 synthesized alongside fluxes (Liu et al., 2022; Stanley et al., 2023).

257 Similar to studies performing data-driven modelling for terrestrial ecosystems, upscaling studies
258 were performed for inland waters for CO₂ (De Eyto et al., 2025; Denfeld et al., 2018; Mu et al.,
259 2025; Ramage et al., 2024; Raymond et al., 2013; Song et al., 2024) and CH₄ (Ramage et al.,
260 2024; Rocher-Ros et al., 2023; Song et al., 2024) varying in methodology, spatial extent, type of
261 water body and magnitude of carbon budget (Table 1).

262 3.2 Ancillary in-situ data

263 The accuracy of flux upscaling models may be improved when *in-situ* environmental and
264 biogeochemical information is available, as extracting from coarser geospatial data may not
265 represent local conditions well. For example, soil moisture models often struggle, especially
266 across the whole Arctic-boreal region (Kemppinen et al., 2023), and are often provided at the 10-
267 50 km scale, which often does not represent fine-scale heterogeneity. While in-situ observations
268 provide the most accurate and spatiotemporally resolved biogeochemical data possible for flux
269 predictions (Knox et al., 2019), leveraging this information requires establishing a link to the
270 gridded predictor dataset that will ultimately be used to scale up fluxes to the larger study
271 domain, and moving between the two may introduce other errors.

272 For terrestrial systems, the incorporation of in-situ soil and vegetation datasets can improve the
273 predictions of flux upscaling models (Voigt et al., 2023; Watts et al., 2023). Key dynamic
274 variables include air and soil temperature, moisture, thaw-depth, and radiation. Semi-static
275 characteristics are also important to measure, including vegetation community composition,
276 aboveground biomass, canopy height, disturbance history, soil type, and soil carbon density.

277 For inland water systems, in-situ water quality measurements can be crucial to successfully
278 predicting ebullitive and diffusive fluxes (Sø et al., 2023). In addition, lake freeze status derived
279 from temperature sensors or field cameras at flux measurement sites can improve the modeled
280 relationships to fluxes (Karlsson et al., 2013) while being readily scalable to associated
281 geospatial layers. Conversely, the freeze status of small lakes derived from high resolution

282 optical imagery can have significant temporal gaps due to limited overpass frequency, cloud
 283 coverage and sun-sensor geometry (Giroux-Bougard et al., 2023). Key dynamic variables include
 284 water depth, depth-resolved temperature (including sediments), dissolved oxygen, dissolved
 285 organic carbon, and variables reflecting biological productivity (Bastviken et al., 2004;
 286 Natchimuthu et al., 2016; Rocher-Ros et al., 2023). Key static variables include water body
 287 surface area, sediment characteristics, and geologic origin (Wik et al., 2016).

288 3.3 Data Repositories and Carbon Flux Syntheses

289 Choosing and compiling input data for data-driven upscaling is a key first step towards running
 290 any model. There are more than 2,000 sites with carbon flux observations using different systems
 291 across the Arctic-boreal region (Vogt et al., 2025), with most flux sites run by independent
 292 researchers studying individual scientific questions. Many of these sites are regionally clustered
 293 in Alaska and Scandinavia (Metcalf et al., 2018). While this clustering facilitates a more
 294 detailed analysis of small-scale spatio-temporal carbon flux dynamics, these clusters limit the
 295 spatial representativeness on broader scales. A considerable fraction of flux datasets have been
 296 collected in data repositories that are publicly accessible. EC data repositories are either regional
 297 networks or global synthesis initiatives, in both cases providing data that are well-organized and
 298 standardized to facilitate integrating measurements from multiple sites (Table 2). Other data
 299 sources, like those related to a specific project or publication, also cover observations from
 300 chambers or concentration measurements; however, these sources are often less systematic and
 301 specialized, therefore making it more difficult to find data, and integrate into larger databases.
 302 This highlights the value of synthesis activities such as e.g. ABCFlux or BAWLD-CH₄ (Kuhn et
 303 al., 2021; Virkkala et al., 2025b, 2022) which standardize and collate data from across various
 304 networks and research groups.

305 **Table 2.** Existing repositories and synthesis data sources for terrestrial and inland water flux data
 306 in the Arctic-boreal region.

Repository, Flux Network, or Synthesis	Measurement method(s)	Geographic Coverage	Reference or URL
--	--------------------------	------------------------	------------------

Fluxnet	EC	Global	https://fluxnet.org/
Ameriflux	EC	Americas	https://ameriflux.lbl.gov/
NEON	EC & Chamber	United States	https://data.neonscience.org/
ORNL DAAC	EC, Chamber & concentration	Global	https://daac.ornl.gov/
ICOS	EC & Chamber	Europe	https://www.icos-cp.eu/
European Fluxes Database Cluster	EC	Europe	https://www.europe-fluxdata.eu/
AsiaFlux	EC	Asia	https://www.asiaflux.net/
Arctic Data Center	EC, Chamber & concentration	Arctic-boreal zone	https://arcticdata.io/
BAWLD-CH4	Chamber	Arctic-boreal zone	Kuhn et al., (2021)
ABCflux	EC & Chamber	Arctic-boreal zone	Virkkala et al. (2025b, 2022)
GRiMe	Chamber and concentration	Global	Stanley et al. (2023)
JapanFlux2024	EC	Asia	Ueyama et al. (2025)
SITES	EC, Chamber & concentration	Sweden	https://www.fieldsites.se/
Golub et al. 2023	EC	Global	Golub et al. (2023)
Natali & Watts et al. 2019	EC & Chamber	Arctic-boreal zone	Natali & Watts et al. (2019)

Treat et al., 2018	EC & Chamber	Arctic-boreal zone	Treat et al. (2018)
Cryosphere Inland Water Greenhouse Gases Database (CIWD-GHG)	Chamber & concentration	Arctic-boreal zone and Tibetan Plateau	https://zenodo.org/records/11054180
Greenland Ecosystem Monitoring	EC & Chamber	Greenland	https://data.g-e-m.dk/
Svalbard Integrated Arctic Earth Observing System (SIOS)	EC, Chamber & concentration	Svalbard	https://www.sios-svalbard.org/

307 **4 Geospatial environmental data**

308 Effective upscaling of carbon fluxes requires accurate geospatial products representing key
 309 predictor variables. These variables should represent the expected processes controlling the
 310 target flux and thus may vary depending on the carbon flux and ecosystem considered, although
 311 there are some common key predictor variables (e.g., air/soil/water temperature). Categories of
 312 environmental correlates used in data-driven upscaling include land cover and waterbody type,
 313 vegetation, soil, permafrost, topography, meteorology and climate (see Table 3 for used
 314 products).

315 **4.1 Current gridded datasets: strengths and limitations**

316 Global optical remote sensing and meteorological datasets have been available for several
 317 decades and have formed the foundation for data-driven carbon flux upscaling. Optical remote
 318 sensing, providing indices like the normalized difference vegetation index (NDVI; using red and
 319 near-infrared spectral bands) from MODIS, have shown strong correlations with carbon fluxes
 320 and often explain a significant portion of carbon flux variability (Tramontana et al., 2016;
 321 Virkkala et al., 2025a), while gridded meteorological datasets (particularly air temperature, solar

322 radiation) provided from products such as the ECMWF reanalysis v5 (ERA5-Land Muñoz-
323 Sabater et al., 2021) are primary covariates for temporal dynamics (Feron et al., 2024; Ying et
324 al., 2025). However, while these predictors capture important spatial and temporal dynamics
325 needed for scaling carbon fluxes for many key covariates within the Arctic-boreal region such as
326 surface inundation, soil moisture, soil freeze/thaw status, snow depth, and snow water
327 equivalent, comprehensive datasets with adequate spatial resolution and quality are still lacking.
328 For example, linked to the lack of high-quality subsurface datasets for the high northern
329 latitudes, moisture status covariates have often been underrepresented in carbon flux upscaling
330 studies or, when included, have shown limited importance (Natali & Watts et al., 2019; Virkkala
331 et al., 2025a), despite obvious impacts at the site level. Moreover, optical remote sensing data for
332 the Arctic-boreal domain are often affected by cloud cover, snow, and low sun angles, all of
333 which impact the availability and quality of spaceborne measurements (Duncan et al., 2020).

334 Beyond dynamic predictors, static geospatial datasets, such as topography, land cover, and soil
335 properties, play a crucial role in carbon flux upscaling. While regional and local datasets of
336 moderate resolution (≤ 1 km) have been available for years, the scarcity of high-quality geospatial
337 products covering the full Arctic-boreal domain with uniform formatting has limited large-scale
338 carbon flux upscaling efforts. Many global land cover classifications do not include unique
339 characteristics of these regions, including periglacial processes, glacial history, or permafrost
340 characteristics, and misclassify land cover types. For example, the global land cover dataset ESA
341 CCI Landcover underestimates wetland extent (19% accuracy for the entire permafrost region,
342 Palmtag et al., 2022) and misclassifies 60% of Arctic shrub tundra as barren (Bartsch et al.,
343 2024). This misrepresentation is partially attributed to the low spatial and thematic resolution of
344 high-latitude land cover classes in global products and can propagate into carbon flux upscaling,
345 including cases where sources are misrepresented as sinks (Hashemi et al., 2025). Similarly, the
346 SoilGrids 250m dataset, a state-of-the-art high-resolution global product of soil properties based
347 on upscaling observational data with machine learning, is constrained by data sparsity, with the
348 tundra bioclimatic region being represented by only ~800 observations, compared to nearly
349 50,000 for the temperate broadleaf and mixed forests bioclimatic region, despite being roughly
350 equal in area (Poggio et al., 2021).

351 Even for the numerous local and regional geospatial datasets that describe the complex and
352 heterogeneous Arctic-boreal environment, the high spatial heterogeneity of these landscapes
353 poses a particular challenge. Case studies capturing such fine-scale variability with high-
354 resolution remote sensing data (≤ 30 m, e.g., optical vegetation and thermal indices calculated
355 from Planet, Sentinel and Landsat satellites) are emerging, and demonstrate strong performance
356 when paired with spatial chamber campaigns or EC flux footprint decomposition (Ludwig et al.,
357 2024, 2023; Räsänen et al., 2021). However, substantial work remains to be invested in
358 integrating and extrapolating these high spatial resolution remote sensing data with the high
359 temporal resolution of flux measurements across the entire Arctic-boreal region. Of particular
360 importance for carbon flux upscaling is the high heterogeneity in soil moisture content (Lara et
361 al., 2020). Bartsch et al. (2024) demonstrated in their high-resolution land cover product for the
362 Arctic biome that about 66% of the analyzed landscape was highly heterogeneous with respect to
363 wetness at a 1-km scale. Since wetland type differentiation is still mostly limited to local studies,
364 and ground-truth data are largely lacking in many regions, the ability of data-driven upscaling
365 approaches to accurately represent conditions within larger Arctic-boreal regions remains
366 severely hampered.

367 For inland water carbon fluxes, scaling is also limited by available geospatial data (Kuhn et al.,
368 2025; Rosentreter et al., 2021; Wik et al., 2016). The scaling efforts to arrive at waterbody
369 carbon budgets often rely on estimates of total waterbody area by regions, sometimes stratified
370 by water body size categories. There are three main challenges to scaling waterbody carbon
371 emissions; first, many of the relevant driver variables are not available as spatial datasets (e.g.
372 water and sediment temperature, dissolved oxygen, dissolved organic carbon concentration and
373 quality, bathymetry, (e.g. water and sediment temperature, dissolved oxygen, dissolved organic
374 carbon concentration and quality, bathymetry, Ludwig et al., 2022). Second, mapping small
375 waterbodies is essential for scaling inland water carbon emissions, particularly in Arctic-boreal
376 regions where small ponds and lakes are abundant and can experience rapid change in area both
377 seasonally and inter-annually (Kyzivat and Smith, 2023; Mullen et al., 2023; Muster et al.,
378 2019). Ponds (<0.01 km²) often have the highest emission rates of CO₂ and CH₄ (Holgerson and
379 Raymond, 2016), but are not mapped accurately enough by 30-m or coarser imagery to delineate
380 area and separate open surface water from vegetated wetlands and pixel edge effects, leading to
381 double counting (Thornton et al., 2016). Currently, water bodies are mapped at the 10 ha and 1

382 ha scale (Messenger et al., 2016; Wang et al., 2025). Third, temporal components like the ice-
383 covered period are estimated based on remotely sensed data (Zhao et al., 2022); however this
384 technique may miss events based on retrieval times and may miss intermittent ice off periods
385 where emissions occur.

386 4.2 Future upgrades towards Arctic-boreal specific geospatial datasets

387 Customized geospatial datasets for the Arctic-boreal region have become increasingly available
388 over the past decades. One example is the Boreal Arctic Wetland and Lake Dataset (BAWLD),
389 which provides a novel thematically complex classification of wetland landscapes across the full
390 Arctic-boreal region, and has been used for carbon flux upscaling (Kuhn et al., 2025; Ramage et
391 al., 2024). This data product integrates multiple data sources at broader scales; however, the
392 resulting information is provided at comparably coarse resolution (0.5 degree; Olefeldt et al.,
393 2021), and the thematic classes are designed for CH₄ flux upscaling and miss many important
394 classes for CO₂ fluxes (e.g., different types of boreal forest or upland tundra vegetation). Spatial
395 and thematic resolution could, however, be improved by fusing available regional products
396 (Briones et al., 2025). Other customized datasets include those describing soil types and carbon
397 stocks as well as active layer thickness and mean annual ground temperatures for the permafrost
398 region (Hugelius et al., 2014; Westermann et al., 2025), though these miss the non-permafrost
399 boreal regions that cover more than 20% of the Arctic-boreal domain.

400 Microwave satellite observations offer a potential solution to address some of the current gaps in
401 providing proxies for belowground conditions, as they can penetrate clouds and provide critical
402 information on high-latitude processes such as active layer thaw or near surface moisture status
403 (Bartsch et al., 2023). However, the high landscape heterogeneity of Arctic-boreal regions poses
404 significant challenges for retrieving soil moisture information via microwaves, available at
405 spatial resolutions of ~10–25 km (Högström et al., 2018; Högström and Bartsch, 2017; Wrona et
406 al., 2017). Recent studies have demonstrated that microwave derived soil freeze/thaw status
407 could enhance flux estimates and provide deeper insights into seasonal carbon dynamics
408 (Pulliainen et al., 2024; Widhalm et al., 2025). While there are still substantial differences
409 between freeze/thaw products to date, there is the potential for spatial resolution enhancement
410 and improvement through product combination (Bartsch et al., 2025). Further, these more active

411 remote sensing techniques could aid in data collection over the dark Arctic winters where there is
412 a large paucity of data given the need for solar radiation in passive remote sensing technologies.

413 Regarding inland water datasets, there are promising avenues that leverage the light absorbed by
414 chlorophyll and chromophoric dissolved organic matter to remotely sense these concentrations in
415 surface waters, which have then been related to CO₂ and CH₄ in empirical models and used in
416 data-driven models (Griffin et al., 2018; Kutser et al., 2005; Lapierre and Del Giorgio, 2012;
417 Ludwig et al., 2023). Regarding the mapping of small water bodies, there are growing efforts to
418 create very high resolution landcover and inland water maps for the pan-Arctic (Bartsch et al.,
419 2024; Mullen et al., 2023; Wang et al., 2025), which could support high resolution, data-driven
420 scaling of inland water carbon emissions. Both directions hold the potential to boost the quality
421 of upscaled inland water carbon products in future modeling frameworks.

422 Finally, the geospatial mapping of extent, severity and frequency of occurrence of disturbance
423 features across the Arctic-boreal region poses a special challenge to upscaling efforts. Typical
424 disturbances are wildfires, windthrow, insects, rain-on-snow events and permafrost thaw,
425 including different types of abrupt thaw, lake drainage, ice wedge degradation, and thermokarst
426 (Bhuiyan et al., 2020; Grosse et al., 2011; Schuur and Mack, 2018). Such rapid changes and
427 disturbances greatly impact carbon fluxes, and the ability to monitor and characterize them
428 (Phoenix et al., 2025). Ramage et al (2024) suggest that disturbances, primarily abrupt thaw and
429 fires, pushed the northern permafrost region from a net sink to a source of atmospheric carbon
430 for the period 2000 – 2020, in line with findings from earlier regional studies (e.g., Commane et
431 al., 2017). The rapid landscape changes that occur from these processes cannot be captured by
432 static land cover datasets, instead we require observations from space that are continuous in time
433 and have sufficient spatial resolution. Wildfires are the most documented, including global
434 products such as Copernicus Fire and GFED (Copernicus Atmosphere Monitoring Service, 2022;
435 Van Der Werf et al., 2017); however, these products often disagree, especially in Siberia
436 (Clelland et al., 2024). In addition to fire, some products have been developed specifically for
437 Arctic-boreal disturbance regimes. Some circumpolar datasets map the spatial patterns of
438 disturbances (e.g., Nitze et al., 2025), providing valuable information on regional dynamics in
439 spatial extent and severity. Zhang et al. (2022) used a continuous change detection and
440 classification algorithm to document and classify boreal forest disturbances based on Landsat

441 satellite imagery, while Runge et al. (2022) reported an 331% increase of areas affected by
 442 retrogressive thaw slumps between 2000 and 2019 based on a large-scale, automated detection
 443 algorithm using combined Landsat and Sentinel-2 satellite imagery. Available data on ground ice
 444 distribution (e.g., O’Neill et al., 2019) could be linked to these studies to project the likelihood of
 445 thermokarst disturbances under future climate scenarios. Still, current information on disturbance
 446 features is based on only a limited number of observational data years, compared to the typical
 447 duration of a disturbance cycle (e.g., Turetsky et al., 2020), and the rate of disturbance formation,
 448 recovery and associated fluxes is mostly lacking, all of which are needed to understand the net
 449 impact of the disturbances on fluxes. Consequently, such predictors have not yet been utilized
 450 adequately in Arctic-boreal carbon flux upscaling.

451 **Table 3.** Examples of geospatial datasets used as input for Arctic-boreal data-driven upscaling
 452 studies. The subclasses describe the specific predictor variables within the broad classes.

Broad class	Subclass	Geospatial dataset
Land cover	Land cover: thematic land cover classes and fractional coverages, including wetland and lake extent	Boreal-Arctic Wetland and Lake Dataset (Olefeldt et al., 2021) Global Lakes and Wetland Database (Lehner et al., 2025)
Vegetation	Vegetation fractional cover: fraction coverage of different types of vegetation (species or generalized classes)	MODIS Continuous Vegetation Fields (DiMiceli et al., 2022)
	Vegetation communities: species data, plant community assemblages, plant functional type	Circum-Arctic Vegetation Map (Raynolds et al., 2019)
	Productivity/Biomass: Leaf area index, normalized difference vegetation index, enhanced vegetation index, above ground and below ground biomass	MODIS Vegetation Indices (Didan, 2021)
Soil properties	Soil texture: Volumetric fraction of sand, silt and clay.	SoilGrids1.0 (Hengl et al., 2017) SoilGrids2.0 (Poggio et al.,

		2021)
	Soil carbon: Soil organic carbon (OC) content, calculated from OC and soil bulk density data.	SoilGrids1.0 (Hengl et al., 2017) SoilGrids2.0 (Poggio et al., 2021) Permafrost Carbon (Hugelius et al., 2014)
Permafrost	Extent of permafrost: Probability or aerial coverage.	(Obu et al., 2019; Westermann et al., 2025)
	Active layer depth: Depth of active layer at the end of the growing season. Data on seasonal and interannual active layer depth variability	(Westermann et al., 2025)
	Permafrost temperature: Degrees, depth of annual zero amplitude	(Obu et al., 2019; Westermann et al., 2025)
	Soil freeze/thaw status	(Kim et al., 2017; Luo et al., 2021)
Topography	Elevation and topographic indices such as slope angle, aspect, topographic wetness index and topographic position index	Geomorpho90m (Amatulli et al., 2020)
Meteorology	Air, surface and soil temperature	ERA5-Land (Muñoz-Sabater et al., 2021) MERRA2 (Global Modeling And Assimilation Office and Pawson, 2015) MODIS Land Surface Temperature (Wan et al., 2021) TerraClimate (Abatzoglou et al., 2018)
	Incoming solar radiation	ERA5-Land (Muñoz-Sabater et al., 2021)
	Precipitation, vapor pressure deficit	ERA5-Land (Muñoz-Sabater et al., 2021)

	Soil moisture	ERA5-Land (Muñoz-Sabater et al., 2021) SMAP (Lakshmi and Fang, 2023)
	Snow cover and depth	ERA5-Land (Muñoz-Sabater et al., 2021) MODIS Snow / Ice Global Mapping Product (Hall and Riggs, 2021)
Climate	Long-term annual and seasonal averages: mean annual air temperature and precipitation, growing degree days, freezing degree days	WorldclimV2 (Fick and Hijmans, 2017) TerraClimate (Abatzoglou et al., 2018)
Waterbody types & characteristics	Lake and river types: Thematic lake and river classes and fractional coverages	Boreal-Arctic Wetland and Lake Dataset (Olefelt et al., 2021)
Inland water characteristics	River discharge	(Lin et al., 2019)
	Lake, river and catchment shapefiles	HydroLAKES, HydroRIVERS, HydroBASINS (Lehner and Grill, 2013)
	Gas transfer velocity	(Liu et al., 2022)

453

454 **5 Model development for data-driven upscaling**

455 **5.1 Model selection and set-up**

456 Given the pronounced landscape heterogeneity and resulting data biases described in the
 457 previous section, selecting an appropriate model architecture is a critical next step. The
 458 characteristics and size of the input dataset drive downstream decisions on which modeling
 459 approach and type of machine learning model is appropriate and feasible (see the flowchart in

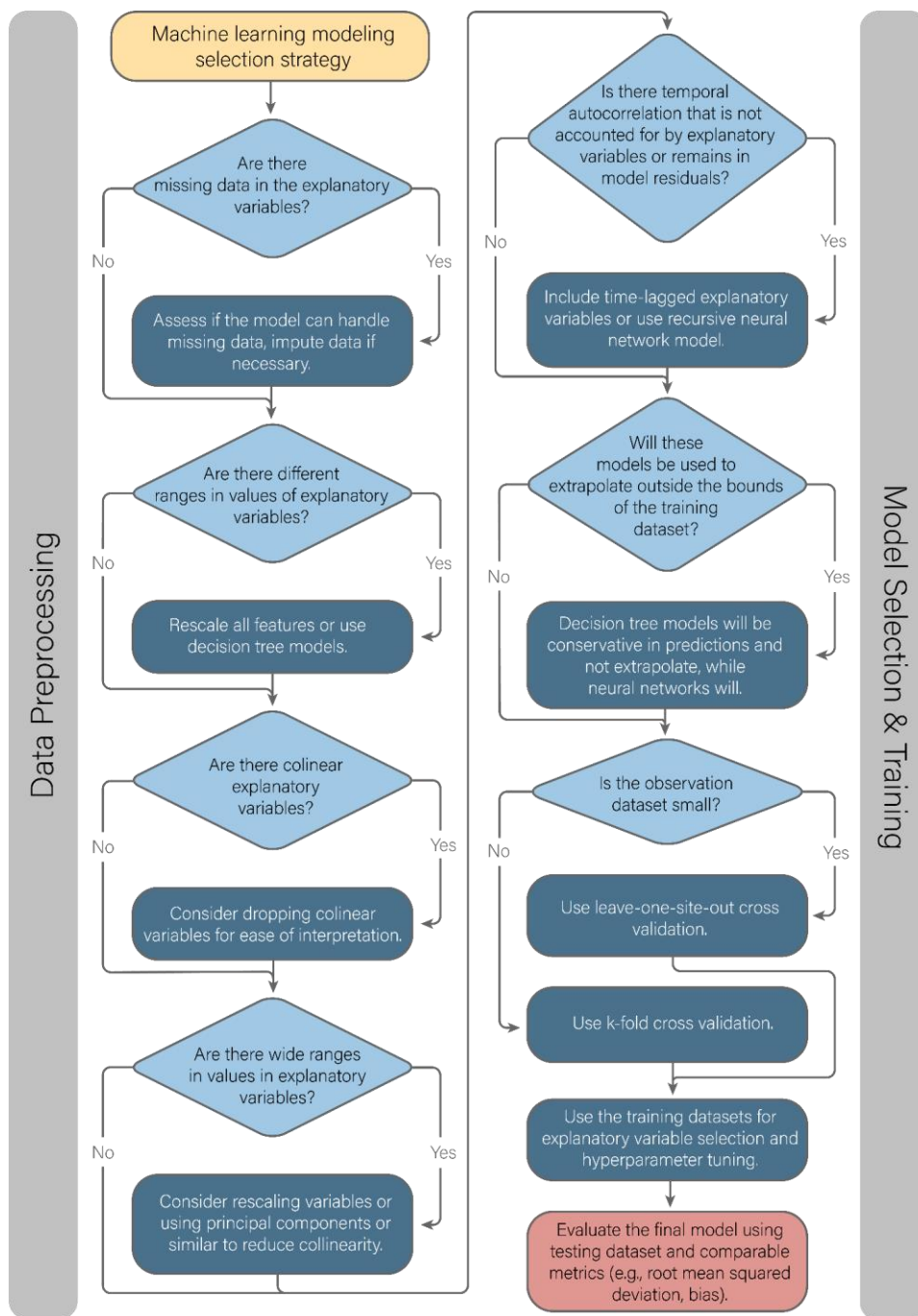
460 figure 3 as one possible approach to decide on a strategy). Complex nonlinear methods such as
461 neural networks (Hochreiter and Schmidhuber, 1997; Jain and Chandrasekaran, 1982; Lipton et
462 al., 2015; Van Der Ploeg et al., 2014) are difficult to construct and computationally intensive,
463 especially when employed with spatial or temporal context, but they excel at handling complex
464 data and have greater ability to extrapolate beyond the normal range of input data. Decision tree-
465 based models (Breiman, 2001; Chen and Guestrin, 2016) offer robustness and scalability, but
466 struggle with extrapolation and tend to produce estimates closer to the mean of training data.
467 However, decision tree models often behave more robustly than neural networks when presented
468 with limited training data (Jiang et al., 2020), which is important in the Arctic-boreal context
469 where training data are sparse. Consequently, the majority of recent upscaling studies exploring
470 carbon budgets at high northern latitudes focused on random forest approaches (Peltola et al.,
471 2019; Ramage et al., 2024; Virkkala et al., 2025a; Yuan et al., 2022). Smaller datasets would
472 preferably be analyzed with simple linear or non-linear regression approaches (e.g. linear mixed-
473 effects models), while simple regional averaging is also a commonly used method.

474 5.2 Data pre-processing

475 Careful pre-processing is critical to ensure that only high-quality data are used in upscaling
476 models. For example, data may need to be standardized or normalized, outliers removed, missing
477 values imputed (i.e., gap-filled), and/or collinearity addressed (see also figure 3). It is critical to
478 consider detailed method procedures, local conditions, and mechanistic understanding behind the
479 flux dynamics when evaluating data quality. Some large fluxes can be event-driven, making
480 “outlier” flux values real and important to keep (e.g. ebullition events), while other outliers can
481 be artifacts. Measurement artifacts (e.g. low turbulence conditions in EC data, low sun angles in
482 remote sensing data, the presence of snow in remote sensing indices) risk propagation to
483 upscaled fluxes if not corrected in quality checks. For missing data, careful imputation may be
484 necessary from a technical standpoint, as some machine learning methods cannot handle data
485 gaps. Even if the chosen upscaling approach can handle gaps, gap-filling may be advisable to
486 ensure the dataset is representative; however, data imputation also holds the potential to
487 introduce new artifacts in the input data or circularity in the modelling approach by common
488 predictor variables in the imputation and model training steps. Therefore, careful consideration

489 should be given to whether/how to impute the data, which method to use, and imputed data
490 should be carefully checked.

491 Scale mismatches between in-situ and associated coarser geospatial data sets may potentially
492 result in dissimilar behavior of the data across scales, and hence between the training and the
493 inference step. This is another potential source of inaccuracies in upscaling studies, and different
494 approaches exist for addressing them. For instance, the global FLUXCOM-X-BASE dataset
495 (Nelson & Walther et al., 2024) uses in-situ meteorological and land cover data, and MODIS
496 remote sensing data for training, which are then upscaled across the globe using corresponding
497 gridded data at a coarser spatial resolution. While this minimizes scale mismatches among
498 predictors and the target variable in training, the distribution in the training data may be different
499 for the same variable in the predictor data and therefore lead to higher uncertainties in the
500 upscaled products. In contrast, other recent efforts have relied solely on gridded data for model
501 training (e.g., Natali & Watts et al., 2019; Rocher-Ros et al., 2023; Virkkala et al., 2025a), thus
502 avoiding the distribution shift at the cost of potentially reduced accuracy of training data at the
503 site level.



504

505 **Figure 3.** Decision flowchart for a potential way forward for selecting an appropriate strategy for
 506 a carbon flux machine learning model. Please note that the outlined selection process focuses on
 507 some core aspects discussed within this overview text and does not aim at being comprehensive.
 508 Accordingly, there are methods that may not be represented here.

509 5.3 Model testing and evaluation: strategies and metrics

510 For the comparatively small datasets that are commonly available for carbon flux upscaling
511 studies, cross validation methods are recommended for this purpose, which involve resampling
512 and sample splitting to use different portions of the available data to validate and train a model.
513 For example, in the global FLUXCOM framework cross validation is done using a ‘X-fold
514 leave-site-out’ strategy (Nelson & Walther et al., 2024). This splits the available data into a
515 number (X) of folds, or groups of sites, iteratively leaves a fold out of model training, and tests
516 model performance at the sites in the fold that has been left out. It is therefore a good measure to
517 test the model’s ability to extrapolate beyond training conditions (Ploton et al., 2020); however,
518 while X-fold leave-site-out would be a gold standard for cross validation, it might not be feasible
519 if categorical predictors (e.g. land cover) include some classes that have very little data, because
520 this can lead to a situation where the training and/or test sets completely lack data from some of
521 the classes (Meyer and Pebesma, 2022).

522 When data are limited, cross-validation approaches based on leaving a smaller part than a fold of
523 the full dataset out for validation have been used, with leave-one-site-out being the most frequent
524 (Virkkala et al., 2021). Other strategies, including leave-X-fold (Natali & Watts et al., 2019),
525 leave-one-observation/row-out, and random k-fold cross validation, may provide overly
526 optimistic model performance estimates (Roberts et al., 2017), not explicitly testing the model’s
527 ability to extrapolate since data from the same site could be included both in the training and
528 validation data. Although the leave-one-site-out approach solves this issue, nearby sites with
529 similar flux dynamics might still be included in training and validation datasets, similarly biasing
530 the performance metrics. To remedy this issue, a spatially blocked cross validation can be used.
531 Instead of relying on site identification as the grouping, this type of validation will block out
532 spatial areas to ensure nearby sites are similarly included in the same groupings (Orndahl et al.,
533 2025; Peltola et al., 2019; Roberts et al., 2017).

534 Acceptable accuracy is identified by good performance in complementary metrics (e.g. bias,
535 RMSE, Nash-Sutcliffe- efficiency, correlation, etc.; Kvalseth, 1985; Nash and Sutcliffe, 1970).
536 These metrics quantify the relationship between the in-situ carbon flux observations and
537 predictions for both the training data *and* the test data which has not been used in training. A

538 model is overfit if model performance is high on the training data but low on the test data.
539 Insufficient performance on both the training and test data indicates an underfit model. Both
540 underfit and overfit models will not be able to extrapolate reliably.

541 In addition, model accuracy may change when analyzed at different levels of temporal
542 aggregation, e.g. using daily, monthly, or intra-annual timesteps (Nelson & Walther et al., 2024;
543 Virkkala et al., 2025a; Ying et al., 2025). For example, assessments consistently show that while
544 dominant intraannual flux patterns can be predicted relatively well, data-driven upscaling often
545 struggles to accurately capture long-term trends and interannual variability. This is mostly linked
546 to the short data time series available, especially for CH₄ and inland water fluxes compared to
547 CO₂ and terrestrial fluxes, respectively. This should be a growing research field as in-situ
548 datasets grow in length and long-term trends can better be addressed with real validation data.

549 Extrapolation into regions that are different from those represented by available data can result in
550 higher model uncertainty and systematic errors. This underscores the importance of a
551 representative distribution of training data – both spatially, temporally, and statistically – for
552 effective upscaling as well as of a thorough quantification of the model representativeness and
553 uncertainty. Transitioning from site level to upscaled flux estimates covering large spatial scales
554 requires researchers to assess the generalizability of the trained model in situations with limited
555 data coverage. Comparison of the range of conditions included in training data with those
556 spanned by the data used in upscaling indicates potential extrapolation areas (Elith et al., 2010;
557 Jung et al., 2020; Meyer and Pebesma, 2021; Pallandt et al., 2024). In the data-poor Arctic-
558 boreal region, extrapolation areas are often extensive (Pallandt et al., 2022), requiring data-
559 driven models to operate well beyond observed environmental conditions. To deal with these
560 errors, researchers may consider carefully utilizing other in-situ datasets for validation (e.g.,
561 chambers over relatively homogenous areas when only EC was used in training data) or
562 comparing results to other modeled products to test agreement. Of course, other modeled
563 products may have their own errors and comparisons should be made here.

564 Finally, cross-comparisons and benchmarking of flux estimates between scaling approaches,
565 including data-driven upscaling, process-based upscaling and atmospheric inversions, are a
566 standard practice; however, drawing conclusions from such is challenging given strong

567 differences in model set-up, training data, and uncertainty estimates (e.g., Bruhwiler et al., 2021;
568 Peltola et al., 2019; Treat et al., 2024; Virkkala et al., 2025a). Further tests for evaluating model
569 fitness include e.g. testing for particularly influential sites or predictors. For instance, earlier
570 upscaling studies have shown that Arctic-boreal CO₂ flux budgets can vary by as much as ±150
571 Tg C yr⁻¹ (approximately ±30% of the total budget) due to relatively minor changes in flux site
572 distribution introduced through bootstrapping (Virkkala et al., 2025a, 2021), or repeated model
573 runs while leaving out some, often random, portion of the data. Regarding predictors, the option
574 to weigh certain observations more than others (e.g., Jung et al., 2020; Pallandt et al., 2024), for
575 example to better capture patterns for a particular carbon species, reproduce extreme events or
576 deal with disproportionate data coverage, should be further explored.

577 6 New insights and future needs

578 6.1 Improvements in data provision

579 The ongoing expansion of in situ flux sites continues to improve spatio-temporal data coverage
580 and has promise to reduce uncertainty (Pallandt et al., 2024, 2022). Still, important gaps in
581 Arctic-boreal data coverage persist, calling for coordination within the research and funding
582 community to upgrade observational capacities (Table 4). Temporal gaps in winter data coverage
583 call for expansion of year-round monitoring sites, which is limited due to the harsh climate in the
584 Arctic-boreal region. Regular maintenance and continuous power pose an enormous challenge
585 outside the growing season, particularly for remote sites. Consequently, the winter observational
586 network lagging behind growing season and the winter network is currently the size the growing
587 season network was 15 years ago (Pallandt et al., 2022); though winters are changing rapidly and
588 are critical for annual carbon budgets (Falvo et al., 2025; Natali & Watts et al., 2019; See et al.,
589 2024). Considerable network gaps exist in Siberia, and the high-Arctic and specific
590 representativeness analysis should be followed if designing a wider flux site network (Pallandt et
591 al., 2022; Schuur et al., 2024).

592 Moreover, current observation sites often are situated in ecosystems with expected high fluxes,
593 such as wetlands for CH₄. Consequently, low-flux ecosystems such as high-Arctic polar deserts
594 and high-altitude alpine ecosystems are under sampled. Even though such ‘cold spots’ likely do

595 not substantially contribute to regional carbon budgets, constraining their carbon fluxes with
596 representative observation sites should reduce uncertainties in upscaling efforts and provide
597 insight into the dynamics of these systems. Finally, limited information is provided on managed
598 ecosystems such as drained peatlands, forests harvested for lumber, and reservoirs which should
599 also be a priority as these are intricately linked parts of the landscape and have direct
600 management implications (e.g., Kim et al., 2016; Korkiakoski et al., 2023; Tikkasalo et al.,
601 2025).

602 To improve the representation of disturbances in models, more advanced geospatial products
603 should be used in models supported by complementary in situ data. Current data-driven models
604 have shown wildfires may have some response to vegetation indices in models given the ties to
605 biomass and greenness (Virkkala et al., 2025a), but more work is needed to properly represent
606 recovery processes common in regrowth following fire. In situ data exists on forest recovery
607 sites, often in a chrono-sequence of time since fire which could be used to inform how models
608 should respond, although these data are sparse (Goulden et al., 2011; Oliveira et al., 2021;
609 Schulze et al., 2025; Ueyama et al., 2019). Permafrost thaw, especially abrupt thaw resulting in
610 active layer detachments and drastic landscape changes, are increasing over the landscape and
611 understanding how they impact fluxes will be crucial with 20% of the permafrost region
612 vulnerable to these types of thaw (Turetsky et al., 2020). Missing predictor datasets from remote
613 sensing for thaw are nearing development at circumpolar scales thanks largely to high-resolution
614 satellite imagery (Nitze et al., 2025) and could be used for a post-hoc estimate of the changing
615 carbon balance due to these features as many are sub-grid cell size (<1 km).

616 Geospatial information on sub-surface parameters including soil properties, moisture levels, and
617 carbon content lack representation in global datasets and thus often result in inaccuracies in the
618 high latitudes. This could be improved with more representative data across the region but also
619 specialized high latitude products could aid in more accurate products as they would be informed
620 by data only from similar ecosystems. Also, a clear definition of uniform formatting rules,
621 including the development of a standardized approach to better harmonize data, could advance
622 the quality of data-driven upscaling products by making products easier to merge and cross
623 compare.

624 New geospatial products require both appropriate thematic resolution (i.e. differentiating
625 between land-covers which have distinct carbon flux magnitudes) and appropriate spatial
626 resolution to avoid issues of mosaic averaging (Hashemi et al., 2025). Robust high-resolution
627 mapping and data would allow better understanding of drivers of carbon fluxes in resultant
628 products, especially for inland water ecosystems where ecosystems can have large impacts on the
629 carbon balance despite or because of their small size (Holgerson and Raymond, 2016). However,
630 thought should be given to what is reasonable given the scale of input data, for example,
631 upscaling carbon fluxes at a one-meter scale using only flux tower data may not be advisable.
632 However, more value could be pulled from flux tower observations by partitioning EC data into
633 flux fingerprints for different land cover types in the footprint (Ludwig et al., 2024; Pirk et al.,
634 2024), in addition to chamber flux observations that cover smaller areas. Moreover, a sufficient
635 number of spatially dispersed and georeferenced in situ measurements should be made around a
636 measurement site's central location (e.g., Siewert, 2018) to appropriately match the chosen grid
637 of the geospatial dataset. These data should be ideally collected according to a standardized
638 protocol and in a manner such that they can be harmonized with the land cover classification
639 scheme used during flux upscaling (Raynolds et al., 2019). To keep heterogeneity of ecosystems
640 and use a coarser scale, more products like BAWLDs approach could be created which have
641 percent landcover breakdowns within coarser 0.25-degree grid cells.

642 6.2 Improvements in data-driven modeling frameworks

643 New statistical data-driven modeling approaches beyond the commonly used random forest
644 models should be tested. Deep learning tools hold the potential to assist in developing fast and
645 efficient models, identifying the best tradeoff between effort and complexity of data-driven
646 modeling frameworks, and accuracy and understandability of novel model output. There are
647 indications that deep learning can partly compensate for missing pieces of information (Kraft et
648 al., 2025). Identifying the most powerful machine learning applications, and customizing and
649 upgrading them to support frameworks for upscaling of carbon fluxes, should therefore be a
650 primary priority for this research community (Lucarini et al., 2024).

651 One major priority is the development of combined machine learning-based estimates for both
652 terrestrial and inland water CO₂ and CH₄ fluxes together, using similar modeling frameworks

653 wherever possible. This would allow for seamless integration across ecosystems, facilitate direct
654 comparisons, and provide a clearer understanding of how different landscapes contribute to the
655 net carbon balance. At the same time, potential biases like the above-mentioned double counting,
656 or pixel edge effects, could be avoided. Spatio-temporally explicit upscaling of lake and river
657 CO₂ fluxes needs special attention, as such data-driven modeling efforts remain rare, and
658 estimates have substantial variability and uncertainties.

659 6.3 Strengthening links between data-driven carbon flux models and 660 other scaling approaches

661 The combined use of data-driven upscaling frameworks with other modeling concepts will
662 advance insights into feedbacks between the carbon cycle and climate change within the Arctic-
663 boreal region. For example, data-driven upscaling outputs can be integrated to model evaluation
664 platforms such as International Land Model Benchmarking (ILAMB) that include statistical
665 analyses and figures designed to provide insights into the strengths and weaknesses of multiple
666 models or model versions (Braghiere et al., 2023; Collier et al., 2018). In addition, data-driven
667 upscaling frameworks hold a strong potential for deriving links between carbon flux processes
668 and control factors that may deviate from functional relationships commonly implemented in
669 process models. Comparing gridded output fluxes between model types (e.g., process-based and
670 data-driven model derived) can reveal such differences, and insights from resulting patterns
671 should be used to upgrade process-based models to subsequently extrapolate such relationships
672 into future climate scenarios.

673 Moreover, spatio-temporally continuous, data-driven estimates of carbon fluxes are highly
674 suitable to serve as priors in atmospheric inverse modeling frameworks. As opposed to coarse-
675 resolution flux grids provided by process-based models, using high-resolution grids from data-
676 driven approaches can help reconcile top-down and bottom-up approaches by reducing biases
677 and improving model convergence. Comparisons between data-driven upscaling and
678 geostatistical inverse modeling (Michalak et al., 2004) offers another promising pathway to
679 reconcile scaling approaches. Geostatistical inversions do not use prior flux fields, but instead
680 they generate these prior patterns from a superposition of geospatial data layers, so-called
681 auxiliary variables. Comparing the choice and weighing of environmental relationships selected

682 to reproduce different carbon observations from very different sources (data-driven upscaling:
683 surface fluxes; atmospheric inversion: atmospheric mixing ratios) offers opportunities to better
684 understand differences in modeling approaches, and the role of environmental predictors in this
685 context. Since inland water carbon flux upscaling outputs may not be spatio-temporally
686 continuous, their usefulness as prior inputs in atmospheric inversions are still limited. As a
687 potential solution, terrestrial and inland water flux fields could be combined into a merged prior
688 flux field for inversions. As a result, comparisons with inversion outputs have largely focused on
689 terrestrial flux estimates, leaving a significant gap in our understanding of the full-system
690 differences across approaches (Bruhwiler et al., 2021; Treat et al., 2024).

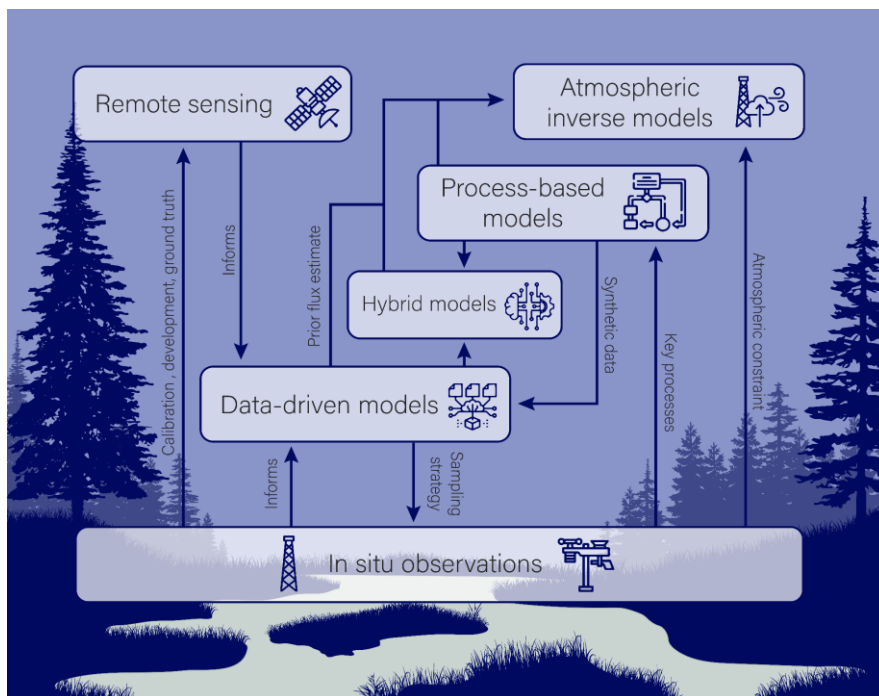
691 Fusing data-driven approaches with process modeling or inverse modeling frameworks holds the
692 potential of maximizing the information gain from diverse databases and thus minimizing output
693 uncertainties. Adding key ecosystem processes from process-based models as additional
694 constraints into machine learning approaches offers a great opportunity to develop hybrid models
695 that can better capture current and future ecosystem dynamics. The combination of the high
696 predictive power of machine learning tools with the mechanistic structure of process-based
697 models can lead to robust estimates of carbon cycle processes across spatial and temporal
698 dimensions (Liu et al., 2024).

699 6.4 Advancing near real-time data integration and upscaling, and 700 fostering collaboration between scientists and modeling approaches

701 The required upgrades in modeling tools and in particular the extension of observational
702 capacities constitute enormous challenges and thus can only be approached in a collaborative
703 manner. To achieve this goal, a continuous exchange of information between the modelling
704 community, field scientists collecting in-situ measurements, and remote sensing specialists
705 developing geospatial data products will be essential. Effective collaboration could help
706 overcome a lack of observational data by allowing the scientific community to maximize
707 currently available information and jointly work on a targeted improvement of the future
708 observational coverage. This includes offering incentives to share new observational datasets in a
709 timely manner to facilitate near real-time data integration products (Falvo et al., 2025), and
710 include efforts by larger networks like the integrated carbon observing system (ICOS) or the

711 National Ecological Observing Network (NEON) which offer near-real time data from many of
712 their observing sites.

713 Enhanced collaboration should include shared field work and field visits between researchers
714 across disciplines to develop an understanding of critical processes and the challenges, benefits,
715 and limitations of field measurements and/or models. Furthermore, there are opportunities to
716 better include and engage local stake- and rights-holders in the design and implementation of
717 observational networks. Discussions on how best to design and manage observational networks
718 should be guided by standardized concepts for environmental monitoring and data processing
719 (e.g., Boike et al., 2022) across scientific and Arctic-boreal communities. There is a need for
720 observational platforms as well as modeling frameworks that could quantify uncertainties in data
721 and model performance and output, and rank sources of uncertainties by their relevance.
722 Information on the impact of missing parameters, uncertainties in provided observational
723 products, and spatial and/or temporal gaps in observational coverage on model performance,
724 could help the observational community upgrade monitoring networks and remote sensing
725 products towards gaining a substantial improvement of upscaling approaches.



726

727 **Figure 4.** The role of data-driven models in understanding Arctic-boreal carbon cycle dynamics.
728 These models can be used to inform other types of models such as process-based models and
729 atmospheric inversions, can inform future in situ sampling strategies.

730 A collaborative data assimilation scheme will leverage a tailored computing infrastructure that
731 facilitates data input across the Arctic-boreal domain in near-real-time. It would also allow
732 researchers to communicate insights such as the impact of an anomalously wet or hot and dry
733 year to policymakers and the public. Such infrastructure would have important societal and
734 climate policy benefits, and could help raise awareness for Arctic climate change, ideally before
735 the worst consequences of climate change are realized. Moreover, these modeling tools would
736 facilitate more accurate reporting of carbon emissions, and help in assessing the impact of
737 potential interventions of climate mitigation (Hugelius et al., 2024). Finally, this infrastructure
738 could be leveraged by researchers to accelerate process-level understanding across multiple
739 disciplines, which in turn can inform process-model development and improvements (Figure 4).

740 There are multiple pathways through which the continued improvement of data-driven upscaling
741 methods contributes to high-latitude carbon cycle science. Given the importance of the Arctic-
742 boreal region in the global carbon budget, and especially how sensitively it will react to climate
743 change in the coming decades, an integration of data-driven methods with other modeling
744 platforms will maximize the use of existing information and reduce associated uncertainties.
745 Furthermore, these integrated methods can provide enhanced and closer to real-time estimates of
746 carbon emissions from the Arctic-boreal region and highlight their relevance to the global
747 climate system to stakeholders. This is foundational to establishing proper baselines with which
748 to develop and demonstrate the efficacy of emission reduction goals.

749 **Table 4.** A summary of key gaps contributing to uncertainties in data-driven carbon flux models and potential solutions.

Theme	Topic	Current status	Potential solutions	Importance (1=highest, 3=lowest)
Carbon Flux	General gaps in CO ₂ and CH ₄ flux data	<ul style="list-style-type: none"> -Data gaps during the non-growing season and in certain regions (Siberia, Canada, high-Arctic and alpine regions) and ecosystems (larch forests, sparsely/barren vegetated ecosystems), and primarily in undisturbed ecosystems -Many chamber datasets are sporadic and limited to daytime measurements 	<ul style="list-style-type: none"> -Establish year-round monitoring sites in these ecosystems and regions -Foster data collection in disturbed ecosystems -Carefully assess the uncertainties related to utilizing different flux measurement techniques in upscaling 	1
	Gaps in terrestrial CO ₂ and CH ₄ flux data	<ul style="list-style-type: none"> -The distribution of year-round long-term CO₂ and CH₄ flux sites is limited -Most CH₄ flux sites are in wetland ecosystems 	<ul style="list-style-type: none"> -Maintain existing flux sites - Coordinate the flux network to target underrepresented regions -Establish CH₄ flux sites in upland ecosystems to avoid observation bias towards high-emitting sites - Sustained and frequent synthesis updates to ensure data are available and public 	2
	Gaps in inland water CO ₂ and CH ₄ flux data	<ul style="list-style-type: none"> - Few long-term observation sites 	<ul style="list-style-type: none"> - Develop new long-term monitoring sites - Collect data during ice-on/ice-off periods 	1

		<ul style="list-style-type: none"> -High variability within and across river networks and individual lakes that is not fully understood -Few measurements from spring ice-break up 	<ul style="list-style-type: none"> - Improve spatial representativeness of sampling within waterbodies - Integrate flux measurements across techniques and emission pathways (e.g., EC vs. other methods, including ebullition) 	
Predictor variables	Uncertain or missing gridded terrestrial predictors	<ul style="list-style-type: none"> - GPP is generally well predicted due to the availability of climate and vegetation-related predictor data - Key predictors for other fluxes (e.g., soil moisture, disturbance, soil carbon, nutrients, ice content, temperature) are often only available at regional scales or coarse spatial resolutions 	<ul style="list-style-type: none"> - Develop remote sensing-based soil datasets with lower uncertainties and improve below ground parameter estimates (e.g., soil properties, moisture, etc.) - Create ongoing disturbance datasets of fires, thaw slumps, insect outbreaks etc. 	2
	Uncertain or missing gridded inland water predictors	<ul style="list-style-type: none"> - Lack of inland water depth and water quality and sediment characteristics - Poor representation of circumpolar seasonal changes in water extent and productivity 	<ul style="list-style-type: none"> -Develop missing predictor datasets -Integrate indices from optical remote sensing to data-driven models 	1
	Land–waterbody type separation	<ul style="list-style-type: none"> - Coarse-resolution wetland and lake classifications across the domain - Lack of high-resolution, intra-annual lake extent datasets 	<ul style="list-style-type: none"> -Use high-resolution satellite data to track dynamic small and seasonal waterbodies - Prefer continuous predictors over categorical - Merge existing higher-resolution regional datasets to harmonize land cover products 	2

	Eddy covariance flux footprint-informed predictor data extraction	<ul style="list-style-type: none"> - Gridded predictors are often extracted from the single pixel containing the flux tower - No accounting for actual flux footprint 	<ul style="list-style-type: none"> - Use site-specific flux footprints to better represent predictor variables where large heterogeneity exists 	3
Modeling resolution	Spatial resolution	<ul style="list-style-type: none"> - Terrestrial CO₂ upscaled at ~1 km - Wetland, lake, and river CH₄ fluxes and river CO₂ fluxes often modeled at 10–50 km - No spatially explicit lake CO₂ flux upscaled outputs 	<ul style="list-style-type: none"> - Improve upscaling to 0.5–1 km resolution across ecosystems - Aim for meter-scale resolution using Landsat, Sentinel, PlanetScope, etc., utilizing chamber data and plot-level data from eddy covariance footprint decomposition 	2
	Temporal resolution	Fluxes are often modeled at monthly or seasonal scales, though some daily outputs are available	<ul style="list-style-type: none"> - Move toward daily resolution to better capture short-term and extreme events 	2
Modeling approaches and performance	Limited diversity in modeling approaches	<ul style="list-style-type: none"> - Most studies rely on random forest models 	<ul style="list-style-type: none"> - Test several types of neural networks (e.g., convolution neural network) and deep learning (e.g. U-net) 	2
	Poor performance for temporal trends	<ul style="list-style-type: none"> - Models perform worse for long-term trends than for mean annual fluxes 	<ul style="list-style-type: none"> - Use time-lagged predictors - Apply recursive neural networks to capture temporal and spatial variability (requires sufficient long-term data) 	1
Model evaluation strategies	Factorial model experiments	<ul style="list-style-type: none"> - Rarely applied in Arctic–boreal context (except for some chamber vs. tower comparisons, e.g., FLUXCOM) 	<ul style="list-style-type: none"> - Apply factorial modeling experiments to systematically test drivers and configurations 	2
	Extrapolation	<ul style="list-style-type: none"> - Area of extrapolation only rarely thoroughly reported and discussed although approaches for such assessment exist 	<ul style="list-style-type: none"> - Adopt standard reporting frameworks, including documentation of extrapolated areas 	1

Uncertainty
evaluation
framework

- Basic approaches (e.g.,
bootstrapping) assess sensitivity to
site distribution and model
structure

- Develop more comprehensive frameworks
incorporating site distribution, model structure
variability, residuals, and measurement
uncertainties for robust and comparable model
evaluations

2

750 7 Conclusion

751 Data-driven upscaling has grown significantly over the past few decades as new technologies, in-situ data collecting techniques and
752 machine learning models have been developed. There is still much to be done to continue to improve modeling techniques and
753 workflows, especially around data collection of both in-situ flux data and gridded products to use for predicting and extrapolating
754 carbon flux estimates. These models are not only useful estimating carbon budgets but can also be useful tools in other modeling types
755 such as informing top-down and process-based bottom-up models and should be integrated into other modeling structures. There is
756 vast potential to significantly improve estimations of carbon fluxes from the Arctic-boreal region at a time when these estimates are
757 crucial to our global climate agreements and continuing to refine our upscaling techniques is a vital tool to meeting climate goals.

758 Acknowledgements

759 This work is the result of a workshop hosted by the Stockholm University and funded with support from the European Space Agency
760 AMPAC-Net project under Grant 4000137912/22/I-DT. GH acknowledges support from the European Union's Horizon Europe
761 Research and Innovation Programme to the ILLUQ project (no. 773421), the ESA RECCAP2 project, the Schmidt Sciences
762 CALIPSO project and the Swedish Research Council VR (no. 2022-04839). AMV, KAA, SNM, BR, MAK, and IW were supported
763 by funding catalyzed through the TED Audacious project (Permafrost Pathways). AB, MG and JV were supported by the European
764 Research Council synergy project Q-Arctic under Grant 951288. MG and JV were supported by the European Commission under the

765 Horizon Europe (GreenFeedback project, grant agreement no. 101056921), MG was further supported by the German Ministry for
766 Research, Technology and Space (MOMENT project, support code 03F0931G). BW was supported by the European Research
767 Council Starting Grant project PRIMETIME (Grant 101039588). FJWP was supported by the Research Council of Norway (Snowless,
768 project no. 352260). EAGS and GF were supported by the Arctic Carbon Warning Network (AWARE) funded by the Minderoo
769 Foundation; LTREB: Renewal Award #2309467; National Science Foundation Bonanza Creek LTER Network, Award #2224776,
770 #1636476; GR-R was supported by the European Union (ERC, ARIMETH, 101161308). SW acknowledges support from the
771 European Space Agency Sen4GPP project under grant 4000134598/21/I-NB. The authors would like to thank Danielle Trangmoe at
772 Woodwell Climate Research Center for detail checks and reviews.

773 Data Availability Statement

774 All data used in this paper are open and free to use. Data created for Figure 1 can be found in the Supplementary Information (SI) in
775 SI Table 1. Data for sites in Figure 2 can be found in Virkkala et al., (2025b); <https://doi.org/10.3334/ORNLDAAAC/2448>. Carbon
776 dioxide upscaled data are from Virkkala et al., (2025a); <https://doi.org/10.3334/ORNLDAAAC/2377>, and methane upscaled data are
777 from Ying et al., (2025); <https://doi.org/10.5281/zenodo.10802153>.

References

- Abatzoglou, J.T., Dobrowski, S.Z., Parks, S.A., Hegewisch, K.C., 2018. TerraClimate, a high-resolution global dataset of monthly climate and climatic water balance from 1958–2015. *Sci. Data* 5, 170191. <https://doi.org/10.1038/sdata.2017.191>
- Amatulli, G., McInerney, D., Sethi, T., Strobl, P., Domisch, S., 2020. Geomorpho90m, empirical evaluation and accuracy assessment of global high-resolution geomorphometric layers. *Sci. Data* 7, 162. <https://doi.org/10.1038/s41597-020-0479-6>
- Arndt, K.A., Hashemi, J., Natali, S.M., Schiferl, L.D., Virkkala, A.-M., 2023. Recent Advances and Challenges in Monitoring and Modeling Non-Growing Season Carbon Dioxide Fluxes from the Arctic Boreal Zone. *Curr. Clim. Change Rep.* 9, 27–40. <https://doi.org/10.1007/s40641-023-00190-4>
- Aubinet, M., Vesala, T., Papale, D. (Eds.), 2012. *Eddy Covariance: A Practical Guide to Measurement and Data Analysis*. Springer Netherlands, Dordrecht. <https://doi.org/10.1007/978-94-007-2351-1>
- Baldocchi, D.D., 2003. Assessing the eddy covariance technique for evaluating carbon dioxide exchange rates of ecosystems: past, present and future. *Glob. Change Biol.* 9, 479–492. <https://doi.org/10.1046/j.1365-2486.2003.00629.x>
- Bartlett, K.B., Harriss, R.C., 1993. Review and assessment of methane emissions from wetlands. *Chemosphere* 26, 261–320. [https://doi.org/10.1016/0045-6535\(93\)90427-7](https://doi.org/10.1016/0045-6535(93)90427-7)
- Bartsch, A., Efimova, A., Widhalm, B., Muri, X., Von Baeckmann, C., Bergstedt, H., Ermokhina, K., Hugelius, G., Heim, B., Leibman, M., 2024. Circumarctic land cover diversity considering wetness gradients. *Hydrol. Earth Syst. Sci.* 28, 2421–2481. <https://doi.org/10.5194/hess-28-2421-2024>
- Bartsch, A., Strozzi, T., Nitze, I., 2023. Permafrost Monitoring from Space. *Surv. Geophys.* 44, 1579–1613. <https://doi.org/10.1007/s10712-023-09770-3>
- Bartsch, A., Tanguy, R., Bergstedt, H., Von Baeckmann, C., Tømmervik, H., Macias-Fauria, M., Lemmetyinen, J., Rautiainen, K., Gruber, C., Forbes, B.C., 2025. Similarities between sea ice area variations and satellite-derived terrestrial biosphere and cryosphere parameters across the Arctic. *The Cryosphere* 19, 4929–4967. <https://doi.org/10.5194/tc-19-4929-2025>
- Bastviken, D., Cole, J., Pace, M., Tranvik, L., 2004. Methane emissions from lakes: Dependence of lake characteristics, two regional assessments, and a global estimate. *Glob. Biogeochem. Cycles* 18, 2004GB002238. <https://doi.org/10.1029/2004GB002238>
- Bastviken, D., Johnson, M.S., 2025. Future methane emissions from lakes and reservoirs. *Nat. Water*. <https://doi.org/10.1038/s44221-025-00532-6>
- Belshe, E.F., Schuur, E.A.G., Bolker, B.M., 2013. Tundra ecosystems observed to be CO₂ sources due to differential amplification of the carbon cycle. *Ecol. Lett.* 16, 1307–1315. <https://doi.org/10.1111/ele.12164>
- Bhuiyan, M.A.E., Witharana, C., Liljedahl, A.K., 2020. Use of Very High Spatial Resolution Commercial Satellite Imagery and Deep Learning to Automatically Map Ice-Wedge

- Polygons across Tundra Vegetation Types. *J. Imaging* 6, 137.
<https://doi.org/10.3390/jimaging6120137>
- Biskaborn, B.K., Smith, S.L., Noetzli, J., Matthes, H., Vieira, G., Streletskiy, D.A., Schoeneich, P., Romanovsky, V.E., Lewkowicz, A.G., Abramov, A., Allard, M., Boike, J., Cable, W.L., Christiansen, H.H., Delaloye, R., Diekmann, B., Drozdov, D., Etzelmüller, B., Grosse, G., Guglielmin, M., Ingeman-Nielsen, T., Isaksen, K., Ishikawa, M., Johansson, M., Johannsson, H., Joo, A., Kaverin, D., Kholodov, A., Konstantinov, P., Kröger, T., Lambiel, C., Lanckman, J.-P., Luo, D., Malkova, G., Meiklejohn, I., Moskalenko, N., Oliva, M., Phillips, M., Ramos, M., Sannel, A.B.K., Sergeev, D., Seybold, C., Skryabin, P., Vasiliev, A., Wu, Q., Yoshikawa, K., Zheleznyak, M., Lantuit, H., 2019. Permafrost is warming at a global scale. *Nat. Commun.* 10, 264. <https://doi.org/10.1038/s41467-018-08240-4>
- Boike, J., Chadburn, S., Martin, J., Zwieback, S., Althuizen, I.H.J., Anselm, N., Cai, L., Coulombe, S., Lee, H., Liljedahl, A.K., Schneebeli, M., Sjöberg, Y., Smith, N., Smith, S.L., Streletskiy, D.A., Stuenzi, S.M., Westermann, S., Wilcox, E.J., 2022. Standardized monitoring of permafrost thaw: a user-friendly, multiparameter protocol. *Arct. Sci.* 8, 153–182. <https://doi.org/10.1139/as-2021-0007>
- Braghiere, R.K., Fisher, J.B., Miner, K.R., Miller, C.E., Worden, J.R., Schimel, D.S., Frankenberg, C., 2023. Tipping point in North American Arctic-Boreal carbon sink persists in new generation Earth system models despite reduced uncertainty. *Environ. Res. Lett.* 18. <https://doi.org/10.1088/1748-9326/acb226>
- Breiman, L., 2001. Random Forests. *Mach. Learn.* 45, 5–32.
<https://doi.org/10.1023/A:1010933404324>
- Briones, V., Genet, H., Jafarov, E.E., Rogers, B.M., Watts, J.D., Virkkala, A.-M., Bartsch, A., Maglio, B.C., Rady, J., Natali, S.M., 2025. Fusing Regional and Global Datasets to Develop a Composite Land Cover Product Across High Latitudes.
<https://doi.org/10.5194/essd-2025-226>
- Bruhwyler, L., Parmentier, F.-J.W., Crill, P., Leonard, M., Palmer, P.I., 2021. The Arctic Carbon Cycle and Its Response to Changing Climate. *Curr. Clim. Change Rep.*
<https://doi.org/10.1007/s40641-020-00169-5>
- Chen, S., Liu, L., Ma, Y., Zhuang, Q., Shurpali, N.J., 2024. Quantifying Global Wetland Methane Emissions With In Situ Methane Flux Data and Machine Learning Approaches. *Earths Future* 12, e2023EF004330. <https://doi.org/10.1029/2023EF004330>
- Chen, T., Guestrin, C., 2016. XGBoost: A Scalable Tree Boosting System, in: *Proceedings of the 22nd ACM SIGKDD International Conference on Knowledge Discovery and Data Mining*. Presented at the KDD '16: The 22nd ACM SIGKDD International Conference on Knowledge Discovery and Data Mining, ACM, San Francisco California USA, pp. 785–794. <https://doi.org/10.1145/2939672.2939785>
- Ciais, P., Bastos, A., Chevallier, F., Lauerwald, R., Poulter, B., Canadell, J.G., Hugelius, G., Jackson, R.B., Jain, A., Jones, M., Kondo, M., Luijkx, I.T., Patra, P.K., Peters, W., Pongratz, J., Petrescu, A.M.R., Piao, S., Qiu, C., Von Randow, C., Regnier, P., Saunois, M., Scholes, R., Shvidenko, A., Tian, H., Yang, H., Wang, X., Zheng, B., 2022. Definitions and methods to estimate regional land carbon fluxes for the second phase of the REgional Carbon Cycle Assessment and Processes Project (RECCAP-2). *Geosci. Model Dev.* 15, 1289–1316. <https://doi.org/10.5194/gmd-15-1289-2022>

- Clelland, A.A., Marshall, G.J., Baxter, R., Potter, S., Talucci, A.C., Rady, J.M., Genet, H., Rogers, B.M., Natali, S.M., 2024. Annual and Seasonal Patterns of Burned Area Products in Arctic-Boreal North America and Russia for 2001–2020. *Remote Sens.* 16, 3306. <https://doi.org/10.3390/rs16173306>
- Collier, N., Hoffman, F.M., Lawrence, D.M., Keppel-Aleks, G., Koven, C.D., Riley, W.J., Mu, M., Randerson, J.T., 2018. The International Land Model Benchmarking (ILAMB) System: Design, Theory, and Implementation. *J. Adv. Model. Earth Syst.* 10, 2731–2754. <https://doi.org/10.1029/2018MS001354>
- Commane, R., Lindaas, J., Benmergui, J., Luus, K.A., Chang, R.Y., Daube, B.C., Euskirchen, E.S., Henderson, J.M., Karion, A., Miller, J.B., Miller, S.M., Parazoo, N.C., Randerson, J.T., Sweeney, C., Tans, P., Thoning, K., Veraverbeke, S., Miller, C.E., Wofsy, S.C., 2017. Carbon dioxide sources from Alaska driven by increasing early winter respiration from Arctic tundra. *Proc Natl Acad Sci U S A* 114, 5361–5366. <https://doi.org/10.1073/pnas.1618567114>
- Copernicus Atmosphere Monitoring Service, 2022. CAMS global biomass burning emissions based on fire radiative power (GFAS). <https://doi.org/10.24381/A05253C7>
- Davidson, S.J., Sloan, V.L., Phoenix, G.K., Wagner, R., Fisher, J.P., Oechel, W.C., Zona, D., 2016. Vegetation Type Dominates the Spatial Variability in CH₄ Emissions Across Multiple Arctic Tundra Landscapes. *Ecosystems* 19, 1116–1132. <https://doi.org/10.1007/s10021-016-9991-0>
- De Eyto, E., Smyth, R.L., Pilla, R.M., Laas, A., Shahabinia, A.R., Baldocchi, A., Desai, A.R., Lupon, A., Lohila, A., Obrador, B., Denfeld, B.A., Carey, C.C., Bastviken, D., Reed, D., Rudberg, D., Rööhm, E., Clayer, F., Weyhenmeyer, G.A., Chmiel, H.E., Grossart, H.P., De Wit, H.A., Kokorite, I., Thrane, J., Bikše, J., Rusak, J.A., Fernández, J.E., Bezerra-Neto, J.F., Brighenti, L.S., Koschorreck, M., Aurela, M., Barros, N., Keller, P.S., Woolway, R.I., Marcé, R., McClure, R.P., Haverinen, S., Juutinen, S., Kosten, S., Sadro, S., Doyle, B.C., 2025. Diel variation in CO₂ flux is substantial in many lakes. *Limnol. Oceanogr. Lett.* 10, 977–989. <https://doi.org/10.1002/lol2.70066>
- De Vrese, P., Georgievski, G., Gonzalez Rouco, J.F., Notz, D., Stacke, T., Steinert, N.J., Wilkenskjeld, S., Brovkin, V., 2023. Representation of soil hydrology in permafrost regions may explain large part of inter-model spread in simulated Arctic and subarctic climate. *The Cryosphere* 17, 2095–2118. <https://doi.org/10.5194/tc-17-2095-2023>
- Denfeld, B.A., Baulch, H.M., Del Giorgio, P.A., Hampton, S.E., Karlsson, J., Stanley, E., Del Giorgio, P., 2018. A synthesis of carbon dioxide and methane dynamics during the ice-covered period of northern lakes. *Limnol. Oceanogr. Lett.* 3. <https://doi.org/10.6073/pasta/8cf05d3ba01b54b6748b5b87caa4c505>
- Didan, K., 2021. MODIS/Terra Vegetation Indices Monthly L3 Global 1km SIN Grid V061. <https://doi.org/10.5067/MODIS/MOD13A3.061>
- DiMiceli, C., Sohlberg, R., Townshend, J., 2022. MODIS/Terra Vegetation Continuous Fields Yearly L3 Global 250m SIN Grid V061. <https://doi.org/10.5067/MODIS/MOD44B.061>
- Dinerstein, E., Olson, D., Joshi, A., Vynne, C., Burgess, N.D., Wikramanayake, E., Hahn, N., Palminteri, S., Hedao, P., Noss, R., Hansen, M., Locke, H., Ellis, E.C., Jones, B., Barber, C.V., Hayes, R., Kormos, C., Martin, V., Crist, E., Sechrest, W., Price, L., Baillie, J.E.M., Weeden, D., Suckling, K., Davis, C., Sizer, N., Moore, R., Thau, D., Birch, T., Potapov, P., Turubanova, S., Tyukavina, A., De Souza, N., Pintea, L., Brito, J.C., Llewellyn, O.A., Miller, A.G., Patzelt, A., Ghazanfar, S.A., Timberlake, J., Klöser, H., Shennan-Farpon,

- Y., Kindt, R., Lillesø, J.-P.B., Van Breugel, P., Graudal, L., Voge, M., Al-Shammari, K.F., Saleem, M., 2017. An Ecoregion-Based Approach to Protecting Half the Terrestrial Realm. *BioScience* 67, 534–545. <https://doi.org/10.1093/biosci/bix014>
- Duncan, B.N., Ott, L.E., Abshire, J.B., Brucker, L., Carroll, M.L., Carton, J., Comiso, J.C., Dinnat, E.P., Forbes, B.C., Gonsamo, A., Gregg, W.W., Hall, D.K., Ialongo, I., Jandt, R., Kahn, R.A., Karpechko, A., Kawa, S.R., Kato, S., Kumpula, T., Kyrölä, E., Loboda, T.V., McDonald, K.C., Montesano, P.M., Nassar, R., Neigh, C.S.R., Parkinson, C.L., Poulter, B., Pulliainen, J., Rautiainen, K., Rogers, B.M., Rousseaux, C.S., Soja, A.J., Steiner, N., Tamminen, J., Taylor, P.C., Tzortziou, M.A., Virta, H., Wang, J.S., Watts, J.D., Winker, D.M., Wu, D.L., 2020. Space-Based Observations for Understanding Changes in the Arctic-Boreal Zone. *Rev. Geophys.* 58. <https://doi.org/10.1029/2019RG000652>
- Ehhalt, D.H., 1974. The atmospheric cycle of methane. *Tellus* 26, 58–70. <https://doi.org/10.1111/j.2153-3490.1974.tb01952.x>
- Elith, J., Kearney, M., Phillips, S., 2010. The art of modelling range-shifting species: *The art of modelling range-shifting species*. *Methods Ecol. Evol.* 1, 330–342. <https://doi.org/10.1111/j.2041-210X.2010.00036.x>
- Erkkilä, K.-M., Ojala, A., Bastviken, D., Biermann, T., Heiskanen, J.J., Lindroth, A., Peltola, O., Rantakari, M., Vesala, T., Mammarella, I., 2018. Methane and carbon dioxide fluxes over a lake: comparison between eddy covariance, floating chambers and boundary layer method. *Biogeosciences* 15, 429–445. <https://doi.org/10.5194/bg-15-429-2018>
- Euskirchen, E.S., Serbin, S.P., Carman, T.B., Fraterrigo, J.M., Genet, H., Iversen, C.M., Salmon, V., McGuire, A.D., 2022. Assessing dynamic vegetation model parameter uncertainty across Alaskan arctic tundra plant communities. *Ecol. Appl.* 32, e2499. <https://doi.org/10.1002/eap.2499>
- Falvo, G., Schuur, E.A.G., Euskirchen, E.S., Natali, S.M., Sonnentag, O., Alcock, H., Arndt, K., Edgar, C., Hould-Gosselin, G., Hung, J., Ledman, J., 2025. Record 2024 winter carbon emissions coincide with record warmth across boreal forest, tundra, and wetland ecosystems. *Environ. Res. Lett.* 20, 114032. <https://doi.org/10.1088/1748-9326/ae09bb>
- Feron, S., Malhotra, A., Bansal, S., Fluet-Chouinard, E., McNicol, G., Knox, S.H., Delwiche, K.B., Cordero, R.R., Ouyang, Z., Zhang, Z., Poulter, B., Jackson, R.B., 2024. Recent increases in annual, seasonal, and extreme methane fluxes driven by changes in climate and vegetation in boreal and temperate wetland ecosystems. *Glob. Change Biol.* 30, e17131. <https://doi.org/10.1111/gcb.17131>
- Fick, S.E., Hijmans, R.J., 2017. WorldClim 2: new 1-km spatial resolution climate surfaces for global land areas. *Int. J. Climatol.* 37, 4302–4315. <https://doi.org/10.1002/joc.5086>
- Gier, B.K., Schlund, M., Friedlingstein, P., Jones, C.D., Jones, C., Zaehle, S., Eyring, V., 2024. Representation of the terrestrial carbon cycle in CMIP6. *Biogeosciences* 21, 5321–5360. <https://doi.org/10.5194/bg-21-5321-2024>
- Giroux-Bougard, X., Fluet-Chouinard, E., Crowley, M.A., Cardille, J.A., Humphries, M.M., 2023. Multi-sensor detection of spring breakup phenology of Canada’s lakes. *Remote Sens. Environ.* 295, 113656. <https://doi.org/10.1016/j.rse.2023.113656>
- Global Modeling And Assimilation Office, Pawson, S., 2015. MERRA-2 tavg1_2d_slv_Nx: 2d,1-Hourly,Time-Averaged,Single-Level,Assimilation,Single-Level Diagnostics V5.12.4. <https://doi.org/10.5067/VJAFPLI1CSIV>

- Golub, M., Koupaei-Abyazani, N., Vesala, T., Mammarella, I., Ojala, A., Bohrer, G., Weyhenmeyer, G.A., Blanken, P.D., Eugster, W., Koebisch, F., Chen, J., Czajkowski, K., Deshmukh, C., Guérin, F., Heiskanen, J., Humphreys, E., Jonsson, A., Karlsson, J., Kling, G., Lee, X., Liu, H., Lohila, A., Lundin, E., Morin, T., Podgrajsek, E., Provenzale, M., Rutgersson, A., Sachs, T., Sahlée, E., Serça, D., Shao, C., Spence, C., Strachan, I.B., Xiao, W., Desai, A.R., 2023. Diel, seasonal, and inter-annual variation in carbon dioxide effluxes from lakes and reservoirs. *Environ. Res. Lett.* 18, 034046. <https://doi.org/10.1088/1748-9326/acb834>
- Golub, M., Thiery, W., Marcé, R., Pierson, D., Vanderkelen, I., Mercado-Bettin, D., Woolway, R.I., Grant, L., Jennings, E., Kraemer, B.M., Schewe, J., Zhao, F., Frieler, K., Mengel, M., Bogomolov, V.Y., Bouffard, D., Côté, M., Couture, R.-M., Debolskiy, A.V., Droppers, B., Gal, G., Guo, M., Janssen, A.B.G., Kirillin, G., Ladwig, R., Magee, M., Moore, T., Perroud, M., Piccolroaz, S., Raaman Vinnaa, L., Schmid, M., Shatwell, T., Stepanenko, V.M., Tan, Z., Woodward, B., Yao, H., Adrian, R., Allan, M., Anneville, O., Arvola, L., Atkins, K., Boegman, L., Carey, C., Christianson, K., De Eyto, E., DeGasperi, C., Grechushnikova, M., Hejzlar, J., Joehnk, K., Jones, I.D., Laas, A., Mackay, E.B., Mammarella, I., Markensten, H., McBride, C., Özkundakci, D., Potes, M., Rinke, K., Robertson, D., Rusak, J.A., Salgado, R., Van Der Linden, L., Verburg, P., Wain, D., Ward, N.K., Wollrab, S., Zdrovennova, G., 2022. A framework for ensemble modelling of climate change impacts on lakes worldwide: the ISIMIP Lake Sector. *Geosci. Model Dev.* 15, 4597–4623. <https://doi.org/10.5194/gmd-15-4597-2022>
- Goulden, M.L., Mcmillan, A.M.S., Winston, G.C., Rocha, A.V., Manies, K.L., Harden, J.W., Bond-Lamberty, B.P., 2011. Patterns of NPP, GPP, respiration, and NEP during boreal forest succession. *Glob. Change Biol.* 17, 855–871. <https://doi.org/10.1111/j.1365-2486.2010.02274.x>
- Griffin, C.G., Finlay, J.C., Brezonik, P.L., Olmanson, L., Hozalski, R.M., 2018. Limitations on using CDOM as a proxy for DOC in temperate lakes. *Water Res.* 144, 719–727. <https://doi.org/10.1016/j.watres.2018.08.007>
- Grosse, G., Romanovsky, V., Jorgenson, T., Anthony, K.W., Brown, J., Overduin, P.P., 2011. Vulnerability and Feedbacks of Permafrost to Climate Change. *Eos Trans. Am. Geophys. Union* 92, 73–74. <https://doi.org/10.1029/2011EO090001>
- Hall, D., Riggs, G., 2021. MODIS/Terra Snow Cover Daily L3 Global 0.05Deg CMG, Version 61. <https://doi.org/10.5067/MODIS/MOD10C1.061>
- Hall, R.O., Ulseth, A.J., 2020. Gas exchange in streams and rivers. *WIREs Water* 7, e1391. <https://doi.org/10.1002/wat2.1391>
- Hashemi, J., Räsänen, A., Virtanen, T., Juutinen, S., Grosse, G., Aurela, M., Bartsch, A., Chasmer, L., Davidson, S.J., Korkiakoski, M., Kuhn, M.A., Lara, M.J., Luoto, M., Niittynen, P., Olefeldt, D., Sonntag, O., Virkkala, A.-M., Voigt, C., Treat, C.C., 2025. Coarse land cover datasets bias Arctic-Boreal wetland methane budgets. *Commun. Earth Environ.* 6, 903. <https://doi.org/10.1038/s43247-025-02963-1>
- Heffernan, L., Estop-Aragonés, C., Kuhn, M.A., Holger-Knorr, K., Olefeldt, D., 2024. Changing climatic controls on the greenhouse gas balance of thermokarst bogs during succession after permafrost thaw. *Glob. Change Biol.* 30, e17388. <https://doi.org/10.1111/gcb.17388>
- Hengl, T., Mendes De Jesus, J., Heuvelink, G.B.M., Ruiperez Gonzalez, M., Kilibarda, M., Blagotić, A., Shangguan, W., Wright, M.N., Geng, X., Bauer-Marschallinger, B., Guevara, M.A., Vargas, R., MacMillan, R.A., Batjes, N.H., Leenaars, J.G.B., Ribeiro, E.,

- Wheeler, I., Mantel, S., Kempen, B., 2017. SoilGrids250m: Global gridded soil information based on machine learning. *PLOS ONE* 12, e0169748. <https://doi.org/10.1371/journal.pone.0169748>
- Hochreiter, S., Schmidhuber, J., 1997. Long Short-Term Memory. *Neural Comput.* 9, 1735–1780. <https://doi.org/10.1162/neco.1997.9.8.1735>
- Högström, E., Bartsch, A., 2017. Impact of Backscatter Variations Over Water Bodies on Coarse-Scale Radar Retrieved Soil Moisture and the Potential of Correcting With Meteorological Data. *IEEE Trans. Geosci. Remote Sens.* 55, 3–13. <https://doi.org/10.1109/TGRS.2016.2530845>
- Högström, E., Heim, B., Bartsch, A., Bergstedt, H., Pointner, G., 2018. Evaluation of a MetOp ASCAT-Derived Surface Soil Moisture Product in Tundra Environments. *J. Geophys. Res. Earth Surf.* 123, 3190–3205. <https://doi.org/10.1029/2018JF004658>
- Holgerson, M.A., Raymond, P.A., 2016. Large contribution to inland water CO₂ and CH₄ emissions from very small ponds. *Nat. Geosci.* 9, 222–226. <https://doi.org/10.1038/ngeo2654>
- Houweling, S., Bergamaschi, P., Chevallier, F., Heimann, M., Kaminski, T., Krol, M., Michalak, A.M., Patra, P., 2017. Global inverse modeling of CH₄ sources and sinks: an overview of methods. *Atmospheric Chem. Phys.* 17, 235–256. <https://doi.org/10.5194/acp-17-235-2017>
- Hugelius, G., Loisel, J., Chadburn, S., Jackson, R.B., Jones, M., Macdonald, G., Marushchak, M., Olefeldt, D., Packalen, M., Siewert, M.B., Treat, C., Turetsky, M., Voigt, C., Yu, Z., 2020. Large stocks of peatland carbon and nitrogen are vulnerable to permafrost thaw. *Proc. Natl. Acad. Sci.* 117. <https://doi.org/10.1073/pnas.1916387117/-/DCSupplemental>
- Hugelius, G., Ramage, J., Burke, E., Chatterjee, A., Smallman, T.L., Aalto, T., Bastos, A., Biasi, C., Canadell, J.G., Chandra, N., Chevallier, F., Ciais, P., Chang, J., Feng, L., Jones, M.W., Kleinen, T., Kuhn, M., Lauerwald, R., Liu, J., López-Blanco, E., Luijkx, I.T., Marushchak, M.E., Natali, S.M., Niwa, Y., Olefeldt, D., Palmer, P.I., Patra, P.K., Peters, W., Potter, S., Poulter, B., Rogers, B.M., Riley, W.J., Saunio, M., Schuur, E.A.G., Thompson, R.L., Treat, C., Tsuruta, A., Turetsky, M.R., Virkkala, A. -M., Voigt, C., Watts, J., Zhu, Q., Zheng, B., 2024. Permafrost Region Greenhouse Gas Budgets Suggest a Weak CO₂ Sink and CH₄ and N₂ O Sources, But Magnitudes Differ Between Top-Down and Bottom-Up Methods. *Glob. Biogeochem. Cycles* 38, e2023GB007969. <https://doi.org/10.1029/2023GB007969>
- Hugelius, G., Strauss, J., Zubrzycki, S., Harden, J.W., Schuur, E.A.G., Ping, C.-L., Schirmer, L., Grosse, G., Michaelson, G.J., Koven, C.D., O'Donnell, J.A., Elberling, B., Mishra, U., Camill, P., Yu, Z., Palmtag, J., Kuhry, P., 2014. Estimated stocks of circumpolar permafrost carbon with quantified uncertainty ranges and identified data gaps. *Biogeosciences* 11, 6573–6593. <https://doi.org/10.5194/bg-11-6573-2014>
- Huntzinger, D.N., Schaefer, K., Schwalm, C., Fisher, J.B., Hayes, D., Stofferahn, E., Carey, J., Michalak, A.M., Wei, Y., Jain, A.K., Kolus, H., Mao, J., Poulter, B., Shi, X., Tang, J., Tian, H., 2020. Evaluation of simulated soil carbon dynamics in Arctic-Boreal ecosystems. *Environ. Res. Lett.* 15, 025005. <https://doi.org/10.1088/1748-9326/ab6784>
- Jain, A.K., Chandrasekaran, B., 1982. 39 Dimensionality and sample size considerations in pattern recognition practice, in: *Handbook of Statistics*. Elsevier, pp. 835–855. [https://doi.org/10.1016/S0169-7161\(82\)02042-2](https://doi.org/10.1016/S0169-7161(82)02042-2)

- Jaynes, D.B., Rogowski, A.S., 1983. Applicability of Fick's Law to Gas Diffusion. *Soil Sci. Soc. Am. J.* 47, 425–430. <https://doi.org/10.2136/sssaj1983.03615995004700030007x>
- Jiang, J., Wang, R., Wang, M., Gao, K., Nguyen, D.D., Wei, G.-W., 2020. Boosting Tree-Assisted Multitask Deep Learning for Small Scientific Datasets. *J. Chem. Inf. Model.* 60, 1235–1244. <https://doi.org/10.1021/acs.jcim.9b01184>
- Jiang, J., Yan, Z., Jian, J., Peng, S., Tian, H., Morris, K.A., Ellam, R.M., Christiansen, J.R., Chen, H., Dong, J., Li, S., Fu, P., Guan, D., Yu, G., Liu, C., Ciais, P., Bond-Lamberty, B., 2025. Global Soil Methane Uptake Estimated by Scaling Up Local Measurements. *Glob. Change Biol.* 31, e70194. <https://doi.org/10.1111/gcb.70194>
- Johnson, M.S., Matthews, E., Du, J., Genovese, V., Bastviken, D., 2022. Methane Emission From Global Lakes: New Spatiotemporal Data and Observation-Driven Modeling of Methane Dynamics Indicates Lower Emissions. *J. Geophys. Res. Biogeosciences* 127, e2022JG006793. <https://doi.org/10.1029/2022JG006793>
- Jung, M., Schwalm, C., Migliavacca, M., Walther, S., Camps-Valls, G., Koirala, S., Anthoni, P., Besnard, S., Bodesheim, P., Carvalhais, N., Chevallier, F., Gans, F., Goll, D.S., Haverd, V., Köhler, P., Ichii, K., Jain, A.K., Liu, J., Lombardozzi, D., Nabel, J.E.M.S., Nelson, J.A., O'Sullivan, M., Pallandt, M., Papale, D., Peters, W., Pongratz, J., Rödenbeck, C., Sitch, S., Tramontana, G., Walker, A., Weber, U., Reichstein, M., 2020. Scaling carbon fluxes from eddy covariance sites to globe: synthesis and evaluation of the FLUXCOM approach. *Biogeosciences* 17, 1343–1365. <https://doi.org/10.5194/bg-17-1343-2020>
- Juutinen, S., Aurela, M., Tuovinen, J.-P., Ivakhov, V., Linkosalmi, M., Räsänen, A., Virtanen, T., Mikola, J., Nyman, J., Vähä, E., Loskutova, M., Makshtas, A., Laurila, T., 2022. Variation in CO₂ and CH₄ fluxes among land cover types in heterogeneous Arctic tundra in northeastern Siberia. *Biogeosciences* 19, 3151–3167. <https://doi.org/10.5194/bg-19-3151-2022>
- Karlsson, J., Giesler, R., Persson, J., Lundin, E., 2013. High emission of carbon dioxide and methane during ice thaw in high latitude lakes. *Geophys. Res. Lett.* 40, 1123–1127. <https://doi.org/10.1002/grl.50152>
- Kemppinen, J., Niittynen, P., Rissanen, T., Tyystjärvi, V., Aalto, J., Luoto, M., 2023. Soil Moisture Variations From Boreal Forests to the Tundra. *Water Resour. Res.* 59, e2022WR032719. <https://doi.org/10.1029/2022WR032719>
- Kim, Y., Kimball, J.S., Glassy, J., Du, J., 2017. An extended global Earth system data record on daily landscape freeze–thaw status determined from satellite passive microwave remote sensing. *Earth Syst. Sci. Data* 9, 133–147. <https://doi.org/10.5194/essd-9-133-2017>
- Kim, Y., Roulet, N.T., Li, C., Frohling, S., Strachan, I.B., Peng, C., Teodoru, C.R., Prairie, Y.T., Tremblay, A., 2016. Simulating carbon dioxide exchange in boreal ecosystems flooded by reservoirs. *Ecol. Model.* 327, 1–17. <https://doi.org/10.1016/j.ecolmodel.2016.01.006>
- Klaus, M., Vachon, D., 2020. Challenges of predicting gas transfer velocity from wind measurements over global lakes. *Aquat. Sci.* 82, 53. <https://doi.org/10.1007/s00027-020-00729-9>
- Kleinen, T., Gromov, S., Steil, B., Brovkin, V., 2021. Atmospheric methane underestimated in future climate projections. *Environ. Res. Lett.* 16, 094006. <https://doi.org/10.1088/1748-9326/ac1814>
- Kling, G.W., Kipphut, G.W., Miller, M.C., 1992. The flux of CO₂ and CH₄ from lakes and rivers in arctic Alaska. *Hydrobiologia* 240, 23–36. <https://doi.org/10.1007/BF00013449>

- Knox, S.H., Jackson, R.B., Poulter, B., McNicol, G., Fluet-Chouinard, E., Zhang, Z., Hugelius, G., Bousquet, P., Canadell, J.G., Saunois, M., Papale, D., Chu, H., Keenan, T.F., Baldocchi, D., Torn, M.S., Mammarella, I., Trotta, C., Aurela, M., Bohrer, G., Campbell, D.I., Cescatti, A., Chamberlain, S., Chen, J., Chen, W., Dengel, S., Desai, A.R., Euskirchen, E., Friborg, T., Gasbarra, D., Goded, I., Goeckede, M., Heimann, M., Helbig, M., Hirano, T., Hollinger, D.Y., Iwata, H., Kang, M., Klatt, J., Krauss, K.W., Kutzbach, L., Lohila, A., Mitra, B., Morin, T.H., Nilsson, M.B., Niu, S., Noormets, A., Oechel, W.C., Peichl, M., Peltola, O., Reba, M.L., Richardson, A.D., Runkle, B.R.K., Ryu, Y., Sachs, T., Schäfer, K.V.R., Schmid, H.P., Shurpali, N., Sonnentag, O., Tang, A.C.I., Ueyama, M., Vargas, R., Vesala, T., Ward, E.J., Windham-Myers, L., Wohlfahrt, G., Zona, D., 2019. FLUXNET-CH₄ Synthesis Activity: Objectives, Observations, and Future Directions. *Bull. Am. Meteorol. Soc.* 100, 2607–2632.
<https://doi.org/10.1175/bams-d-18-0268.1>
- Korkiakoski, M., Ojanen, P., Tuovinen, J.-P., Minkkinen, K., Nevalainen, O., Penttilä, T., Aurela, M., Laurila, T., Lohila, A., 2023. Partial cutting of a boreal nutrient-rich peatland forest causes radically less short-term on-site CO₂ emissions than clear-cutting. *Agric. For. Meteorol.* 332, 109361. <https://doi.org/10.1016/j.agrformet.2023.109361>
- Kraft, B., Nelson, J.A., Walther, S., Gans, F., Weber, U., Duveiller, G., Reichstein, M., Zhang, W., Rußwurm, M., Tuia, D., Körner, M., Hamdi, Z., Jung, M., 2025. On the added value of sequential deep learning for the upscaling of evapotranspiration. *Biogeosciences* 22, 3965–3987. <https://doi.org/10.5194/bg-22-3965-2025>
- Kuhn, M., Olefeldt, D., Arndt, K.A., Bastviken, D., Bruhwiler, L., Crill, P., DelSontro, T., Fluet-Chouinard, E., Grosse, G., Hovemyr, M., Hugelius, G., MacIntyre, S., Malhotra, A., McGuire, A.D., Oh, Y., Poulter, B., Treat, C.C., Turetsky, M.R., Varner, R.K., Walter Anthony, K.M., Watts, J.D., Zhang, Z., 2025. Current and future methane emissions from boreal-Arctic wetlands and lakes. *Nat. Clim. Change* 15, 986–991.
<https://doi.org/10.1038/s41558-025-02413-y>
- Kuhn, M.A., Varner, R.K., Bastviken, D., Crill, P., MacIntyre, S., Turetsky, M., Walter Anthony, K., McGuire, A.D., Olefeldt, D., 2021. BAWLD-CH₄: a comprehensive dataset of methane fluxes from boreal and arctic ecosystems. *Earth Syst. Sci. Data* 13, 5151–5189. <https://doi.org/10.5194/essd-13-5151-2021>
- Kutser, T., Pierson, D.C., Kallio, K.Y., Reinart, A., Sobek, S., 2005. Mapping lake CDOM by satellite remote sensing. *Remote Sens. Environ.* 94, 535–540.
<https://doi.org/10.1016/j.rse.2004.11.009>
- Kvalseth, T.O., 1985. Cautionary Note about R². *Am. Stat.* 39, 279.
<https://doi.org/10.2307/2683704>
- Kwon, M.J., Natali, S.M., Hicks Pries, C.E., Schuur, E.A.G., Steinhof, A., Crummer, K.G., Zimov, N., Zimov, S.A., Heimann, M., Kolle, O., Goeckede, M., 2019. Drainage enhances modern soil carbon contribution but reduces old soil carbon contribution to ecosystem respiration in tundra ecosystems. *Glob. Change Biol.* 25, 1315–1325.
<https://doi.org/10.1111/gcb.14578>
- Kyzivat, E.D., Smith, L.C., 2023. A Closer Look at the Effects of Lake Area, Aquatic Vegetation, and Double-Counted Wetlands on Pan-Arctic Lake Methane Emissions Estimates. *Geophys. Res. Lett.* 50, e2023GL104825.
<https://doi.org/10.1029/2023GL104825>

- Lakshmi, V., Fang, B., 2023. SMAP-Derived 1-km Downscaled Surface Soil Moisture Product, Version 1. <https://doi.org/10.5067/U8QZ2AXE5V7B>
- Lapierre, J., Del Giorgio, P.A., 2012. Geographical and environmental drivers of regional differences in the lake p CO₂ versus DOC relationship across northern landscapes. *J. Geophys. Res. Biogeosciences* 117, 2012JG001945. <https://doi.org/10.1029/2012JG001945>
- Lara, M.J., McGuire, A.D., Euskirchen, E.S., Genet, H., Yi, S., Rutter, R., Iversen, C., Sloan, V., Wullschleger, S.D., 2020. Local-scale Arctic tundra heterogeneity affects regional-scale carbon dynamics. *Nat. Commun.* 11, 4925. <https://doi.org/10.1038/s41467-020-18768-z>
- Lauerwald, R., Allen, G.H., Deemer, B.R., Liu, S., Maavara, T., Raymond, P., Alcott, L., Bastviken, D., Hastie, A., Holgerson, M.A., Johnson, M.S., Lehner, B., Lin, P., Marzadri, A., Ran, L., Tian, H., Yang, X., Yao, Y., Regnier, P., 2023. Inland Water Greenhouse Gas Budgets for RECCAP2: 2. Regionalization and Homogenization of Estimates. *Glob. Biogeochem. Cycles* 37, e2022GB007658. <https://doi.org/10.1029/2022GB007658>
- Lehner, B., Anand, M., Fluet-Chouinard, E., Tan, F., Aires, F., Allen, G.H., Bousquet, P., Canadell, J.G., Davidson, N., Ding, M., Finlayson, C.M., Gumbrecht, T., Hilarides, L., Hugelius, G., Jackson, R.B., Korver, M.C., Liu, L., McIntyre, P.B., Nagy, S., Olefeldt, D., Pavelsky, T.M., Pekel, J.-F., Poulter, B., Prigent, C., Wang, J., Worthington, T.A., Yamazaki, D., Zhang, X., Thieme, M., 2025. Mapping the world's inland surface waters: an upgrade to the Global Lakes and Wetlands Database (GLWD v2). *Earth Syst. Sci. Data* 17, 2277–2329. <https://doi.org/10.5194/essd-17-2277-2025>
- Lehner, B., Grill, G., 2013. Global river hydrography and network routing: baseline data and new approaches to study the world's large river systems. *Hydrol. Process.* 27, 2171–2186. <https://doi.org/10.1002/hyp.9740>
- Lin, P., Pan, M., Beck, H.E., Yang, Y., Yamazaki, D., Frasson, R., David, C.H., Durand, M., Pavelsky, T.M., Allen, G.H., Gleason, C.J., Wood, E.F., 2019. Global Reconstruction of Naturalized River Flows at 2.94 Million Reaches. *Water Resour. Res.* 55, 6499–6516. <https://doi.org/10.1029/2019WR025287>
- Lipton, Z.C., Berkowitz, J., Elkan, C., 2015. A Critical Review of Recurrent Neural Networks for Sequence Learning. <https://doi.org/10.48550/ARXIV.1506.00019>
- Liu, L., Zhou, W., Guan, K., Peng, B., Xu, S., Tang, J., Zhu, Q., Till, J., Jia, X., Jiang, C., Wang, S., Qin, Z., Kong, H., Grant, R., Mezbahuddin, S., Kumar, V., Jin, Z., 2024. Knowledge-guided machine learning can improve carbon cycle quantification in agroecosystems. *Nat. Commun.* 15. <https://doi.org/10.1038/s41467-023-43860-5>
- Liu, S., Kuhn, C., Amatulli, G., Aho, K., Butman, D.E., Allen, G.H., Lin, P., Pan, M., Yamazaki, D., Brinkerhoff, C., Gleason, C., Xia, X., Raymond, P.A., 2022. The importance of hydrology in routing terrestrial carbon to the atmosphere via global streams and rivers. *Proc. Natl. Acad. Sci.* 119, e2106322119. <https://doi.org/10.1073/pnas.2106322119>
- Loescher, H.W., Vargas, R., Mirtl, M., Morris, B., Pauw, J., Yu, X., Kutsch, W., Mabee, P., Tang, J., Ruddell, B.L., Pulsifer, P., Bäck, J., Zacharias, S., Grant, M., Feig, G., Zhang, L., Waldmann, C., Genazzio, M.A., 2022. Building a Global Ecosystem Research Infrastructure to Address Global Grand Challenges for Macrosystem Ecology. *Earths Future* 10, e2020EF001696. <https://doi.org/10.1029/2020EF001696>
- Lucarini, A., Cascio, M.L., Marras, S., Sirca, C., Spano, D., 2024. Artificial intelligence and Eddy covariance: A review. *Sci. Total Environ.* 950, 175406. <https://doi.org/10.1016/j.scitotenv.2024.175406>

- Ludwig, S.M., Natali, S.M., Mann, P.J., Schade, J.D., Holmes, R.M., Powell, M., Fiske, G., Commane, R., 2022. Using Machine Learning to Predict Inland Aquatic CO₂ and CH₄ Concentrations and the Effects of Wildfires in the Yukon-Kuskokwim Delta, Alaska. *Glob. Biogeochem. Cycles* 36. <https://doi.org/10.1029/2021GB007146>
- Ludwig, S.M., Natali, S.M., Schade, J.D., Powell, M., Fiske, G., Schiferl, L.D., Commane, R., 2023. Scaling waterbody carbon dioxide and methane fluxes in the arctic using an integrated terrestrial-aquatic approach. *Environ. Res. Lett.* 18, 064019. <https://doi.org/10.1088/1748-9326/acd467>
- Ludwig, S.M., Schiferl, L., Hung, J., Natali, S.M., Commane, R., 2024. Resolving heterogeneous fluxes from tundra halves the growing season carbon budget. *Biogeosciences* 21, 1301–1321. <https://doi.org/10.5194/bg-21-1301-2024>
- Luoju, K., Pulliainen, J., Takala, M., Lemmetyinen, J., Mortimer, C., Derksen, C., Mudryk, L., Moisander, M., Hiltunen, M., Smolander, T., Ikonen, J., Cohen, J., Salminen, M., Norberg, J., Veijola, K., Venäläinen, P., 2021. GlobSnow v3.0 Northern Hemisphere snow water equivalent dataset. *Sci. Data* 8, 163. <https://doi.org/10.1038/s41597-021-00939-2>
- Matthews, E., Fung, I., 1987. Methane emission from natural wetlands: Global distribution, area, and environmental characteristics of sources. *Glob. Biogeochem. Cycles* 1, 61–86. <https://doi.org/10.1029/GB001i001p00061>
- Matthews, E., Johnson, M.S., Genovese, V., Du, J., Bastviken, D., 2020. Methane emission from high latitude lakes: methane-centric lake classification and satellite-driven annual cycle of emissions. *Sci. Rep.* 10, 12465. <https://doi.org/10.1038/s41598-020-68246-1>
- Mavrovic, A., Sonnentag, O., Voigt, C., Lemmetyinen, J., Aurela, M., Roy, A., 2025. Winter Methane Fluxes Over Boreal and Arctic Environments. *Geophys. Res. Lett.* 52, e2025GL118367. <https://doi.org/10.1029/2025GL118367>
- McGuire, A.D., Christensen, T.R., Hayes, D., Heroult, A., Euskirchen, E., Kimball, J.S., Koven, C., Laflour, P., Miller, P.A., Oechel, W., Peylin, P., Williams, M., Yi, Y., 2012. An assessment of the carbon balance of Arctic tundra: comparisons among observations, process models, and atmospheric inversions. *Biogeosciences* 9, 3185–3204. <https://doi.org/10.5194/bg-9-3185-2012>
- McNicol, G., Fluet-Chouinard, E., Ouyang, Z., Knox, S., Zhang, Z., Aalto, T., Bansal, S., Chang, K., Chen, M., Delwiche, K., Feron, S., Goeckede, M., Liu, J., Malhotra, A., Melton, J.R., Riley, W., Vargas, R., Yuan, K., Ying, Q., Zhu, Q., Alekseychik, P., Aurela, M., Billesbach, D.P., Campbell, D.I., Chen, J., Chu, H., Desai, A.R., Euskirchen, E., Goodrich, J., Griffis, T., Helbig, M., Hirano, T., Iwata, H., Jurasinski, G., King, J., Koebisch, F., Kolka, R., Krauss, K., Lohila, A., Mammarella, I., Nilson, M., Noormets, A., Oechel, W., Peichl, M., Sachs, T., Sakabe, A., Schulze, C., Sonnentag, O., Sullivan, R.C., Tuittila, E., Ueyama, M., Vesala, T., Ward, E., Wille, C., Wong, G.X., Zona, D., Windham-Myers, L., Poulter, B., Jackson, R.B., 2023. Upscaling Wetland Methane Emissions From the FLUXNET-CH₄ Eddy Covariance Network (UpCH₄ v1.0): Model Development, Network Assessment, and Budget Comparison. *AGU Adv.* 4, e2023AV000956. <https://doi.org/10.1029/2023AV000956>
- Meredith, M., Sommerkorn, M., Cassotta, S., Derksen, C., Ekaykin, A., Hollowed, A., Kofinas, G., Mackintosh, A., Melbourne-Thomas, J., Muelbert, M.M.C., Ottersen, G., Pritchard, H., Schuur, E.A.G., 2019. Polar Regions, in: Pörtner, H.-O., Roberts, D.C., Masson-Delmotte, V., Zhai, P., Tignor, M., Poloczanska, E., Mintenbeck, K., Alegria, A., Nicolai,

- M., Okem, A., Petzold, J., Rama, B. (Eds.), IPCC Special Report on the Ocean and Cryosphere in a Changing Climate. Cambridge University Press, Cambridge, UK and New York, NY, USA, pp. 203–320. <https://doi.org/10.1017/9781009157964.005>
- Messenger, M.L., Lehner, B., Grill, G., Nedeva, I., Schmitt, O., 2016. Estimating the volume and age of water stored in global lakes using a geo-statistical approach. *Nat. Commun.* 7, 13603. <https://doi.org/10.1038/ncomms13603>
- Metcalfe, D.B., Hermans, T.D.G., Ahlstrand, J., Becker, M., Berggren, M., Björk, R.G., Björkman, M.P., Blok, D., Chaudhary, N., Chisholm, C., Classen, A.T., Hasselquist, N.J., Jonsson, M., Kristensen, J.A., Kumordzi, B.B., Lee, H., Mayor, J.R., Prevéy, J., Pantazatou, K., Rousk, J., Sponseller, R.A., Sundqvist, M.K., Tang, J., Uddling, J., Wallin, G., Zhang, W., Ahlström, A., Tenenbaum, D.E., Abdi, A.M., 2018. Patchy field sampling biases understanding of climate change impacts across the Arctic. *Nat. Ecol. Evol.* 2, 1443–1448. <https://doi.org/10.1038/s41559-018-0612-5>
- Mevenkamp, H., Wunderling, N., Bhatt, U., Carman, T., Friedemann Donges, J., Genet, H., Serbin, S., Winkelmann, R., Susanne Euskirchen, E., 2023. Reducing uncertainty of high-latitude ecosystem models through identification of key parameters. *Environ. Res. Lett.* 18, 084032. <https://doi.org/10.1088/1748-9326/ace637>
- Meyer, H., Pebesma, E., 2022. Machine learning-based global maps of ecological variables and the challenge of assessing them. *Nat. Commun.* 13, 2208. <https://doi.org/10.1038/s41467-022-29838-9>
- Meyer, H., Pebesma, E., 2021. Predicting into unknown space? Estimating the area of applicability of spatial prediction models. *Methods Ecol. Evol.* 12, 1620–1633. <https://doi.org/10.1111/2041-210X.13650>
- Michalak, A.M., Bruhwiler, L., Tans, P.P., 2004. A geostatistical approach to surface flux estimation of atmospheric trace gases. *J. Geophys. Res. Atmospheres* 109, 2003JD004422. <https://doi.org/10.1029/2003JD004422>
- Mishra, U., Hugelius, G., Shelef, E., Yang, Y., Strauss, J., Lupachev, A., Harden, J.W., Jastrow, J.D., Ping, C.-L., Riley, W.J., Schuur, E.A.G., Matamala, R., Siewert, M., Nave, L.E., Koven, C.D., Fuchs, M., Palmtag, J., Kuhry, P., Treat, C.C., Zubrzycki, S., Hoffman, F.M., Elberling, B., Camill, P., Veremeeva, A., Orr, A., 2021. Spatial heterogeneity and environmental predictors of permafrost region soil organic carbon stocks. *Sci. Adv.* 7, eaaz5236. <https://doi.org/10.1126/sciadv.aaz5236>
- Mu, C., Li, K., Liu, S., Wei, Y., Mu, M., Shang, X., Liu, F., Zhang, C., Liu, H., Gao, T., Song, C., Zhang, L., Karlsson, J., 2025. Recent intensified riverine CO₂ emission across the Northern Hemisphere permafrost region. *Nat. Commun.* 16, 3616. <https://doi.org/10.1038/s41467-025-58716-3>
- Mullen, A.L., Watts, J.D., Rogers, B.M., Carroll, M.L., Elder, C.D., Noomah, J., Williams, Z., Caraballo-Vega, J.A., Bredder, A., Rickenbaugh, E., Levenson, E., Cooley, S.W., Hung, J.K.Y., Fiske, G., Potter, S., Yang, Y., Miller, C.E., Natali, S.M., Douglas, T.A., Kyzivat, E.D., 2023. Using High-Resolution Satellite Imagery and Deep Learning to Track Dynamic Seasonality in Small Water Bodies. *Geophys. Res. Lett.* 50, e2022GL102327. <https://doi.org/10.1029/2022GL102327>
- Muñoz-Sabater, J., Dutra, E., Agustí-Panareda, A., Albergel, C., Arduini, G., Balsamo, G., Boussetta, S., Choulga, M., Harrigan, S., Hersbach, H., Martens, B., Miralles, D.G., Piles, M., Rodríguez-Fernández, N.J., Zsoter, E., Buontempo, C., Thépaut, J.-N., 2021. ERA5-

- Land: a state-of-the-art global reanalysis dataset for land applications. *Earth Syst. Sci. Data* 13, 4349–4383. <https://doi.org/10.5194/essd-13-4349-2021>
- Munson, M.A., 2012. A study on the importance of and time spent on different modeling steps. *ACM SIGKDD Explor. Newsl.* 13, 65–71. <https://doi.org/10.1145/2207243.2207253>
- Muster, S., Riley, W.J., Roth, K., Langer, M., Cresto Aleina, F., Koven, C.D., Lange, S., Bartsch, A., Grosse, G., Wilson, C.J., Jones, B.M., Boike, J., 2019. Size Distributions of Arctic Waterbodies Reveal Consistent Relations in Their Statistical Moments in Space and Time. *Front. Earth Sci.* 7, 5. <https://doi.org/10.3389/feart.2019.00005>
- Nash, J.E., Sutcliffe, J.V., 1970. River flow forecasting through conceptual models part I — A discussion of principles. *J. Hydrol.* 10, 282–290. [https://doi.org/10.1016/0022-1694\(70\)90255-6](https://doi.org/10.1016/0022-1694(70)90255-6)
- Natali, S.M., Holdren, J.P., Rogers, B.M., Treharne, R., Duffy, P.B., Pomerance, R., MacDonald, E., 2021. Permafrost carbon feedbacks threaten global climate goals. *Proc. Natl. Acad. Sci.* 118, e2100163118. <https://doi.org/10.1073/pnas.2100163118>
- Natali, S.M., Watts, J.D., Rogers, B.M., Potter, S., Ludwig, S.M., Selbmann, A.-K., Sullivan, P.F., Abbott, B.W., Arndt, K.A., Birch, L., Björkman, M.P., Bloom, A.A., Celis, G., Christensen, T.R., Christiansen, C.T., Commane, R., Cooper, E.J., Crill, P., Czimczik, C., Davydov, S., Du, J., Egan, J.E., Elberling, B., Euskirchen, E.S., Friborg, T., Genet, H., Göckede, M., Goodrich, J.P., Grogan, P., Helbig, M., Jafarov, E.E., Jastrow, J.D., Kalhori, A.A.M., Kim, Y., Kimball, J.S., Kutzbach, L., Lara, M.J., Larsen, K.S., Lee, B.-Y., Liu, Z., Lorant, M.M., Lund, M., Lupascu, M., Madani, N., Malhotra, A., Matamala, R., McFarland, J., McGuire, A.D., Michelsen, A., Minions, C., Oechel, W.C., Olefeldt, D., Parmentier, F.-J.W., Pirk, N., Poulter, B., Quinton, W., Rezanezhad, F., Risk, D., Sachs, T., Schaefer, K., Schmidt, N.M., Schuur, E.A.G., Semenchuk, P.R., Shaver, G., Sonntag, O., Starr, G., Treat, C.C., Waldrop, M.P., Wang, Y., Welker, J., Wille, C., Xu, X., Zhang, Z., Zhuang, Q., Zona, D., 2019. Large loss of CO₂ in winter observed across the northern permafrost region. *Nat. Clim. Change* 9, 852–857. <https://doi.org/10.1038/s41558-019-0592-8>
- Natchimuthu, S., Sundgren, I., Gålfalk, M., Klemetsson, L., Crill, P., Danielsson, Å., Bastviken, D., 2016. Spatio-temporal variability of lake CH₄ fluxes and its influence on annual whole lake emission estimates. *Limnol. Oceanogr.* 61. <https://doi.org/10.1002/lno.10222>
- Nelson, J.A., Walther, S., Gans, F., Kraft, B., Weber, U., Novick, K., Buchmann, N., Migliavacca, M., Wohlfahrt, G., Šigut, L., Ibrom, A., Papale, D., Göckede, M., Duveiller, G., Knohl, A., Hörtnagl, L., Scott, R.L., Zhang, W., Hamdi, Z.M., Reichstein, M., Aranda-Barranco, S., Ardö, J., Op De Beeck, M., Billdesbach, D., Bowling, D., Bracho, R., Brümmner, C., Camps-Valls, G., Chen, S., Cleverly, J.R., Desai, A., Dong, G., El-Madany, T.S., Euskirchen, E.S., Feigenwinter, I., Galvagno, M., Gerosa, G., Gielen, B., Godeed, I., Goslee, S., Gough, C.M., Heinesch, B., Ichii, K., Jackowicz-Korczynski, M.A., Klosterhalfen, A., Knox, S., Kobayashi, H., Kohonen, K.-M., Korkiakoski, M., Mammarella, I., Mana, G., Marzuoli, R., Matamala, R., Metzger, S., Montagnani, L., Nicolini, G., O’Halloran, T., Ourcival, J.-M., Peichl, M., Pendall, E., Ruiz Reverter, B., Roland, M., Sabbatini, S., Sachs, T., Schmidt, M., Schwalm, C.R., Shekhar, A., Silberstein, R., Silveira, M.L., Spano, D., Tagesson, T., Tramontana, G., Trotta, C., Turco, F., Vesala, T., Vincke, C., Vitale, D., Vivoni, E.R., Wang, Y., Woodgate, W., Yopez, E.A., Zhang, J., Zona, D., Jung, M., 2024. X-BASE: the first terrestrial carbon

- and water flux products from an extended data-driven scaling framework, FLUXCOM-X. <https://doi.org/10.5194/egusphere-2024-165>
- Nitze, I., Heidler, K., Nesterova, N., Küpper, J., Schütt, E., Hölzer, T., Barth, S., Lara, M.J., Liljedahl, A.K., Grosse, G., 2025. DARTS: Multi-year database of AI-detected retrogressive thaw slumps in the circum-arctic permafrost region. *Sci. Data* 12, 1512. <https://doi.org/10.1038/s41597-025-05810-2>
- Obu, J., Westermann, S., Bartsch, A., Berdnikov, N., Christiansen, H.H., Dashtseren, A., Delaloye, R., Elberling, B., Etzelmüller, B., Kholodov, A., Khomutov, A., Kääh, A., Leibman, M.O., Lewkowicz, A.G., Panda, S.K., Romanovsky, V., Way, R.G., Westergaard-Nielsen, A., Wu, T., Yamkhin, J., Zou, D., 2019. Northern Hemisphere permafrost map based on TTOP modelling for 2000–2016 at 1 km² scale. *Earth-Sci. Rev.* 193, 299–316. <https://doi.org/10.1016/j.earscirev.2019.04.023>
- Oechel, W.C., Hastings, S.J., Vourlitis, G., Jenkins, M., Riechers, G., Grulke, N., 1993. Recent change of Arctic tundra ecosystems from a net carbon dioxide sink to a source. *Nature* 361, 520–523. <https://doi.org/10.1038/361520a0>
- Oechel, W.C., Laskowski, C.A., Burba, G., Gioli, B., Kalhori, A.A.M., 2014. Annual patterns and budget of CO₂ flux in an Arctic tussock tundra ecosystem. *J. Geophys. Res. Biogeosciences* 119, 323–339. <https://doi.org/10.1002/2013JG002431>
- Oh, Y., Zhuang, Q., Liu, L., Welp, L.R., Lau, M.C.Y., Onstott, T.C., Medvigy, D., Bruhwiler, L., Dlugokencky, E.J., Hugelius, G., D’Imperio, L., Elberling, B., 2020. Reduced net methane emissions due to microbial methane oxidation in a warmer Arctic. *Nat. Clim. Change* 10, 317–321. <https://doi.org/10.1038/s41558-020-0734-z>
- Olefeldt, D., Hovemyr, M., Kuhn, M.A., Bastviken, D., Bohn, T.J., Connolly, J., Crill, P., Euskirchen, E.S., Finkelstein, S.A., Genet, H., Grosse, G., Harris, L.I., Heffernan, L., Helbig, M., Hugelius, G., Hutchins, R., Juutinen, S., Lara, M.J., Malhotra, A., Manies, K., McGuire, A.D., Natali, S.M., O’Donnell, J.A., Parmentier, F.-J.W., Räsänen, A., Schädel, C., Sonntag, O., Strack, M., Tank, S.E., Treat, C., Varner, R.K., Virtanen, T., Warren, R.K., Watts, J.D., 2021. The Boreal–Arctic Wetland and Lake Dataset (BAWLD). *Earth Syst. Sci. Data* 13, 5127–5149. <https://doi.org/10.5194/essd-13-5127-2021>
- Oliveira, B.R.F., Schaller, C., Jacob Keizer, J., Foken, T., 2021. Estimating immediate post-fire carbon fluxes using the eddy-covariance technique. *Biogeosciences* 18, 285–302. <https://doi.org/10.5194/bg-18-285-2021>
- O’Neill, H.B., Wolfe, S.A., Duchesne, C., 2019. New ground ice maps for Canada using a paleogeographic modelling approach. *The Cryosphere* 13, 753–773. <https://doi.org/10.5194/tc-13-753-2019>
- Orndahl, K.M., Berner, L.T., Macander, M.J., Arndal, M.F., Alexander, H.D., Humphreys, E.R., Loranty, M.M., Ludwig, S.M., Nyman, J., Juutinen, S., Aurela, M., Mikola, J., Mack, M.C., Rose, M., Vankoughnett, M.R., Iversen, C.M., Kumar, J., Salmon, V.G., Yang, D., Grogan, P., Danby, R.K., Scott, N.A., Olofsson, J., Siewert, M.B., Deschamps, L., Maire, V., Lévesque, E., Gauthier, G., Boudreau, S., Gaspard, A., Bret-Harte, M.S., Reynolds, M.K., Walker, D.A., Michelsen, A., Kumpula, T., Villoslada, M., Yläne, H., Luoto, M., Virtanen, T., Greaves, H.E., Forbes, B.C., Heim, R.J., Hölzel, N., Epstein, H., Bunn, A.G., Holmes, R.M., Natali, S.M., Virkkala, A.-M., Goetz, S.J., 2025. Next generation Arctic vegetation maps: Aboveground plant biomass and woody dominance mapped at

- 30 m resolution across the tundra biome. *Remote Sens. Environ.* 323, 114717.
<https://doi.org/10.1016/j.rse.2025.114717>
- Pallandt, M.M.T.A., Jung, M., Arndt, K., Natali, S.M., Rogers, B.M., Virkkala, A., Göckede, M., 2024. High-Latitude Eddy Covariance Temporal Network Design and Optimization. *J. Geophys. Res. Biogeosciences* 129, e2024JG008406.
<https://doi.org/10.1029/2024JG008406>
- Pallandt, M.M.T.A., Kumar, J., Mauritz, M., Schuur, E.A.G., Virkkala, A.-M., Celis, G., Hoffman, F.M., Göckede, M., 2022. Representativeness assessment of the pan-Arctic eddy covariance site network and optimized future enhancements. *Biogeosciences* 19, 559–583. <https://doi.org/10.5194/bg-19-559-2022>
- Palmtag, J., Obu, J., Kuhry, P., Richter, A., Siewert, M.B., Weiss, N., Westermann, S., Hugelius, G., 2022. A high-spatial resolution soil carbon and nitrogen dataset for the northern permafrost region, based on circumpolar land cover upscaling.
<https://doi.org/10.5194/essd-2022-8>
- Parmentier, F.-J.W., Thornton, B.F., Silyakova, A., Christensen, T.R., 2024. Vulnerability of Arctic-Boreal methane emissions to climate change. *Front. Environ. Sci.* 12, 1460155.
<https://doi.org/10.3389/fenvs.2024.1460155>
- Parmentier, F.J.W., Van Huissteden, J., Van Der Molen, M.K., Schaepman-Strub, G., Karsanaev, S.A., Maximov, T.C., Dolman, A.J., 2011. Spatial and temporal dynamics in eddy covariance observations of methane fluxes at a tundra site in northeastern Siberia. *J. Geophys. Res.* 116, G03016. <https://doi.org/10.1029/2010JG001637>
- Pastorello, G., Trotta, C., Canfora, E., Chu, H., Christianson, D., Cheah, Y.-W., Poindexter, C., Chen, J., Elbashandy, A., Humphrey, M., Isaac, P., Polidori, D., Reichstein, M., Ribeca, A., Van Ingen, C., Vuichard, N., Zhang, L., Amiro, B., Ammann, C., Arain, M.A., Ardö, J., Arkebauer, T., Arndt, S.K., Arriga, N., Aubinet, M., Aurela, M., Baldocchi, D., Barr, A., Beamesderfer, E., Marchesini, L.B., Bergeron, O., Beringer, J., Bernhofer, C., Berveiller, D., Billesbach, D., Black, T.A., Blanken, P.D., Bohrer, G., Boike, J., Bolstad, P.V., Bonal, D., Bonnefond, J.-M., Bowling, D.R., Bracho, R., Brodeur, J., Brümmer, C., Buchmann, N., Burban, B., Burns, S.P., Buysse, P., Cale, P., Cavagna, M., Cellier, P., Chen, S., Chini, I., Christensen, T.R., Cleverly, J., Collalti, A., Consalvo, C., Cook, B.D., Cook, D., Coursolle, C., Cremonese, E., Curtis, P.S., D’Andrea, E., Da Rocha, H., Dai, X., Davis, K.J., Cinti, B.D., Grandcourt, A.D., Ligne, A.D., De Oliveira, R.C., Delpierre, N., Desai, A.R., Di Bella, C.M., Tommasi, P.D., Dolman, H., Domingo, F., Dong, G., Dore, S., Duce, P., Dufrière, E., Dunn, A., Dušek, J., Eamus, D., Eichelmann, U., ElKhidir, H.A.M., Eugster, W., Ewenz, C.M., Ewers, B., Famulari, D., Fares, S., Feigenwinter, I., Feitz, A., Fensholt, R., Filippa, G., Fischer, M., Frank, J., Galvagno, M., Gharun, M., Gianelle, D., Gielen, B., Gioli, B., Gitelson, A., Goded, I., Goeckede, M., Goldstein, A.H., Gough, C.M., Goulden, M.L., Graf, A., Griebel, A., Gruening, C., Grünwald, T., Hammerle, A., Han, S., Han, X., Hansen, B.U., Hanson, C., Hatakka, J., He, Y., Hehn, M., Heinesch, B., Hinko-Najera, N., Hörtnagl, L., Hutley, L., Ibrom, A., Ikawa, H., Jackowicz-Korczynski, M., Janouš, D., Jans, W., Jassal, R., Jiang, S., Kato, T., Khomik, M., Klatt, J., Knohl, A., Knox, S., Kobayashi, H., Koerber, G., Kolle, O., Kosugi, Y., Kotani, A., Kowalski, A., Kruijt, B., Kurbatova, J., Kutsch, W.L., Kwon, H., Launiainen, S., Laurila, T., Law, B., Leuning, R., Li, Yingnian, Liddell, M., Limousin, J.-M., Lion, M., Liska, A.J., Lohila, A., López-Ballesteros, A., López-Blanco, E., Loubet, B., Loustau, D., Lucas-Moffat, A., Lüers, J., Ma, S., Macfarlane, C., Magliulo, V., Maier,

- R., Mammarella, I., Manca, G., Marcolla, B., Margolis, H.A., Marras, S., Massman, W., Mastepanov, M., Matamala, R., Matthes, J.H., Mazzenga, F., McCaughey, H., McHugh, I., McMillan, A.M.S., Merbold, L., Meyer, W., Meyers, T., Miller, S.D., Minerbi, S., Moderow, U., Monson, R.K., Montagnani, L., Moore, C.E., Moors, E., Moreaux, V., Moureaux, C., Munger, J.W., Nakai, T., Neiryneck, J., Nesic, Z., Nicolini, G., Noormets, A., Northwood, M., Noretto, M., Nouvellon, Y., Novick, K., Oechel, W., Olesen, J.E., Ourcival, J.-M., Papuga, S.A., Parmentier, F.-J., Paul-Limoges, E., Pavelka, M., Peichl, M., Pendall, E., Phillips, R.P., Pilegaard, K., Pirk, N., Posse, G., Powell, T., Prasse, H., Prober, S.M., Rambal, S., Rannik, Ü., Raz-Yaseef, N., Rebmann, C., Reed, D., Dios, V.R.D., Restrepo-Coupe, N., Reverter, B.R., Roland, M., Sabbatini, S., Sachs, T., Saleska, S.R., Sánchez-Cañete, E.P., Sanchez-Mejia, Z.M., Schmid, H.P., Schmidt, M., Schneider, K., Schrader, F., Schroder, I., Scott, R.L., Sedlák, P., Serrano-Ortiz, P., Shao, C., Shi, P., Shironya, I., Siebicke, L., Šigut, L., Silberstein, R., Sirca, C., Spano, D., Steinbrecher, R., Stevens, R.M., Sturtevant, C., Suyker, A., Tagesson, T., Takanashi, S., Tang, Y., Tapper, N., Thom, J., Tomassucci, M., Tuovinen, J.-P., Urbanski, S., Valentini, R., Van Der Molen, M., Van Gorsel, E., Van Huissteden, K., Varlagin, A., Verfaillie, J., Vesala, T., Vincke, C., Vitale, D., Vygodskaya, N., Walker, J.P., Walter-Shea, E., Wang, H., Weber, R., Westermann, S., Wille, C., Wofsy, S., Wohlfahrt, G., Wolf, S., Woodgate, W., Li, Yuelin, Zampedri, R., Zhang, J., Zhou, G., Zona, D., Agarwal, D., Biraud, S., Torn, M., Papale, D., 2020. The FLUXNET2015 dataset and the ONEFlux processing pipeline for eddy covariance data. *Sci. Data* 7, 225. <https://doi.org/10.1038/s41597-020-0534-3>
- Peltola, O., Vesala, T., Gao, Y., Rätty, O., Alekseychik, P., Aurela, M., Chojnicki, B., Desai, A.R., Dolman, A.J., Euskirchen, E.S., Friborg, T., Göckede, M., Helbig, M., Humphreys, E., Jackson, R.B., Jocher, G., Joos, F., Klatt, J., Knox, S.H., Kowalska, N., Kutzbach, L., Lienert, S., Lohila, A., Mammarella, I., Nadeau, D.F., Nilsson, M.B., Oechel, W.C., Peichl, M., Pypker, T., Quinton, W., Rinne, J., Sachs, T., Samson, M., Schmid, H.P., Sonntag, O., Wille, C., Zona, D., Aalto, T., 2019. Monthly gridded data product of northern wetland methane emissions based on upscaling eddy covariance observations. *Earth Syst. Sci. Data* 11, 1263–1289. <https://doi.org/10.5194/essd-11-1263-2019>
- Phoenix, G.K., Bjerke, J.W., Björk, R.G., Blok, D., Bryn, A., Callaghan, T.V., Christiansen, C.T., Cunliffe, A.M., Davidson, S.J., Epstein, H.E., Loranty, M.M., Martin, A.C., Myers-Smith, I.H., Olofsson, J., Parker, T.C., Parmentier, F.-J.W., Stordal, F., Treharne, R., Tømmervik, H., Voigt, C., 2025. Browning events in Arctic ecosystems: Diverse causes with common consequences. *PLOS Clim.* 4, e0000570. <https://doi.org/10.1371/journal.pclm.0000570>
- Pirk, N., Aalstad, K., Mannerfelt, E.S., Clayer, F., De Wit, H., Christiansen, C.T., Althuizen, I., Lee, H., Westermann, S., 2024. Disaggregating the Carbon Exchange of Degrading Permafrost Peatlands Using Bayesian Deep Learning. *Geophys. Res. Lett.* 51, e2024GL109283. <https://doi.org/10.1029/2024GL109283>
- Ploton, P., Mortier, F., Réjou-Méchain, M., Barbier, N., Picard, N., Rossi, V., Dormann, C., Cornu, G., Viennois, G., Bayol, N., Lyapustin, A., Gourlet-Fleury, S., Péliissier, R., 2020. Spatial validation reveals poor predictive performance of large-scale ecological mapping models. *Nat. Commun.* 11, 4540. <https://doi.org/10.1038/s41467-020-18321-y>
- Podgrajsek, E., Sahlée, E., Rutgersson, A., 2014. Diurnal cycle of lake methane flux. *J. Geophys. Res. Biogeosciences* 119, 236–248. <https://doi.org/10.1002/2013JG002327>

- Poggio, L., De Sousa, L.M., Batjes, N.H., Heuvelink, G.B.M., Kempen, B., Ribeiro, E., Rossiter, D., 2021. SoilGrids 2.0: producing soil information for the globe with quantified spatial uncertainty. *SOIL* 7, 217–240. <https://doi.org/10.5194/soil-7-217-2021>
- Pulliainen, J., Aurela, M., Aalto, T., Böttcher, K., Cohen, J., Derksen, C., Heimann, M., Helbig, M., Kolari, P., Kontu, A., Krasnova, A., Launiainen, S., Lemmetyinen, J., Lindqvist, H., Lindroth, A., Lohila, A., Luojus, K., Mammarella, I., Markkanen, T., Nevala, E., Noe, S., Peichl, M., Pumpanen, J., Rautiainen, K., Salminen, M., Sonnentag, O., Takala, M., Thum, T., Vesala, T., Vestin, P., 2024. Increase in gross primary production of boreal forests balanced out by increase in ecosystem respiration. *Remote Sens. Environ.* 313, 114376. <https://doi.org/10.1016/j.rse.2024.114376>
- Ramage, J., Kuhn, M., Virkkala, A., Voigt, C., Marushchak, M.E., Bastos, A., Biasi, C., Canadell, J.G., Ciais, P., López-Blanco, E., Natali, S.M., Olefeldt, D., Potter, S., Poulter, B., Rogers, B.M., Schuur, E.A.G., Treat, C., Turetsky, M.R., Watts, J., Hugelius, G., 2024. The Net GHG Balance and Budget of the Permafrost Region (2000–2020) From Ecosystem Flux Upscaling. *Glob. Biogeochem. Cycles* 38, e2023GB007953. <https://doi.org/10.1029/2023GB007953>
- Räsänen, A., Manninen, T., Korkiakoski, M., Lohila, A., Virtanen, T., 2021. Predicting catchment-scale methane fluxes with multi-source remote sensing. *Landsc. Ecol.* 36, 1177–1195. <https://doi.org/10.1007/s10980-021-01194-x>
- Rasilo, T., Prairie, Y.T., Del Giorgio, P.A., 2015. Large-scale patterns in summer diffusive CH₄ fluxes across boreal lakes, and contribution to diffusive C emissions. *Glob. Change Biol.* 21, 1124–1139. <https://doi.org/10.1111/gcb.12741>
- Raymond, P.A., Hartmann, J., Lauerwald, R., Sobek, S., McDonald, C., Hoover, M., Butman, D., Striegl, R., Mayorga, E., Humborg, C., Kortelainen, P., Dürr, H., Meybeck, M., Ciais, P., Guth, P., 2013. Global carbon dioxide emissions from inland waters. *Nature* 503, 355–359. <https://doi.org/10.1038/nature12760>
- Raymond, P.A., Zappa, C.J., Butman, D., Bott, T.L., Potter, J., Mulholland, P., Laursen, A.E., McDowell, W.H., Newbold, D., 2012. Scaling the gas transfer velocity and hydraulic geometry in streams and small rivers. *Limnol. Oceanogr. Fluids Environ.* 2, 41–53. <https://doi.org/10.1215/21573689-1597669>
- Raynolds, M.K., Walker, D.A., Balsler, A., Bay, C., Campbell, M., Cherosov, M.M., Daniëls, F.J.A., Eidesen, P.B., Ermokhina, K.A., Frost, G.V., Jedrzejek, B., Jorgenson, M.T., Kennedy, B.E., Kholod, S.S., Lavrinenko, I.A., Lavrinenko, O.V., Magnússon, B., Matveyeva, N.V., Metúsalemsson, S., Nilsen, L., Olthof, I., Pospelov, I.N., Pospelova, E.B., Pouliot, D., Razzhivin, V., Schaepman-Strub, G., Šibík, J., Telyatnikov, M.Yu., Troeva, E., 2019. A raster version of the Circumpolar Arctic Vegetation Map (CAVM). *Remote Sens. Environ.* 232, 111297. <https://doi.org/10.1016/j.rse.2019.111297>
- Rinne, J., Riutta, T., Pihlatie, M., Aurela, M., Haapanala, S., Tuovinen, J.-P., Tuittila, E.-S., Vesala, T., 2007. Annual cycle of methane emission from a boreal fen measured by the eddy covariance technique. *Tellus B Chem. Phys. Meteorol.* 59, 449. <https://doi.org/10.1111/j.1600-0889.2007.00261.x>
- Roberts, D.R., Bahn, V., Ciuti, S., Boyce, M.S., Elith, J., Guillera-Aroita, G., Hauenstein, S., Lahoz-Monfort, J.J., Schröder, B., Thuiller, W., Warton, D.I., Wintle, B.A., Hartig, F., Dormann, C.F., 2017. Cross-validation strategies for data with temporal, spatial, hierarchical, or phylogenetic structure. *Ecography* 40, 913–929. <https://doi.org/10.1111/ecog.02881>

- Rocher-Ros, G., Stanley, E.H., Loken, L.C., Casson, N.J., Raymond, P.A., Liu, S., Amatulli, G., Sponseller, R.A., 2023. Global methane emissions from rivers and streams. *Nature* 621, 530–535. <https://doi.org/10.1038/s41586-023-06344-6>
- Rödenbeck, C., Zaehle, S., Keeling, R., Heimann, M., 2018. History of El Niño impacts on the global carbon cycle 1957–2017: a quantification from atmospheric CO₂ data. *Philos. Trans. R. Soc. B Biol. Sci.* 373, 20170303. <https://doi.org/10.1098/rstb.2017.0303>
- Rosentreter, J.A., Borges, A.V., Deemer, B.R., Holgerson, M.A., Liu, S., Song, C., Melack, J., Raymond, P.A., Duarte, C.M., Allen, G.H., Olefeldt, D., Poulter, B., Battin, T.I., Eyre, B.D., 2021. Half of global methane emissions come from highly variable aquatic ecosystem sources. *Nat. Geosci.* 14, 225–230. <https://doi.org/10.1038/s41561-021-00715-2>
- Runge, A., Nitze, I., Grosse, G., 2022. Remote sensing annual dynamics of rapid permafrost thaw disturbances with LandTrendr. *Remote Sens. Environ.* 268, 112752. <https://doi.org/10.1016/j.rse.2021.112752>
- Schädel, C., Rogers, B.M., Lawrence, D.M., Koven, C.D., Brovkin, V., Burke, E.J., Genet, H., Huntzinger, D.N., Jafarov, E., McGuire, A.D., Riley, W.J., Natali, S.M., 2024. Earth system models must include permafrost carbon processes. *Nat. Clim. Change* 14, 114–116. <https://doi.org/10.1038/s41558-023-01909-9>
- Schulze, C., Sonntag, O., Emmerton, C.A., Harris, L., Alcock, H., Marouelli, K., Hould Gosselin, G., Knox, S.H., Howard, R., Skeeter, J., Moore, P., Nesic, Z., Olefeldt, D., 2025. Large Carbon Losses From Burned Permafrost Peatlands During Post-Fire Succession. *Geophys. Res. Lett.* 52, e2025GL118344. <https://doi.org/10.1029/2025GL118344>
- Schuur, E.A.G., Abbott, B.W., Commane, R., Ernakovich, J., Euskirchen, E., Hugelius, G., Grosse, G., Jones, M., Koven, C., Leshyk, V., Lawrence, D., Loranty, M.M., Mauritz, M., Olefeldt, D., Natali, S., Rodenhizer, H., Salmon, V., Schädel, C., Strauss, J., Treat, C., Turetsky, M., 2022. Permafrost and Climate Change: Carbon Cycle Feedbacks From the Warming Arctic. *Annu. Rev. Environ. Resour.* 47, 343–371. <https://doi.org/10.1146/annurev-environ-012220-011847>
- Schuur, E.A.G., Mack, M.C., 2018. Ecological Response to Permafrost Thaw and Consequences for Local and Global Ecosystem Services. *Annu. Rev. Ecol. Evol. Syst.* 49, 279–301. <https://doi.org/10.1146/annurev-ecolsys-121415-032349>
- Schuur, E.A.G., Pallandt, M., Göckede, M., 2024. Russian collaboration loss risks permafrost carbon emissions network. *Nat. Clim. Change* 14, 410–411. <https://doi.org/10.1038/s41558-024-02001-6>
- Sebacher, D.I., Harriss, R.C., Bartlett, K.B., Sebacher, S.M., Grice, S.S., 1986. Atmospheric methane sources: Alaskan tundra bogs, an alpine fen, and a subarctic boreal marsh. *Tellus B* 38B, 1–10. <https://doi.org/10.1111/j.1600-0889.1986.tb00083.x>
- See, C.R., Virkkala, A.-M., Natali, S.M., Rogers, B.M., Mauritz, M., Biasi, C., Bokhorst, S., Boike, J., Bret-Harte, M.S., Celis, G., Chae, N., Christensen, T.R., Murner, S.J., Dengel, S., Dolman, H., Edgar, C.W., Elberling, B., Emmerton, C.A., Euskirchen, E.S., Göckede, M., Grelle, A., Heffernan, L., Helbig, M., Holl, D., Humphreys, E., Iwata, H., Järveoja, J., Kobayashi, H., Kochendorfer, J., Kolari, P., Kotani, A., Kutzbach, L., Kwon, M.J., Lathrop, E.R., López-Blanco, E., Mammarella, I., Marushchak, M.E., Mastepanov, M., Matsuura, Y., Merbold, L., Meyer, G., Minions, C., Nilsson, M.B., Nojeim, J., Oberbauer, S.F., Olefeldt, D., Park, S.-J., Parmentier, F.-J.W., Peichl, M., Peter, D.,

- Petrov, R., Poyatos, R., Prokushkin, A.S., Quinton, W., Rodenhizer, H., Sachs, T., Savage, K., Schulze, C., Sjögersten, S., Sonnentag, O., St. Louis, V.L., Torn, M.S., Tuittila, E.-S., Ueyama, M., Varlagin, A., Voigt, C., Watts, J.D., Zona, D., Zyryanov, V.I., Schuur, E.A.G., 2024. Decadal increases in carbon uptake offset by respiratory losses across northern permafrost ecosystems. *Nat. Clim. Change* 14, 853–862. <https://doi.org/10.1038/s41558-024-02057-4>
- Sieczko, A.K., Duc, N.T., Schenk, J., Pajala, G., Rudberg, D., Sawakuchi, H.O., Bastviken, D., 2020. Diel variability of methane emissions from lakes. *Proc. Natl. Acad. Sci.* 117, 21488–21494. <https://doi.org/10.1073/pnas.2006024117>
- Siewert, M.B., 2018. High-resolution digital mapping of soil organic carbon in permafrost terrain using machine learning: a case study in a sub-Arctic peatland environment. *Biogeosciences* 15, 1663–1682. <https://doi.org/10.5194/bg-15-1663-2018>
- Sø, J.S., Sand-Jensen, K., Martinsen, K.T., Polauke, E., Kjær, J.E., Reitzel, K., Kragh, T., 2023. Methane and carbon dioxide fluxes at high spatiotemporal resolution from a small temperate lake. *Sci. Total Environ.* 878, 162895. <https://doi.org/10.1016/j.scitotenv.2023.162895>
- Song, C., Liu, S., Wang, G., Zhang, L., Rosentreter, J.A., Zhao, G., Sun, X., Yao, Y., Mu, C., Sun, S., Hu, Z., Lin, S., Sun, J., Li, Yang, Wang, Y., Li, Yuhao, Raymond, P.A., Karlsson, J., 2024. Inland water greenhouse gas emissions offset the terrestrial carbon sink in the northern cryosphere. *Sci. Adv.* 10, eadp0024. <https://doi.org/10.1126/sciadv.adp0024>
- Stanley, E.H., Casson, N.J., Christel, S.T., Crawford, J.T., Loken, L.C., Oliver, S.K., 2016. The ecology of methane in streams and rivers: patterns, controls, and global significance. *Ecol. Monogr.* 86, 146–171. <https://doi.org/10.1890/15-1027>
- Stanley, E.H., Loken, L.C., Casson, N.J., Oliver, S.K., Sponseller, R.A., Wallin, M.B., Zhang, L., Rocher-Ros, G., 2023. GRiMeDB: the Global River Methane Database of concentrations and fluxes. *Earth Syst. Sci. Data* 15, 2879–2926. <https://doi.org/10.5194/essd-15-2879-2023>
- Subke, J.-A., Kutzbach, L., Risk, D., 2021. Soil Chamber Measurements, in: Foken, T. (Ed.), *Springer Handbook of Atmospheric Measurements*, Springer Handbooks. Springer International Publishing, Cham, pp. 1603–1624. https://doi.org/10.1007/978-3-030-52171-4_60
- Suni, T., Rinne, J., Reissell, A., Altimir, N., Keronen, P., Rannik, Ü., Maso, M.D., Kulmala, M., Vesala, T., 2003. Long-term measurements of surface fluxes above a Scots pine forest in Hyttiälä, southern Finland, 1996–2001 287–301.
- Tan, Z., Zhuang, Q., 2015. Methane emissions from pan-Arctic lakes during the 21st century: An analysis with process-based models of lake evolution and biogeochemistry. *J. Geophys. Res. Biogeosciences* 120, 2641–2653. <https://doi.org/10.1002/2015JG003184>
- Thornton, B.F., Wik, M., Crill, P.M., 2016. Double-counting challenges the accuracy of high-latitude methane inventories. *Geophys. Res. Lett.* 43. <https://doi.org/10.1002/2016GL071772>
- Tikkasalo, O.-P., Peltola, O., Alekseychik, P., Heikkinen, J., Launiainen, S., Lehtonen, A., Li, Q., Martínez-García, E., Peltoniemi, M., Salovaara, P., Tuominen, V., Mäkipää, R., 2025. Eddy-covariance fluxes of CO₂, CH₄ and N₂O in a drained peatland forest after clear-cutting. *Biogeosciences* 22, 1277–1300. <https://doi.org/10.5194/bg-22-1277-2025>

- Tramontana, G., Jung, M., Schwalm, C.R., Ichii, K., Camps-Valls, G., Ráduly, B., Reichstein, M., Arain, M.A., Cescatti, A., Kiely, G., Merbold, L., Serrano-Ortiz, P., Sickert, S., Wolf, S., Papale, D., 2016. Predicting carbon dioxide and energy fluxes across global FLUXNET sites with regression algorithms. *Biogeosciences* 13, 4291–4313. <https://doi.org/10.5194/bg-13-4291-2016>
- Treat, Claire C, Bloom, A.A., Marushchak, M.E., 2018. Growing season, non-growing season and annual CH₄ fluxes from temperate, boreal, and Arctic wetlands and uplands. <https://doi.org/10.1594/PANGAEA.886976>
- Treat, Claire C., Marushchak, M.E., Voigt, C., Zhang, Y., Tan, Z., Zhuang, Q., Virtanen, T.A., Räsänen, A., Biasi, C., Hugelius, G., Kaverin, D., Miller, P.A., Stendel, M., Romanovsky, V., Rivkin, F., Martikainen, P.J., Shurpali, N.J., 2018. Tundra landscape heterogeneity, not interannual variability, controls the decadal regional carbon balance in the Western Russian Arctic. *Glob. Change Biol.* 24, 5188–5204. <https://doi.org/10.1111/gcb.14421>
- Treat, C.C., Virkkala, A., Burke, E., Bruhwiler, L., Chatterjee, A., Fisher, J.B., Hashemi, J., Parmentier, F.W., Rogers, B.M., Westermann, S., Watts, J.D., Blanc-Betes, E., Fuchs, M., Kruse, S., Malhotra, A., Miner, K., Strauss, J., Armstrong, A., Epstein, H.E., Gay, B., Goeckede, M., Kalhori, A., Kou, D., Miller, C.E., Natali, S.M., Oh, Y., Shakil, S., Sonntag, O., Varner, R.K., Zolkos, S., Schuur, E.A.G., Hugelius, G., 2024. Permafrost Carbon: Progress on Understanding Stocks and Fluxes Across Northern Terrestrial Ecosystems. *J. Geophys. Res. Biogeosciences* 129, e2023JG007638. <https://doi.org/10.1029/2023JG007638>
- Turetsky, M.R., Abbott, B.W., Jones, M.C., Anthony, K.W., Olefeldt, D., Schuur, E.A.G., Grosse, G., Kuhry, P., Hugelius, G., Koven, C., Lawrence, D.M., Gibson, C., Sannel, A.B.K., McGuire, A.D., 2020. Carbon release through abrupt permafrost thaw. *Nat. Geosci.* 13, 138–143. <https://doi.org/10.1038/s41561-019-0526-0>
- Tweedie, R.L., Mengersen, K.L., Eccleston, J.A., 1994. Garbage In, Garbage Out: Can Statisticians Quantify the Effects of Poor Data? 7, 20–27.
- Ueyama, M., Ichii, K., Iwata, H., Euskirchen, E.S., Zona, D., Rocha, A.V., Harazono, Y., Iwama, C., Nakai, T., Oechel, W.C., 2013. Upscaling terrestrial carbon dioxide fluxes in Alaska with satellite remote sensing and support vector regression. *J. Geophys. Res. Biogeosciences* 118, 1266–1281. <https://doi.org/10.1002/jgrg.20095>
- Ueyama, M., Iwata, H., Nagano, H., Tahara, N., Iwama, C., Harazono, Y., 2019. Carbon dioxide balance in early-successional forests after forest fires in interior Alaska. *Agric. For. Meteorol.* 275, 196–207. <https://doi.org/10.1016/j.agrformet.2019.05.020>
- Ueyama, M., Takao, Y., Yazawa, H., Tanaka, M., Yabuki, H., Kumagai, T., Iwata, H., Awal, Md.A., Du, M., Harazono, Y., Hata, Y., Hirano, T., Hiura, T., Ide, R., Ishida, S., Ishikawa, M., Kitamura, K., Kominami, Y., Komiya, S., Kotani, A., Inoue, Y., Machimura, T., Matsumoto, K., Matsuura, Y., Mizoguchi, Y., Murayama, S., Nagano, H., Nakai, T., Nakaji, T., Nakaya, K., Ohkubo, S., Ohta, T., Ono, K., Saitoh, T.M., Sakabe, A., Shimizu, T., Shimoda, S., Sugita, M., Takagi, K., Takahashi, Y., Takamura, N., Takanashi, S., Takimoto, T., Yasuda, Y., Wang, Q., Asanuma, J., Hasegawa, H., Hiyama, T., Iijima, Y., Ishidoya, S., Itoh, M., Kato, T., Kondo, H., Kosugi, Y., Kume, T., Maeda, T., Matsuura, S., Maximov, T., Miyama, T., Moriwaki, R., Muraoka, H., Petrov, R., Suzuki, J., Taniguchi, S., Ichii, K., 2025. The JapanFlux2024 dataset for eddy

- covariance observations covering Japan and East Asia from 1990 to 2023. *Earth Syst. Sci. Data* 17, 3807–3833. <https://doi.org/10.5194/essd-17-3807-2025>
- Van Der Ploeg, T., Austin, P.C., Steyerberg, E.W., 2014. Modern modelling techniques are data hungry: a simulation study for predicting dichotomous endpoints. *BMC Med. Res. Methodol.* 14, 137. <https://doi.org/10.1186/1471-2288-14-137>
- Van Der Werf, G.R., Randerson, J.T., Giglio, L., Van Leeuwen, T.T., Chen, Y., Rogers, B.M., Mu, M., Van Marle, M.J.E., Morton, D.C., Collatz, G.J., Yokelson, R.J., Kasibhatla, P.S., 2017. Global fire emissions estimates during 1997–2016. *Earth Syst. Sci. Data* 9, 697–720. <https://doi.org/10.5194/essd-9-697-2017>
- Virkkala, A.-M., Aalto, J., Rogers, B.M., Tagesson, T., Treat, C.C., Natali, S.M., Watts, J.D., Potter, S., Lehtonen, A., Mauritz, M., Schuur, E.A.G., Kochendorfer, J., Zona, D., Oechel, W., Kobayashi, H., Humphreys, E., Goeckede, M., Iwata, H., Lafleur, P.M., Euskirchen, E.S., Bokhorst, S., Marushchak, M., Martikainen, P.J., Elberling, B., Voigt, C., Biasi, C., Sonnentag, O., Parmentier, F.J.W., Ueyama, M., Celis, G., St.Louis, V.L., Emmerton, C.A., Peichl, M., Chi, J., Järveoja, J., Nilsson, M.B., Oberbauer, S.F., Torn, M.S., Park, S.J., Dolman, H., Mammarella, I., Chae, N., Poyatos, R., López-Blanco, E., Christensen, T.R., Kwon, M.J., Sachs, T., Holl, D., Luoto, M., 2021. Statistical upscaling of ecosystem CO₂ fluxes across the terrestrial tundra and boreal domain: Regional patterns and uncertainties. *Glob. Change Biol.* 27, 4040–4059. <https://doi.org/10.1111/gcb.15659>
- Virkkala, A.-M., Abdi, A.M., Luoto, M., Metcalfe, D.B., 2019. Identifying multidisciplinary research gaps across Arctic terrestrial gradients. *Environ. Res. Lett.* 14. <https://doi.org/10.1088/1748-9326/ab4291>
- Virkkala, A.-M., Natali, S.M., Rogers, B.M., Watts, J.D., Savage, K., Connon, S.J., Mauritz, M., Schuur, E.A.G., Peter, D., Minions, C., Nojeim, J., Commane, R., Emmerton, C.A., Goeckede, M., Helbig, M., Holl, D., Iwata, H., Kobayashi, H., Kolari, P., López-Blanco, E., Marushchak, M.E., Mastepanov, M., Merbold, L., Parmentier, F.-J.W., Peichl, M., Sachs, T., Sonnentag, O., Ueyama, M., Voigt, C., Aurela, M., Boike, J., Celis, G., Chae, N., Christensen, T.R., Bret-Harte, M.S., Dengel, S., Dolman, H., Edgar, C.W., Elberling, B., Euskirchen, E., Grelle, A., Hatakka, J., Humphreys, E., Järveoja, J., Kotani, A., Kutzbach, L., Laurila, T., Lohila, A., Mammarella, I., Matsuura, Y., Meyer, G., Nilsson, M.B., Oberbauer, S.F., Park, S.-J., Petrov, R., Prokushkin, A.S., Schulze, C., St. Louis, V.L., Tuittila, E.-S., Tuovinen, J.-P., Quinton, W., Varlagin, A., Zona, D., Zyryanov, V.I., 2022. The ABCflux database: Arctic–boreal CO₂ flux observations and ancillary information aggregated to monthly time steps across terrestrial ecosystems. *Earth Syst. Sci. Data* 14, 179–208. <https://doi.org/10.5194/essd-14-179-2022>
- Virkkala, A.-M., Rogers, B.M., Watts, J.D., Arndt, K.A., Potter, S., Wargowsky, I., Schuur, E.A.G., See, C., Mauritz, M., Boike, J., Bret-Harte, S.M., Burke, E.J., Burrell, A., Chae, N., Chatterjee, A., Chevallier, F., Christensen, T.R., Commane, R., Dolman, H., Elberling, B., Emmerton, C.A., Euskirchen, E.S., Feng, L., Goeckede, M., Grelle, A., Helbig, M., Holl, D., Järveoja, J., Kobayashi, H., Kutzbach, L., Liu, J., Liujkx, I., López-Blanco, E., Lunneberg, K., Mammarella, I., Marushchak, M.E., Mastepanov, M., Matsuura, Y., Maximov, T., Merbold, L., Meyer, G., Nilsson, M.B., Niwa, Y., Oechel, W., Park, S.-J., Parmentier, F.-J.W., Peichl, M., Peters, W., Petrov, R., Quinton, W., Rödenbeck, C., Sachs, T., Schulze, C., Sonnentag, O., St.Louis, V., Tuittila, E.-S., Ueyama, M., Varlagin, A., Zona, D., Natali, S.M., 2024. An increasing Arctic-boreal

CO₂sink offset by wildfires and source regions.

<https://doi.org/10.1101/2024.02.09.579581>

- Virkkala, A.-M., Rogers, B.M., Watts, J.D., Arndt, K.A., Potter, S., Wargowsky, I., Schuur, E.A.G., See, C.R., Mauritz, M., Boike, J., Bret-Harte, M.S., Burke, E.J., Burrell, A., Chae, N., Chatterjee, A., Chevallier, F., Christensen, T.R., Commane, R., Dolman, H., Edgar, C.W., Elberling, B., Emmerton, C.A., Euskirchen, E.S., Feng, L., Göckede, M., Grelle, A., Helbig, M., Holl, D., Järveoja, J., Karsanaev, S.V., Kobayashi, H., Kutzbach, L., Liu, J., Luijkx, I.T., López-Blanco, E., Lunneberg, K., Mammarella, I., Marushchak, M.E., Mastepanov, M., Matsuura, Y., Maximov, T.C., Merbold, L., Meyer, G., Nilsson, M.B., Niwa, Y., Oechel, W., Palmer, P.I., Park, S.-J., Parmentier, F.-J.W., Peichl, M., Peters, W., Petrov, R., Quinton, W., Rödenbeck, C., Sachs, T., Schulze, C., Sonnentag, O., St. Louis, V.L., Tuittila, E.-S., Ueyama, M., Varlagin, A., Zona, D., Natali, S.M., 2025a. Wildfires offset the increasing but spatially heterogeneous Arctic–boreal CO₂ uptake. *Nat. Clim. Change* 15, 188–195. <https://doi.org/10.1038/s41558-024-02234-5>
- Virkkala, A.-M., Wargowsky, I., Vogt, J., Kuhn, M.A., Madaan, S., O’Keefe, R., Windholz, T., Arndt, K.A., Rogers, B.M., Watts, J.D., Kent, K., Göckede, M., Olefeldt, D., Rocher-Ros, G., Schuur, E.A.G., Bastviken, D., Aalstad, K., Aho, K., Ala-Könni, J., Alcock, H., Althuisen, I., Arp, C.D., Asanuma, J., Attermeyer, K., Aurela, M., Balathandayuthabani, S., Barr, A., Barret, M., Batkhisig, O., Biasi, C., Björkman, M.P., Black, A., Blanc-Betes, E., Bodmer, P., Boike, J., Bolek, A., Bouchard, F., Bussmann, I., Cabrol, L., Canfora, E., Carey, S., Castro-Morales, K., Chae, N., Christen, A., Christensen, T.R., Christiansen, C.T., Chu, H., Clark, G., Clayer, F., Crill, P., Cunada, C., Davidson, S.J., Dean, J.F., Dengel, S., Detto, M., Dieleman, C., Domine, F., Dyukarev, E., Edgar, C., Elberling, B., Emmerton, C.A., Euskirchen, E., Falvo, G., Friborg, T., Garneau, M., Giamberini, M., Glagolev, M.V., Gonzalez-Meler, M.A., Granath, G., Guðmundsson, J., Happonen, K., Harazono, Y., Harris, L., Hashemi, J., Hasson, N., Heerah, J., Heffernan, L., Helbig, M., Helgason, W., Heliasz, M., Henry, G., Hensgens, G., Hiyama, T., Hock, M., Holl, D., Holmes, B., Holst, J., Holst, T., Hould-Gosselin, G., Humphreys, E., Hung, J., Huotari, J., Ikawa, H., Ilyasov, D.V., Ishikawa, M., Iwahana, G., Iwata, H., Jackowicz-Korczynski, M.A., Jansen, J., Järveoja, J., Jassey, V.E.J., Jensen, R., Jentsch, K., Jespersen, R.G., Johannesson, C.-F., Jones, C.P., Jonsson, A., Jung, J.Y., Juutinen, S., Kane, E., Karlsson, J., Karsanaev, S., Kasak, K., Kelly, J., Kempton, K., Klaus, M., Kling, G.W., Kljun, N., Knutson, J., Kobayashi, H., Kochendorfer, J., Kohonen, K.-M., Kolari, P., Korkiakoski, M., Korrensalo, A., Kortelainen, P., Koster, E., Koster, K., Kotani, A., Krishnan, P., Kurbatova, J., Kutzbach, L., Kwon, M.J., Kyzivat, E.D., Lagroix, J., Langhorst, T., Lapshina, E., Larmola, T., Larsen, K.S., Laurion, I., Ledman, J., Lee, H., Leffler, A.J., Lesack, L., Lindroth, A., Lipson, D., Lohila, A., López-Blanco, E., St. Louis, V.L., Lundin, E., Luoto, M., Machimura, T., Magnani, M., Malhotra, A., Maljanen, M., Mammarella, I., Männistö, E., Marchesini, L.B., Marsh, P., Martkainen, P.J., Marushchak, M.E., Mastepanov, M., Mavrovic, A., Maximov, T., Minions, C., Montemayor, M., Morishita, T., Murphy, P., Nadeau, D.F., Nicholls, E., Nilsson, M.B., Niyazova, A., Nordén, J., Noumonvi, K.D., Nykanen, H., Oechel, W., Ojala, A., Okadera, T., Pal, S., Panov, A.V., Papakyriakou, T., Papale, D., Park, S.-J., Parmentier, F.-J.W., Pastorello, G., Peacock, M., Peichl, M., Petrov, R., St. Pierre, K., Pirk, N., Plein, J., Preskienis, V., Prokushkin, A., Pumpanen, J., Rains, H.A., Rakos, N., Räsänen, A., Rautakoski, H., Rinnan, R., Rinne, J., Rocha, A., Roulet, N., Roy, A., Rutgersson, A.,

- Sabrekov, A.F., Sachs, T., Sahlée, E., Salazar, A., Sawakuchi, H.O., Schulze, C., Seco, R., Sepulveda-Jauregui, A., Serikova, S., Serrone, A., Silvennoinen, H.M., Sjogersten, S., Skeeter, J., Snöäl, J., Sobek, S., Sonnentag, O., Stanley, E.H., Strack, M., Strom, L., Sullivan, P., Sullivan, R., Sytiuk, A., Tagesson, T., Taillardat, P., Talbot, J., Tank, S.E., Tenuta, M., Terenteva, I., Thalasso, F., Thiboult, A., Thorgeirsson, H., Garcia Tigreros, F., Torn, M., Townsend-Small, A., Treat, C., Tremblay, A., Trotta, C., Tuittila, E.-S., Turetsky, M., Ueyama, M., Umair, M., Vähä, A., Van Delden, L., Van Hardenbroek, M., Varlagin, A., Varner, R.K., Veretennikova, E., Vesala, T., Virtanen, T., Voigt, C., Vonk, J.E., Wagner, R., Walter Anthony, K., Wang, Q., Watanabe, M., Webb, H., Welker, J.M., Westergaard-Nielsen, A., Westermann, S., White, J.R., Wille, C., Williamson, S.N., Zolkos, S., Zona, D., Natali, S.M., 2025b. ABCFlux v2: Arctic–boreal CO₂ and CH₄ monthly flux observations and ancillary information across terrestrial and freshwater ecosystems. <https://doi.org/10.5194/essd-2025-585>
- Vogt, J., Pallandt, M.M.T.A., Basso, L.S., Bolek, A., Ivanova, K., Schlutow, M., Celis, G., Kuhn, M., Mauritz, M., Schuur, E.A.G., Arndt, K., Virkkala, A.-M., Wargowsky, I., Göckede, M., 2025. ARGO: ARctic greenhouse Gas Observation metadata version 1. *Earth Syst. Sci. Data* 17, 2553–2573. <https://doi.org/10.5194/essd-17-2553-2025>
- Voigt, C., Virkkala, A.-M., Hould Gosselin, G., Bennett, K.A., Black, T.A., Detto, M., Chevrier-Dion, C., Guggenberger, G., Hashmi, W., Kohl, L., Kou, D., Marquis, C., Marsh, P., Marushchak, M.E., Nesic, Z., Nykänen, H., Saarela, T., Sauheitl, L., Walker, B., Weiss, N., Wilcox, E.J., Sonnentag, O., 2023. Arctic soil methane sink increases with drier conditions and higher ecosystem respiration. *Nat. Clim. Change* 13, 1095–1104. <https://doi.org/10.1038/s41558-023-01785-3>
- Walter Anthony, K.M., Lindgren, P., Hanke, P., Engram, M., Anthony, P., Daanen, R.P., Bondurant, A., Liljedahl, A.K., Lenz, J., Grosse, G., Jones, B.M., Brosius, L., James, S.R., Minsley, B.J., Pastick, N.J., Munk, J., Chanton, J.P., Miller, C.E., Meyer, F.J., 2021. Decadal-scale hotspot methane ebullition within lakes following abrupt permafrost thaw. *Environ. Res. Lett.* 16, 035010. <https://doi.org/10.1088/1748-9326/abc848>
- Walter Anthony, K.M., Vas, Dragos.A., Brosius, L., Chapin, F.S., Zimov, S.A., Zhuang, Q., 2010. Estimating methane emissions from northern lakes using ice-bubble surveys. *Limnol. Oceanogr. Methods* 8, 592–609. <https://doi.org/10.4319/lom.2010.8.0592>
- Walter, K.M., Smith, L.C., Stuart Chapin, F., 2007. Methane bubbling from northern lakes: present and future contributions to the global methane budget. *Philos. Trans. R. Soc. Math. Phys. Eng. Sci.* 365, 1657–1676. <https://doi.org/10.1098/rsta.2007.2036>
- Wan, Z., Hook, S., Hulley, G., 2021. MODIS/Terra Land Surface Temperature/Emissivity Monthly L3 Global 0.05Deg CMG V061. <https://doi.org/10.5067/MODIS/MOD11C3.061>
- Wang, J., Pottier, C., Cazals, C., Battude, M., Sheng, Y., Song, C., Sikder, M.S., Yang, X., Ke, L., Delhoume, M., Gosset, M., Oliveira, R.R.A., Grippa, M., Girard, F., Allen, G.H., Xu, X., Zhu, X., Biancamaria, S., Smith, L.C., Crétaux, J., Pavelsky, T.M., 2025. The Surface Water and Ocean Topography Mission (SWOT) Prior Lake Database (PLD): Lake Mask and Operational Auxiliaries. *Water Resour. Res.* 61, e2023WR036896. <https://doi.org/10.1029/2023WR036896>
- Watts, J.D., Farina, M., Kimball, J.S., Schiferl, L.D., Liu, Z., Arndt, K.A., Zona, D., Ballantyne, A., Euskirchen, E.S., Parmentier, F.J.W., Helbig, M., Sonnentag, O., Tagesson, T., Rinne, J., Ikawa, H., Ueyama, M., Kobayashi, H., Sachs, T., Nadeau, D.F., Kochendorfer, J.,

- Jackowicz-Korczynski, M., Virkkala, A.-M., Aurela, M., Commane, R., Byrne, B., Birch, L., Johnson, M.S., Madani, N., Rogers, B., Du, J., Endsley, A., Savage, K., Poulter, B., Zhang, Z., Bruhwiler, L.M., Miller, C.E., Goetz, S., Oechel, W.C., 2023. Carbon uptake in Eurasian boreal forests dominates the high-latitude net ecosystem carbon budget. *Glob. Change Biol.* 29, 1870–1889. <https://doi.org/10.1111/gcb.16553>
- Watts, J.D., Natali, S.M., Minions, C., Risk, D., Arndt, K., Zona, D., Euskirchen, E.S., Rocha, A.V., Sonnentag, O., Helbig, M., Kalhori, A., Oechel, W., Ikawa, H., Ueyama, M., Suzuki, R., Kobayashi, H., Celis, G., Schuur, E.A.G., Humphreys, E., Kim, Y., Lee, B.-Y., Goetz, S., Madani, N., Schiferl, L.D., Commane, R., Kimball, J.S., Liu, Z., Torn, M.S., Potter, S., Wang, J.A., Jorgenson, M.T., Xiao, J., Li, X., Edgar, C., 2021. Soil respiration strongly offsets carbon uptake in Alaska and Northwest Canada. *Environ. Res. Lett.* 16, 084051. <https://doi.org/10.1088/1748-9326/ac1222>
- Watts, J.D., Potter, S., Rogers, B.M., Virkkala, A., Fiske, G., Arndt, K.A., Burrell, A., Butler, K., Gerlt, B., Grayson, J., Shestakova, T.A., Du, J., Kim, Y., Parmentier, F.W., Natali, S.M., 2025. Regional Hotspots of Change in Northern High Latitudes Informed by Observations From Space. *Geophys. Res. Lett.* 52, e2023GL108081. <https://doi.org/10.1029/2023GL108081>
- Westermann, S., Barboux, C., Bartsch, A., Delaloye, R., Grosse, G., Heim, B., Hugelius, G., Irrgang, A., Kääb, A.M., Matthes, H., Miesner, F., Nitze, I., Pellet, C., Seifert, F.M., Strozzi, T., Wegmüller, U., Wiczorek, M., Wiesmann, A., 2025. ESA Permafrost Climate Change Initiative (Permafrost_cci): Permafrost Ground Temperature for the Northern Hemisphere, v5.0. <https://doi.org/10.5285/5675B0BE944F45A8AF0E7DDBEB47A011>
- Widhalm, B., Bartsch, A., Strozzi, T., Jones, N., Khomutov, A., Babkina, E., Leibman, M., Khairullin, R., Göckede, M., Bergstedt, H., Von Baeckmann, C., Muri, X., 2025. InSAR-derived seasonal subsidence reflects spatial soil moisture patterns in Arctic lowland permafrost regions. *The Cryosphere* 19, 1103–1133. <https://doi.org/10.5194/tc-19-1103-2025>
- Wik, M., Varner, R.K., Anthony, K.W., MacIntyre, S., Bastviken, D., 2016. Climate-sensitive northern lakes and ponds are critical components of methane release. *Nat. Geosci.* 9, 99–105. <https://doi.org/10.1038/ngeo2578>
- Wittig, S., Berchet, A., Pison, I., Saunio, M., Paris, J.-D., 2024. Surface networks in the Arctic may miss a future *methane bomb*. *Atmospheric Chem. Phys.* 24, 6359–6373. <https://doi.org/10.5194/acp-24-6359-2024>
- Wrona, E., Rowlandson, T.L., Nambiar, M., Berg, A.A., Colliander, A., Marsh, P., 2017. Validation of the Soil Moisture Active Passive (SMAP) satellite soil moisture retrieval in an Arctic tundra environment. *Geophys. Res. Lett.* 44, 4152–4158. <https://doi.org/10.1002/2017GL072946>
- Ying, Q., Poulter, B., Watts, J.D., Arndt, K.A., Virkkala, A.-M., Bruhwiler, L., Oh, Y., Rogers, B.M., Natali, S.M., Sullivan, H., Armstrong, A., Ward, E.J., Schiferl, L.D., Elder, C.D., Peltola, O., Bartsch, A., Desai, A.R., Euskirchen, E., Göckede, M., Lehner, B., Nilsson, M.B., Peichl, M., Sonnentag, O., Tuittila, E.-S., Sachs, T., Kalhori, A., Ueyama, M., Zhang, Z., 2025. WetCH₄: a machine-learning-based upscaling of methane fluxes of northern wetlands during 2016–2022. *Earth Syst. Sci. Data* 17, 2507–2534. <https://doi.org/10.5194/essd-17-2507-2025>

- Yuan, K., Li, F., McNicol, G., Chen, M., Hoyt, A., Knox, S., Riley, W.J., Jackson, R., Zhu, Q., 2024. Boreal–Arctic wetland methane emissions modulated by warming and vegetation activity. *Nat. Clim. Change* 14, 282–288. <https://doi.org/10.1038/s41558-024-01933-3>
- Yuan, K., Zhu, Q., Li, F., Riley, W.J., Torn, M., Chu, H., McNicol, G., Chen, M., Knox, S., Delwiche, K., Wu, H., Baldocchi, D., Ma, H., Desai, A.R., Chen, J., Sachs, T., Ueyama, M., Sonnentag, O., Helbig, M., Tuittila, E.-S., Jurasinski, G., Koebsch, F., Campbell, D., Schmid, H.P., Lohila, A., Goeckede, M., Nilsson, M.B., Friborg, T., Jansen, J., Zona, D., Euskirchen, E., Ward, E.J., Bohrer, G., Jin, Z., Liu, L., Iwata, H., Goodrich, J., Jackson, R., 2022. Causality guided machine learning model on wetland CH₄ emissions across global wetlands. *Agric. For. Meteorol.* 324, 109115. <https://doi.org/10.1016/j.agrformet.2022.109115>
- Zhang, Y., Woodcock, C.E., Chen, S., Wang, J.A., Sulla-Menashe, D., Zuo, Z., Olofsson, P., Wang, Y., Friedl, M.A., 2022. Mapping causal agents of disturbance in boreal and arctic ecosystems of North America using time series of Landsat data. *Remote Sens. Environ.* 272, 112935. <https://doi.org/10.1016/j.rse.2022.112935>
- Zhao, G., Li, Y., Zhou, L., Gao, H., 2022. Evaporative water loss of 1.42 million global lakes. *Nat. Commun.* 13, 3686. <https://doi.org/10.1038/s41467-022-31125-6>
- Zimov, S.A., Voropaev, Y.V., Semiletov, I.P., Davidov, S.P., Prosiannikov, S.F., Chapin, F.S., Chapin, M.C., Trumbore, S., Tyler, S., 1997. North Siberian Lakes: A Methane Source Fueled by Pleistocene Carbon. *Science* 277, 800–802. <https://doi.org/10.1126/science.277.5327.800>

Supplementary Information for “Data-driven modeling of carbon dioxide and methane fluxes across the Arctic-boreal region: recent achievements and future opportunities”

Anna-Maria Virkkala*^{1,2}, Mathias Göckede*³, Kyle A. Arndt*¹, McKenzie Kuhn^{1,4}, Sophia Walther³, Jacob Nelson³, Olli Peltola⁵, Gerard Rocher-Ros⁶, Annett Bartsch⁷, David Bastviken⁸, Grant Falvo⁹, Alexandra Hamm², Josh Hashemi¹⁰, Sarah M. Ludwig¹¹, Susan M. Natali¹, David Olefeldt¹², Martijn Pallandt^{2, 13}, Frans-Jan W. Parmentier¹⁴, Brendan M. Rogers¹, Ted Schuur¹⁵, Claire Treat¹⁰, Judith Vogt³, Carolina Voigt^{10,16}, Jennifer D. Watts¹, Isabel Wargowsky¹, Birgit Wild^{17,13}, Yili Yang¹, Amanda Armstrong^{18, 19}, Valeria Briones¹, Elchin Jafarov¹, Kathleen M. Orndahl²⁰, Benjamin Poulter²¹, Qing Ying¹⁸, Gustaf Hugelius^{2, 13}

*shared first-authorship

Affiliations:

1 Woodwell Climate Research Center, Falmouth, USA

2 Department of Physical Geography, Stockholm University, Stockholm, Sweden

3 Max Planck Institute for Biogeochemistry, Jena, Germany

4 Geography Department, University of British Columbia, Vancouver, Canada

5 Natural Resources Institute Finland, Helsinki, Finland

6 IceLab, Department of Ecology Environment and Geoscience, Umeå University, Umeå, Sweden

7 b.geos GmbH, Korneuburg, Austria

8 Department of Thematic Studies - Environmental Change, Linköping University, Linköping, Sweden

9 Department of Biological Sciences, Northern Arizona University, Arizona, USA

10 Alfred-Wegener Institute Helmholtz Centre for Polar and Marine Research, Potsdam, Germany

11 Department of Earth and Environmental Science, Columbia University, New York, NY, United States of America

12 Department of Renewable Resources, University of Alberta, Edmonton, Canada

13 Bolin Centre for Climate Research, Stockholm University, Stockholm, Sweden

14 Centre for Biogeochemistry in the Anthropocene, Department of Geosciences, University of Oslo, Oslo, Norway

15 Center for Ecosystem Science and Society, and Department of Biological Sciences, Northern Arizona University, Flagstaff, AZ, USA

16 University of Hamburg, Hamburg, Germany

17 Department of Environmental Science, Stockholm University

18 Earth System Science Interdisciplinary Center, University of Maryland, College Park, MD, USA

19 Biospheric Sciences Laboratory, NASA Goddard Space Flight Center, Greenbelt, MD, USA

20 School of Informatics, Computing and Cyber Systems, Northern Arizona University, Flagstaff, AZ, USA

21 Spark Climate Solutions, San Francisco, California

Table S1: Upscaling Methods and Input data from previous upscaling studies which include or are within the Arctic-boreal region.

Year	Bin	Manuscript	Upscaling Method	Input Data	GHG	Target ecosystem(s)	Region
1974	1971-1975	Ehhalt et al. (1974)	Area times flux rate	Chambers	CH4	Tundra	Circumpolar
1986	1986-1990	Sebacher et al. (1986)	Area times flux rate	Chambers	CH4	Wetlands	Arctic Boreal Region
1987	1986-1990	Matthews and Fung (1987)	Area times flux rate	Chambers	CH4	Wetlands	North of 60 Degrees N
1992	1991-1995	Kling et al. (1992)	Area times flux rate	Diffusion	CO2, CH4	Lakes & Rivers	North Slope of Alaska
1993	1991-1995	Oechel et al. (1993)	Area times flux rate	Chambers	CO2	Tundra	Circumpolar
1993	1991-1995	Bartlett and Harris (1993)	Area times flux rate	Chambers, Bubble Traps	CH4	Wetlands & Tundra	North of 45 Degrees N
1997	1996-2000	Zimov et al. (1997)	Area times flux rate	Chambers, Diffusion	CH4	Lakes	North Siberia
2006	2006-2010	Walter et al. (2006)	Mass balance stoichiometry	Bubble Traps	CH4	Lakes	North Siberia
2007	2006-2010	Walter et al. (2007)	Mass balance stoichiometry	Bubble Traps	CH4	Lakes	Circumpolar
2008	2006-2010	Bartsch et al. (2008)	Area times flux rate	Chambers	CH4	Lakes	Taymyr peninsula
2009	2006-2010	Schneider et al. (2009)	Area times flux rate	Chambers	CH4	Terrestrial & Inland Water	Lena River Delta
2012	2011-2015	McGuire et al. (2012)	Area times flux rate	EC, Chambers, Diffusion, Models	CO2, CH4	Tundra	Circumpolar
2013	2011-2015	Ueyama et al. (2013)	Machine learning	EC	CO2	Terrestrial	Alaska
2013	2011-2015	Marushchak et al. (2013)	Area times flux rate	EC, Chambers, Diffusion	CO2	Terrestrial & Lakes	Northeast European Russian Tundra
2013	2011-2015	Belshe et al. (2013)	Linear regression	EC, Chambers, Diffusion, Models	CO2	Tundra	Circumpolar
2016	2016-2020	Holgerson & Raymond (2016)	Area times flux rate	Diffusion	CO2, CH4	Lakes & ponds	Global
2016	2016-2020	Wik et al. (2016)	Area times flux rate	EC, Diffusion, Bubble Traps	CH4	Lakes & ponds	North of 50 Degrees N
			Linear mixed-effect				
2018	2016-2020	Treat et al. (2018)	modeling	EC, Chambers, Diffusion	CH4	Wetlands	North of 40 Degrees N
2019	2016-2020	Peltola et al. (2019)	Machine learning	EC	CH4	Wetlands	North of 45 Degrees N
2019	2016-2020	Natali & Watts et al. (2019)	Machine learning	EC, Chambers, Diffusion	CO2	Terrestrial	Permafrost Region
2020	2016-2020	Matthews et al. (2020)	Area times flux rate	Chambers, Diffusion	CH4	Lakes	North of 50 Degrees N

2021	2021-2025	Watts et al. (2021)	Machine learning	EC, Chambers	CO2	Terrestrial	Permafrost Affected Alaska and Western Canada
2021	2021-2025	Virkkala et al. (2021)	Machine learning	EC, Chambers, Diffusion, Models	CO2	Terrestrial	Arctic Boreal Region
2022	2021-2025	Johnson et al. (2022)	Area times flux rate	Chambers, Diffusion	CH4	Lakes	North of 45 Degrees N
2022	2021-2025	Liu et al. (2022)	Machine learning	Diffusion	CO2	Rivers	Arctic Boreal Region
2023	2021-2025	Rocher-Ros et al. (2023)	Machine learning	Chambers, Diffusion	CH4	Rivers	Global
2023	2021-2025	McNichol et al. (2023)	Machine learning	EC	CH4	Wetlands	Global
				Chambers, Diffusion, Bubble			
2024	2021-2025	Song et al., (2024)	Area times flux rate	Traps	CO2, CH4	Inland Water	Permafrost Region
2024	2021-2025	Yuan et al. (2024)	Machine learning	EC, Chambers	CH4	Wetlands	Arctic Boreal Region
2024	2021-2025	Chen et al. (2024)	Machine learning	EC, Chambers	CH4	Wetlands	North of 30 Degrees N
2024	2021-2025	Ramage et al. (2024)	Area times flux rate	EC, Chambers, Diffusion, Models	CO2, CH4, N2O	Terrestrial & Inland Water	Permafrost Region
2025	2021-2025	Virkkala et al. (2025)	Machine learning	EC, Chambers	CO2	Terrestrial	Arctic Boreal Region
2025	2021-2025	Bastviken & Johnson (2025)	Area times flux rate	Chambers, Diffusion	CH4	Lakes & Reservoirs	Arctic Boreal Region
2025	2021-2025	Ying et al. (2025)	Machine learning	EC	CH4	Wetlands	North of 45 Degrees N

1 References

- 2 Bartlett, K.B., Harriss, R.C., 1993. Review and assessment of methane emissions from wetlands.
3 *Chemosphere* 26, 261–320. [https://doi.org/https://doi.org/10.1016/0045-6535\(93\)90427-7](https://doi.org/10.1016/0045-6535(93)90427-7)
- 4 Bartsch, A., Pathe, C., Wagner, W., Scipal, K., 2008. Detection of permanent open water
5 surfaces in central Siberia with ENVISAT ASAR wide swath data with special emphasis
6 on the estimation of methane fluxes from tundra wetlands. *Hydrol. Res.* 39, 89–100.
7 <https://doi.org/10.2166/nh.2008.041>
- 8 Bastviken, D., Johnson, M.S., 2025. Future methane emissions from lakes and reservoirs. *Nat.*
9 *Water.* <https://doi.org/10.1038/s44221-025-00532-6>
- 10 Belshe, E.F., Schuur, E.A.G., Bolker, B.M., 2013. Tundra ecosystems observed to be CO₂
11 sources due to differential amplification of the carbon cycle. *Ecol. Lett.* 16, 1307–1315.
12 <https://doi.org/10.1111/ele.12164>
- 13 Chen, S., Liu, L., Ma, Y., Zhuang, Q., Shurpali, N.J., 2024. Quantifying Global Wetland
14 Methane Emissions With In Situ Methane Flux Data and Machine Learning Approaches.
15 *Earths Future* 12, e2023EF004330. <https://doi.org/10.1029/2023EF004330>
- 16 Ehhalt, D.H., 1974. The atmospheric cycle of methane. *Tellus* 26, 58–70.
17 <https://doi.org/10.1111/j.2153-3490.1974.tb01952.x>
- 18 Holgerson, M.A., Raymond, P.A., 2016. Large contribution to inland water CO₂ and CH₄
19 emissions from very small ponds. *Nat. Geosci.* 9, 222–226.
20 <https://doi.org/10.1038/ngeo2654>
- 21 Johnson, M.S., Matthews, E., Du, J., Genovese, V., Bastviken, D., 2022. Methane Emission
22 From Global Lakes: New Spatiotemporal Data and Observation-Driven Modeling of
23 Methane Dynamics Indicates Lower Emissions. *J. Geophys. Res. Biogeosciences* 127,
24 e2022JG006793. <https://doi.org/10.1029/2022JG006793>
- 25 Kling, G.W., Kipphut, G.W., Miller, M.C., 1992. The flux of CO₂ and CH₄ from lakes and
26 rivers in arctic Alaska. *Hydrobiologia* 240, 23–36. <https://doi.org/10.1007/BF00013449>
- 27 Liu, S., Kuhn, C., Amatulli, G., Aho, K., Butman, D.E., Allen, G.H., Lin, P., Pan, M., Yamazaki,
28 D., Brinkerhoff, C., Gleason, C., Xia, X., Raymond, P.A., 2022. The importance of
29 hydrology in routing terrestrial carbon to the atmosphere via global streams and rivers.
30 *Proc. Natl. Acad. Sci.* 119, e2106322119. <https://doi.org/10.1073/pnas.2106322119>
- 31 Marushchak, M.E., Kiepe, I., Biasi, C., Elsakov, V., Friborg, T., Johansson, T., Soegaard, H.,
32 Virtanen, T., Martikainen, P.J., 2013. Carbon dioxide balance of subarctic tundra from
33 plot to regional scales. *Biogeosciences* 10, 437–452. [https://doi.org/10.5194/bg-10-437-](https://doi.org/10.5194/bg-10-437-2013)
34 2013
- 35 Matthews, E., Fung, I., 1987. Methane emission from natural wetlands: Global distribution, area,
36 and environmental characteristics of sources. *Glob. Biogeochem. Cycles* 1, 61–86.
37 <https://doi.org/10.1029/GB001i001p00061>
- 38 Matthews, E., Johnson, M.S., Genovese, V., Du, J., Bastviken, D., 2020. Methane emission from
39 high latitude lakes: methane-centric lake classification and satellite-driven annual cycle
40 of emissions. *Sci. Rep.* 10, 12465. <https://doi.org/10.1038/s41598-020-68246-1>
- 41 McGuire, A.D., Christensen, T.R., Hayes, D., Heroult, A., Euskirchen, E., Kimball, J.S., Koven,
42 C., Lafleur, P., Miller, P.A., Oechel, W., Peylin, P., Williams, M., Yi, Y., 2012. An
43 assessment of the carbon balance of Arctic tundra: comparisons among observations,

44 process models, and atmospheric inversions. *Biogeosciences* 9, 3185–3204.
45 <https://doi.org/10.5194/bg-9-3185-2012>

46 McNicol, G., Fluet-Chouinard, E., Ouyang, Z., Knox, S., Zhang, Z., Aalto, T., Bansal, S., Chang,
47 K., Chen, M., Delwiche, K., Feron, S., Goeckede, M., Liu, J., Malhotra, A., Melton, J.R.,
48 Riley, W., Vargas, R., Yuan, K., Ying, Q., Zhu, Q., Alekseychik, P., Aurela, M.,
49 Billesbach, D.P., Campbell, D.I., Chen, J., Chu, H., Desai, A.R., Euskirchen, E.,
50 Goodrich, J., Griffis, T., Helbig, M., Hirano, T., Iwata, H., Jurasinski, G., King, J.,
51 Koepsch, F., Kolka, R., Krauss, K., Lohila, A., Mammarella, I., Nilson, M., Noormets,
52 A., Oechel, W., Peichl, M., Sachs, T., Sakabe, A., Schulze, C., Sonntag, O., Sullivan,
53 R.C., Tuittila, E., Ueyama, M., Vesala, T., Ward, E., Wille, C., Wong, G.X., Zona, D.,
54 Windham-Myers, L., Poulter, B., Jackson, R.B., 2023. Upscaling Wetland Methane
55 Emissions From the FLUXNET-CH4 Eddy Covariance Network (UpCH4 v1.0): Model
56 Development, Network Assessment, and Budget Comparison. *AGU Adv.* 4,
57 e2023AV000956. <https://doi.org/10.1029/2023AV000956>

58 Natali, S.M., Watts, J.D., Rogers, B.M., Potter, S., Ludwig, S.M., Selbmann, A.-K., Sullivan,
59 P.F., Abbott, B.W., Arndt, K.A., Birch, L., Björkman, M.P., Bloom, A.A., Celis, G.,
60 Christensen, T.R., Christiansen, C.T., Commane, R., Cooper, E.J., Crill, P., Czimczik, C.,
61 Davydov, S., Du, J., Egan, J.E., Elberling, B., Euskirchen, E.S., Friborg, T., Genet, H.,
62 Göckede, M., Goodrich, J.P., Grogan, P., Helbig, M., Jafarov, E.E., Jastrow, J.D.,
63 Kalhori, A.A.M., Kim, Y., Kimball, J.S., Kutzbach, L., Lara, M.J., Larsen, K.S., Lee, B.-
64 Y., Liu, Z., Lorant, M.M., Lund, M., Lupascu, M., Madani, N., Malhotra, A., Matamala,
65 R., McFarland, J., McGuire, A.D., Michelsen, A., Minions, C., Oechel, W.C., Olefeldt,
66 D., Parmentier, F.-J.W., Pirk, N., Poulter, B., Quinton, W., Rezanezhad, F., Risk, D.,
67 Sachs, T., Schaefer, K., Schmidt, N.M., Schuur, E.A.G., Semenchuk, P.R., Shaver, G.,
68 Sonntag, O., Starr, G., Treat, C.C., Waldrop, M.P., Wang, Y., Welker, J., Wille, C.,
69 Xu, X., Zhang, Z., Zhuang, Q., Zona, D., 2019. Large loss of CO₂ in winter observed
70 across the northern permafrost region. *Nat. Clim. Change* 9, 852–857.
71 <https://doi.org/10.1038/s41558-019-0592-8>

72 Oechel, W.C., Hastings, S.J., Vourlitis, G., Jenkins, M., Riechers, G., Grulke, N., 1993. Recent
73 change of Arctic tundra ecosystems from a net carbon dioxide sink to a source. *Nature*
74 361, 520–523. <https://doi.org/10.1038/361520a0>

75 Peltola, O., Vesala, T., Gao, Y., Rätty, O., Alekseychik, P., Aurela, M., Chojnicki, B., Desai,
76 A.R., Dolman, A.J., Euskirchen, E.S., Friborg, T., Göckede, M., Helbig, M., Humphreys,
77 E., Jackson, R.B., Jocher, G., Joos, F., Klatt, J., Knox, S.H., Kowalska, N., Kutzbach, L.,
78 Lienert, S., Lohila, A., Mammarella, I., Nadeau, D.F., Nilsson, M.B., Oechel, W.C.,
79 Peichl, M., Pypker, T., Quinton, W., Rinne, J., Sachs, T., Samson, M., Schmid, H.P.,
80 Sonntag, O., Wille, C., Zona, D., Aalto, T., 2019. Monthly gridded data product of
81 northern wetland methane emissions based on upscaling eddy covariance observations.
82 *Earth Syst. Sci. Data* 11, 1263–1289. <https://doi.org/10.5194/essd-11-1263-2019>

83 Ramage, J., Kuhn, M., Virkkala, A., Voigt, C., Marushchak, M.E., Bastos, A., Biasi, C.,
84 Canadell, J.G., Ciais, P., López-Blanco, E., Natali, S.M., Olefeldt, D., Potter, S., Poulter,
85 B., Rogers, B.M., Schuur, E.A.G., Treat, C., Turetsky, M.R., Watts, J., Hugelius, G.,
86 2024. The Net GHG Balance and Budget of the Permafrost Region (2000–2020) From
87 Ecosystem Flux Upscaling. *Glob. Biogeochem. Cycles* 38, e2023GB007953.
88 <https://doi.org/10.1029/2023GB007953>

89 Rocher-Ros, G., Stanley, E.H., Loken, L.C., Casson, N.J., Raymond, P.A., Liu, S., Amatulli, G.,
90 Sponseller, R.A., 2023. Global methane emissions from rivers and streams. *Nature* 621,
91 530–535. <https://doi.org/10.1038/s41586-023-06344-6>

92 Schneider, J., Grosse, G., Wagner, D., 2009. Land cover classification of tundra environments in
93 the Arctic Lena Delta based on Landsat 7 ETM+ data and its application for upscaling of
94 methane emissions. *Remote Sens. Environ.* 113, 380–391.
95 <https://doi.org/10.1016/j.rse.2008.10.013>

96 Sebacher, D.I., Harriss, R.C., Bartlett, K.B., Sebacher, S.M., Grice, S.S., 1986. Atmospheric
97 methane sources: Alaskan tundra bogs, an alpine fen, and a subarctic boreal marsh. *Tellus*
98 B 38B, 1–10. <https://doi.org/10.1111/j.1600-0889.1986.tb00083.x>

99 Song, C., Liu, S., Wang, G., Zhang, L., Rosentreter, J.A., Zhao, G., Sun, X., Yao, Y., Mu, C.,
100 Sun, S., Hu, Z., Lin, S., Sun, J., Li, Yang, Wang, Y., Li, Yuhao, Raymond, P.A.,
101 Karlsson, J., 2024. Inland water greenhouse gas emissions offset the terrestrial carbon
102 sink in the northern cryosphere. *Sci. Adv.* 10, eadp0024.
103 <https://doi.org/10.1126/sciadv.adp0024>

104 Treat, C.C., Bloom, A.A., Marushchak, M.E., 2018. Nongrowing season methane emissions—a
105 significant component of annual emissions across northern ecosystems. *Glob. Change*
106 *Biol.* 24, 3331–3343. <https://doi.org/10.1111/gcb.14137>

107 Ueyama, M., Ichii, K., Iwata, H., Euskirchen, E.S., Zona, D., Rocha, A.V., Harazono, Y., Iwama,
108 C., Nakai, T., Oechel, W.C., 2013. Upscaling terrestrial carbon dioxide fluxes in Alaska
109 with satellite remote sensing and support vector regression. *J. Geophys. Res.*
110 *Biogeosciences* 118, 1266–1281. <https://doi.org/10.1002/jgrg.20095>

111 Virkkala, A.-M., Aalto, J., Rogers, B.M., Tagesson, T., Treat, C.C., Natali, S.M., Watts, J.D.,
112 Potter, S., Lehtonen, A., Mauritz, M., Schuur, E.A.G., Kochendorfer, J., Zona, D.,
113 Oechel, W., Kobayashi, H., Humphreys, E., Goeckede, M., Iwata, H., Lafleur, P.M.,
114 Euskirchen, E.S., Bokhorst, S., Marushchak, M., Martikainen, P.J., Elberling, B., Voigt,
115 C., Biasi, C., Sonnentag, O., Parmentier, F.J.W., Ueyama, M., Celis, G., St.Louis, V.L.,
116 Emmerton, C.A., Peichl, M., Chi, J., Järveoja, J., Nilsson, M.B., Oberbauer, S.F., Torn,
117 M.S., Park, S.J., Dolman, H., Mammarella, I., Chae, N., Poyatos, R., López-Blanco, E.,
118 Christensen, T.R., Kwon, M.J., Sachs, T., Holl, D., Luoto, M., 2021. Statistical upscaling
119 of ecosystem CO₂ fluxes across the terrestrial tundra and boreal domain: Regional
120 patterns and uncertainties. *Glob. Change Biol.* 27, 4040–4059.
121 <https://doi.org/10.1111/gcb.15659>

122 Virkkala, A.-M., Rogers, B.M., Watts, J.D., Arndt, K.A., Potter, S., Wargowsky, I., Schuur,
123 E.A.G., See, C.R., Mauritz, M., Boike, J., Bret-Harte, M.S., Burke, E.J., Burrell, A.,
124 Chae, N., Chatterjee, A., Chevallier, F., Christensen, T.R., Commane, R., Dolman, H.,
125 Edgar, C.W., Elberling, B., Emmerton, C.A., Euskirchen, E.S., Feng, L., Goeckede, M.,
126 Grelle, A., Helbig, M., Holl, D., Järveoja, J., Karsanaev, S.V., Kobayashi, H., Kutzbach,
127 L., Liu, J., Luijkx, I.T., López-Blanco, E., Lunneberg, K., Mammarella, I., Marushchak,
128 M.E., Mastepanov, M., Matsuura, Y., Maximov, T.C., Merbold, L., Meyer, G., Nilsson,
129 M.B., Niwa, Y., Oechel, W., Palmer, P.I., Park, S.-J., Parmentier, F.-J.W., Peichl, M.,
130 Peters, W., Petrov, R., Quinton, W., Rödenbeck, C., Sachs, T., Schulze, C., Sonnentag,
131 O., St. Louis, V.L., Tuittila, E.-S., Ueyama, M., Varlagin, A., Zona, D., Natali, S.M.,
132 2025. Wildfires offset the increasing but spatially heterogeneous Arctic–boreal CO₂
133 uptake. *Nat. Clim. Change* 15, 188–195. <https://doi.org/10.1038/s41558-024-02234-5>

134 Walter, K.M., Smith, L.C., Stuart Chapin, F., 2007. Methane bubbling from northern lakes:
135 present and future contributions to the global methane budget. *Philos. Trans. R. Soc.*
136 *Math. Phys. Eng. Sci.* 365, 1657–1676. <https://doi.org/10.1098/rsta.2007.2036>

137 Walter, K.M., Zimov, S.A., Chanton, J.P., Verbyla, D., Chapin, F.S., 2006. Methane bubbling
138 from Siberian thaw lakes as a positive feedback to climate warming. *Nature* 443, 71–75.
139 <https://doi.org/10.1038/nature05040>

140 Watts, J.D., Natali, S.M., Minions, C., Risk, D., Arndt, K., Zona, D., Euskirchen, E.S., Rocha,
141 A.V., Sonnentag, O., Helbig, M., Kalhori, A., Oechel, W., Ikawa, H., Ueyama, M.,
142 Suzuki, R., Kobayashi, H., Celis, G., Schuur, E.A.G., Humphreys, E., Kim, Y., Lee, B.-
143 Y., Goetz, S., Madani, N., Schiferl, L.D., Commane, R., Kimball, J.S., Liu, Z., Torn,
144 M.S., Potter, S., Wang, J.A., Jorgenson, M.T., Xiao, J., Li, X., Edgar, C., 2021. Soil
145 respiration strongly offsets carbon uptake in Alaska and Northwest Canada. *Environ. Res.*
146 *Lett.* 16, 084051. <https://doi.org/10.1088/1748-9326/ac1222>

147 Wik, M., Varner, R.K., Anthony, K.W., MacIntyre, S., Bastviken, D., 2016. Climate-sensitive
148 northern lakes and ponds are critical components of methane release. *Nat. Geosci.* 9, 99–
149 105. <https://doi.org/10.1038/ngeo2578>

150 Ying, Q., Poulter, B., Watts, J.D., Arndt, K.A., Virkkala, A.-M., Bruhwiler, L., Oh, Y., Rogers,
151 B.M., Natali, S.M., Sullivan, H., Armstrong, A., Ward, E.J., Schiferl, L.D., Elder, C.D.,
152 Peltola, O., Bartsch, A., Desai, A.R., Euskirchen, E., Göckede, M., Lehner, B., Nilsson,
153 M.B., Peichl, M., Sonnentag, O., Tuittila, E.-S., Sachs, T., Kalhori, A., Ueyama, M.,
154 Zhang, Z., 2025. WetCH₄ : a machine-learning-based upscaling of methane fluxes of
155 northern wetlands during 2016–2022. *Earth Syst. Sci. Data* 17, 2507–2534.
156 <https://doi.org/10.5194/essd-17-2507-2025>

157 Yuan, K., Li, F., McNicol, G., Chen, M., Hoyt, A., Knox, S., Riley, W.J., Jackson, R., Zhu, Q.,
158 2024. Boreal–Arctic wetland methane emissions modulated by warming and vegetation
159 activity. *Nat. Clim. Change* 14, 282–288. <https://doi.org/10.1038/s41558-024-01933-3>

160 Zimov, S.A., Voropaev, Y.V., Semiletov, I.P., Davidov, S.P., Prosiannikov, S.F., Chapin, F.S.,
161 Chapin, M.C., Trumbore, S., Tyler, S., 1997. North Siberian Lakes: A Methane Source
162 Fueled by Pleistocene Carbon. *Science* 277, 800–802.
163 <https://doi.org/10.1126/science.277.5327.800>

164

165